EVALUATING GLACIER MOVEMENT FLUCTUATIONS USING REMOTE SENSING: A CASE STUDY OF THE BAIRD, PATTERSON, LECONTE, AND SHAKES GLACIERS IN CENTRAL SOUTHEASTERN ALASKA

By

Robert Howard Davidson

A Thesis Presented to the

FACULTY OF THE USC GRADUATE SCHOOL

UNIVERSITY OF SOUTHERN CALIFORNIA

In Partial Fulfillment of the

Requirements for the Degree

MASTER OF SCIENCE

(GEOGRAPHIC INFORMATION SCIENCE AND TECHNOLOGY)

March 2014

ACKNOWLEDGEMENTS

From conception to finalization of this thesis has been what seemed like a lifetime. Excitement and despair seemed to change places on a weekly basis. There were many times when I was elated to finally be working on this project; other times were spent wondering if I would ever complete it. My chief supporter and encourager is my wife. To this day, I am not sure how she and my two children put up with the long nights that I put in in writing, editing, and finalizing this document. Besides my family, there are others that I should recognize; for without their support and inspiration, you would not be reading this document.

I would like to thank my thesis chair person, Dr. Flora Paganelli, for her guidance and assistance throughout this thesis. I would also like to thank Dr. Su Jin Lee and Dr. Lowell Stott who also served on my thesis committee for their guidance. Many years ago, I had the privilege of learning land surveying from Mr. Paul Bowen. Through his kind instruction and mentoring, I developed a fascination with all things geospatial; especially surveying. It was in his class that I first went to LeConte Glacier and conducted a ground-based survey of that glacier. Years later, that experience would help me as a geospatial analyst/geodetic surveyor in the United States Marine Corps. While serving in the Marine Corps, I developed a close friendship with Mr. Michael Noderer who taught me most of what I know about remote sensing; especially phenomenology.

Throughout my life, I have had the privilege of learning from some of the best people in the “business”. It is to those people that I dedicate this thesis. From the bottom of my heart, thank you.

TABLE OF CONTENTS

LIST OF FIGURES (CHAPTERS 1-6)

LIST OF FIGURES (APPENDIXES A-C)

LIST OF TABLES (CHAPTERS 1-6)

LIST OF TABLES (APPENDIXES A-C)

ABSTRACT

Global Land Survey (GLS) data encompassing Landsat Multispectral Scanner (MSS), Landsat 5's Thematic Mapper (TM), and Landsat 7's Enhanced Thematic Mapper Plus (ETM+) were used to determine the terminus locations of Baird, Patterson, LeConte, and Shakes Glaciers in Alaska in the time period 1975-2010. The sequences of the terminuses locations were investigated to determine the movement rates of these glaciers with respect to specific physical and environmental conditions.

GLS data from 1975, 1990, 2000, 2005, and 2010 in false-color composite images enhancing ice-snow differentiation and Iterative Self-Organizing (ISO) Data Cluster Unsupervised Classifications were used to 1) quantify the movement rates of Baird, Patterson, LeConte, and Shakes Glaciers; 2) analyze the movement rates for glaciers with *similar* terminal terrain conditions and; 3) analyze the movement rates for glaciers with *dissimilar* terminal terrain conditions. From the established sequence of terminus locations, movement distances were quantified between the glacier locations. Movement distances were then compared to see if any correlation existed between glaciers with similar or dissimilar terminal terrain conditions. The Global Land Ice Measurement from Space (GLIMS) data was used as a starting point from which glacier movement was measured for Baird, Patterson, and LeConte Glaciers only as the Shakes Glacier is currently not included in the GLIMS database.

The National Oceanographic and Atmospheric Administration (NOAA) temperature data collected at the Petersburg, Alaska, meteorological station (from January 1, 1973 to December 31, 2009) were used to help in the understanding of the climatic condition in this area and potential impact on glaciers terminus.

Results show that glaciers with similar terminal terrain conditions (Patterson and Shakes Glaciers) and glaciers with dissimilar terminal terrain conditions (Baird, Patterson, and LeConte Glaciers) did not exhibit similar movement rates. Glacier movement rates were greatest for glaciers whose terminuses were in fresh water (Patterson and Shakes Glaciers), less for those with terminuses in salt water (LeConte Glacier), and least for glaciers with terminuses on dry land (Baird Glacier).Based upon these findings, the presence of water, especially fresh water, at the terminal end of the Patterson and Shakes Glaciers had a greater effect on glacier movement than slope. Possible explanations for this effect might include a heat sink effect or tidal motions that hasten glacier disintegration in the ablation zone. In a heat sink scenario, the water bodies in which the Patterson and Shakes Glaciers terminus are located could act as a thermal energy transfer medium that increases glacier melting and subsequent retreat. On the other hand, tidal motions could act as horizontal and vertical push/pull forces, which increase the fracturing rate, calving, and subsequent retreat of glaciers terminus that are is salt water like the LeConte Glacier.

Over the length of the study period, 1975 through 2010, there has been a 0.85°C increase in annual air temperatures that, although may seem low, may prove important when determining glacial mass balance rates. Further studies are necessary to test these hypotheses to determine if a heat sink effect and tidal motions significantly affected the movement rates for the glaciers in this study area.

An additional significant result of this study was the creation of shapefiles delineating the positions of the Shakes Glaciers that are being submitted to the Global Land Ice Measurements from Space (GLIMS) program for inclusion in their master worldwide glacier database.

CHAPTER ONE: INTRODUCTION AND LITERATURE REVIEW

1.1 Introduction

Worldwide, glaciers are estimated to cover about 10% of all land mass and hold 69% of all fresh water on earth (United States Geological Survey, 2012). Glacier "health" is indicative of climate "health" (Michna, 2012). This means that if the world's climate is generally cooler, glaciers should grow larger and advance forward. If glaciers are growing larger and advancing, then by extension the climate should be getting cooler. It can also be said that glaciers, as the extensions of ice caps and sheets, are indicative of overall "health" of the parent ice cap or sheet. As an ice cap or sheet fluctuates in size, its associated glaciers should also fluctuate in size and move accordingly.

Glaciers are an important source of dissolved organic matter (DOM), in the form of labile carbon, for riverine and estuarine ecosystems (Hood et al., 2009). In a study of eleven coastal watersheds along the Gulf of Alaska; Hood et al. (2009) found that glacial runoff is a significant source of beneficial carbon for all ecosystems that are downstream of a glacier. Any reduction in glacier ice mass is detrimental to the availability of DOM in the dependent ecosystems (Hood et al. 2009). It is estimated that the Gulf of Alaska river drainage basins contain more than 10% of all mountain glaciers on Earth and the annual runoff from these systems is the second largest for the Pacific Ocean (Hood et al., 2009). The Gulf of Alaska and connected water bodies contain several of the most productive salmon, ground fish, and shellfish fisheries in the world (Alaska Department of Fish and Game, 2012). In 2011, Alaskan fisheries supported jobs for 78,500 people and generated 5.8 billion dollars from sales and services of which the Gulf of Alaska fisheries provided a significant percentage (Alaska Department of Fish and Game, 2012). For

economic as well as ecologic reasons, precise glacial measurements is necessary to provide scientific data that help the management of Alaskans' fisheries that represent a reliable source of food for native Alaskans and worldwide consumption.

The natural conditions that favor the formation of glaciers, like high elevations and inhospitable climate and weather, make on-site glacier study difficult. While these variables make direct glacier study problematic, they also directly impact glacier movement rates. Waddington (2009) attributes glacier movement rates to several physical and environmental factors; like glacial bed slope and warming temperatures. The warm, moist maritime climate present in the study area, coupled with a relatively wide range of glacial bed slopes, resulted in a variety of glacial movement rates for the glaciers studied for this project. Many glaciers require substantial effort for researchers to approach, necessitating the use of aircraft in often hazardous conditions. Remote sensing, as indirect method of detection of an object or phenomenon without direct human contact (Noderer, 2007), whether by using an imaging sensor flown by aircraft or satellite platform, provide the means for glacial monitoring. Satellite imagery such as Landsat (Irons, 2013), RADARSAT (Canadian Space Agency, 2013), and ASTER (Jet Propulsion Laboratory, 2013.) are successful in providing worldwide imaging capability that is repeatable and consistent.

Glaciers are studied to increase our understanding of glacier processes. A great deal of effort has been spent in documenting world glaciers by the development of databases of worldwide glaciers, such as the Global Land Survey (GLS; http://gls.umd.edu/) and the Global Land Ice Measurements from Space (GLIMS) project (Raup et al., 2007). It is currently estimated that there are between 70,000 and 200,000 glaciers worldwide which, due to the

immense number of glaciers, necessitates automated or automatic methods to map them (Aher and Dalvi, 2012). Remote sensing of glaciers has been expanded to include ice caps, fields, and sheets; all of which are differentiated by size and shape. Ice sheets and caps are domed shaped, icefields are flat; ice caps and fields are less than 50,000km^2 and ice sheets are greater than 50,000km^2 (Pidwirny and Jones, 2010).

Baird, Patterson, LeConte, and Shakes Glaciers originate from the Stikine Icefield. The Stikine Icefield is a very large icefield, approximately 190km in length from its southern border at the Stikine River to its northern border at the Taku River, straddling the southeastern Alaska and British Columbia (Canada) border (Molnia, 2008). Rapper and Braithwaite (2006) concluded that the melting rate for glaciers is different than the rate for ice caps or icefields; i.e. glaciers melt faster. This is analogous to leaving a large block of ice and the contents of an ice cube tray in the sun; the individual cubes will melt faster than the block of ice due to the significantly larger percentage of surface area compared to volume. In order to accurately monitor icecap mass change, it is necessary to consider glaciers and icecaps separately. After determining the mass change for an icecap and its included glaciers separately, the results can be combined to determine a final mass change figure that is indicative of the whole glacier-icecap system.

1.2 Review of remote sensing in glaciers studies

Remote sensing is considered reliable, safe, and a cost-effective method for assessing the world's glaciers. Several projects are gathering and processing data for monitoring purposes and worldwide use that are based on precursory studies that set the path for suitable procedure and the need for historical data archives. A literary search for remote sensing of glaciers returns an overwhelming amount of material and data archives; such as the Global Land Survey (GLS) and

the Global Land Ice Measurements from Space (GLIMS) project. GLS and GLIMS are described in detail based on the data type and main characteristics in support of regional glacier studies. It is important to note that these initiatives took place as a response to standardize glaciers study procedures and therefore several references are a collection of previous studies on which the glaciers study community is built upon. The focus is on low-cost data and procedures for regional glaciers monitoring such as in this study. However, it is important to mention that other remote sensing techniques such as laser altimetry, also known as Light Detection and Ranging, or LiDAR (National Oceanic and Atmospheric Administration, 2013), are used to measure the surfaces of glaciers, although they are currently at large scale, e.g. Mendenhall and Taku Glaciers by Hekkers (2010). LiDAR enable the rendering of very accurate three-dimensional modeling of a glacier's surface. However, this kind of technology is limited at this point to small areas and is not cost-effective for larger studies and therefore was not considered in this study.

The Global Land Survey (GLS), a partnership between the U.S. Geological Survey (USGS) and the National Aeronautics and Space Administration (NASA) in support of the U.S. Climate Change Science Program (CCSP) and the NASA Land-cover and Land-use Change (LCLUC) Program, builds on the existing geo-cover data sets developed for 1975, 1990, and 2000's. Some 9,500 Landsat images, acquired in the period 2004-2007, are processed and made available to the public. Given the failure of the Landsat-7 ETM+ Scan-Line-Corrector (SLC) in 2003, a combination of Landsat-7 gap-filled data and Landsat-5 data is used to create the GLS2010 dataset (Haq et al., 2012). The GLS is a global dataset of 30-meter resolution satellite imagery to support measurement of Earth's land cover and rates of land cover change during the first decade of the 21st century (Haq et al., 2012).

Since GLS data is collected using Landsat multispectral remote sensing satellites, a short review of the Landsat constellation is useful to highlight the capabilities, advantages, and disadvantages of this data source. Landsat satellites orbit in a near-polar orbit; that is they do not pass directly over the poles, rather they are slightly offset (Lillesand, Kiefer, and Chipman, 2008). Although Landsats 1-3 orbits at a different altitude than Landsats 5-8, all have an along track swath width of 185km (United States Geological Survey, 2012). Because of the difference in orbit altitude, Landsats 1-3 have a scene revisit time of 18 days and Landsats 5-8 have a scene revisit time of 16 days (United States Geological Survey, 2012). It should be recognized that Landsats 5 and 7 are eight days apart which reduces a scene revisit time to eight days when the two satellites are used together (Noderer, 2007). Imagery characteristics of the Landsat 1's Multispectral Scanner (MSS) spectral bands are summarized in Table 1, and Landsat 5's Thematic Mapper (TM) spectral bands and Landsat 7's Enhanced Thematic Mapper Plus (ETM+) spectral bands in Table 2.

Table 1. Landsat 1 Multispectral Scanner (MSS) spectral bands summary. Landsat 1 lacks a visible blue image band, which makes constructing a true color composite image difficult. It also lacks shortwave infrared capability. It is important to note that although the band numbers between MSS and later sensors do not correlate, the Electromagnetic Spectrum regions sensed are very similar.

Band Number	Electromagnetic Spectrum Region	Wavelength (µm)	Spatial Resolution (m)
Band 4	Visible Green	0.5-0.6	80
Band 5	Visible Red	0.6-0.7	80
Band 6	Near-Infrared	0.7-0.8	80
Band 7	Near-Infrared	0.8-1.1	80

Table 2. Landsat 5 Thematic Mapper (TM) and Landsat 7 Enhanced Thematic Mapper Plus (ETM+) spectral bands summary. TM and ETM+ differ primarily in the panchromatic band's spatial resolution. For this study, the panchromatic band is not used for analysis; which makes the images obtained by TM and ETM+ interchangeable.

Band Number	Electromagnetic Spectrum Region	Wavelength (μm)	Spatial Resolution (m)
Band 1 (TM & ETM+)	Visible Blue	0.45-0.52	30
Band 2 (TM & ETM+)	Visible Green	0.52-0.61	30
Band 3 (TM & ETM+)	Visible Red	0.63-0.69	30
Band 4 (TM & ETM+)	Near-Infrared	0.76-0.90	30
Band 5 (TM & ETM+)	Shortwave-Infrared	1.55-1.75	30
Band 6 (TM & ETM+)	Thermal-Infrared	10.40-12.50	120
Band 7 (TM & ETM+)	Shortwave-Infrared	2.08-2.35	30
Band 8 (ETM+ Only)	Panchromatic (Visible)	0.52-0.90	15

Landsat imagery has advantages and disadvantages depending upon what question the imagery is used to answer. The Landsat program has been collecting imagery since 1972, which is over forty years (Earth Resources Observation and Science Center, 2012). This longevity has provided a data library with more than 3.3 million images as of February, 2012 (United States Geological Survey, 2012). This very large image library that spans more than 40 years allows for temporal analysis of earth's features, like glaciers. The large image swath width of 185 km reduces the number of images needed for most projects applied to glaciers studies (United States Geological Survey, 2012). While a large image swath is an advantage in most situations, the course multispectral pixel spatial resolution of 80m for Landsat 1 and 30m for Landsats 5 and 7 do not provide the resolution needed for analyzing small features, like parking lot congestion

(United States Geological Survey, 2012). However, the spatial resolution is sufficient for analyzing features that cover large areas, like agriculture, forestry, or glaciers.

Landsat multiple spectral bands (four for Landsat 1 and seven for Landsats 5 & 7) allow a better differentiation of features or phenomena. Ice and snow are often visually identical in the visible region of the electromagnetic (EM) spectrum; however, they are sharply contrasting in the shortwave-infrared regions making it possible to differentiate the many transitional areas that are difficult to distinguish as either glacial ice or surrounding snow (Baolin et al., 2004; Noderer, 2007). Baolin et al. (2004) suggest that the most appropriate method is to perform either a supervised classification or a semi unsupervised classification on every image scene to ensure that the results are accurate (Baolin et al. 2004).

In a recent study by Haq et al. (2012) determined that false-color SWIR composite (RGB: 4, 5, 7) provided the most visual interpretability. This band combination accentuates differences between snow and ice so that the extent of both features can be determined. When this image composite is viewed, ice is a dark red color and snow is a very discernibly lighter shade of red. Figure 1 illustrates the visual difference between areas of snow and ice when viewed in a shortwave-infrared composite. Haq et al. (2012) also points out that the uneven terrain of glaciers necessitates topographically correcting imagery radiance values. Shadowing effects caused by terrain can negatively affect the brightness values of pixels so that material identification is difficult. As a result, a normalized difference snow index function was used to identify image pixels comprised of ice (Haq et al., 2012).

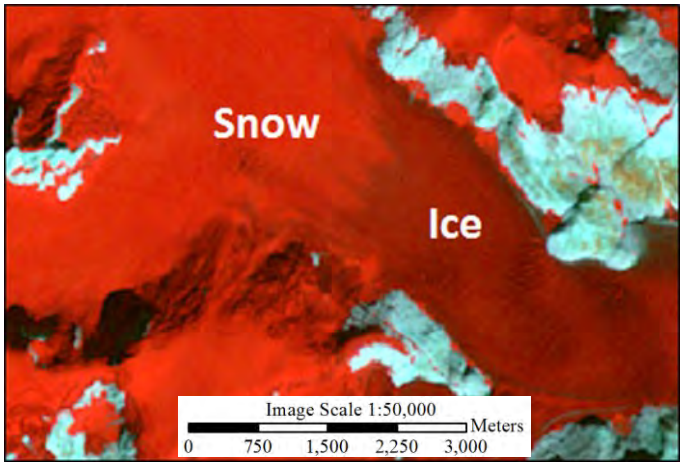

Figure 1. Snow and ice discrimination with Landsat shortwave-infrared composite image (RGB: 4, 5, 7) graphic. In this false-color composite, snow is bright red and ice is dark red. The line between snow and ice is visually discernable. Image source: Haq et al., 2012.

In a study by Baolin et al. (2004) glaciers position information is assessed by detecting glacial marginal fluctuations using multi-temporal images. Digital image classification and change detection yield root mean square errors (RMSE) of less than a pixel, which is sufficient to produce measureable results. The results were checked with ground-truth data that is generated by a visual inspection of the imagery and not by ground-based surveys (Baolin et al. 2004). The advantage to creating in-scene ground-truth data is that it can be done in a controlled environment although it often requires significant experience in image interpretation techniques. In a recent study by Haq et al. (2012) Landsat multispectral imagery from the early 1970s to 2010 is used to compare the size, shape, and location of the Gangotri Glacier. This type of analysis reveals with a reasonable degree of accuracy how a feature changes over time. It should be pointed out that Haq et al. (2012) did not use imagery with a particular anniversary date, which can create problems when trying to compare results and determine the true movement of a glacier.

The GLS data has been used for numerous studies that rely on temporal change detection to monitor earth processes and human development activities. Lindquiest et al. (2008) uses GLS2000 and GLS2005 data to monitor tropical forest cover change in the Democratic Republic of the Congo. Likewise, Beuchle et al. (2011) relies on GLS1990 and GLS2000 to access the deforestation of tropical forests. Gutman et al. (2008) predicts that GLS2005 data will be critical in analyzing trends in:

- forest cover change to include deforestation and replanting efforts;
- agriculture expansion in arid regions that rely heavily on irrigation techniques;
- lingering flooding of low-lying areas and the negative impact these areas have on human health;
- arctic terrain changes as areas with permafrost begin warming and transforming;
- increased human-footprint as evidenced by expanding urban areas and urbanization of traditionally nonurban areas.

While GLS data has been used in numerous independent studies, it is also used as foundational data for several national programs administered by the United States Government. The US Climate Change Science Program has an executive mandate to provide a systematic measurement of changes in global land cover (Justice, 2013). Wolfe et al. (2004) relies on GLS1975, GLS1990, and GLS2000 data as a primary input for the Landsat Ecosystem Disturbance Adaptive Processing System (LEDAPS). LEDAPS has the critical task of mapping change detection for North American forests so that accurate carbon modeling can be developed. Masek (2011) identifies LEDAPS as a cornerstone of the National Aeronautics and Space Administration's contribution to the North American Carbon Program (NACP) and an invaluable

tool for the United States Global Change Research Program (USGCRP) Carbon Cycle Science Program. Although GLS heavily relies upon Landsat imagery, this reliance may shift to alternative imagery sources. Gutman et al. (2008) concluded that with Landsats 5 and 7 reaching the end of their useful life due to onboard fuel cell depletion, future GLS datasets will require international cooperation to produce. This will shift the focus away from a US centric data collection strategy to a worldwide responsibility to continue to monitor the changing world so that human use of natural resources can be planned with sustainability as a cornerstone of any development plan.

Another crucial initiative is The Global Land Ice Measurements from Space (GLIMS) project, which is currently creating a unique glacier inventory storing critical information about the extent and rates of change of the world's estimated 160,000 glaciers. GLIMS is an international collaborative project, that includes more than sixty institutions world-wide, to create a globally comprehensive inventory of land ice including: measurements of glacier area, geometry, surface velocity, and snow line elevation, retreat, wasting, and thinning (Raup et al. 2007). To perform these analyses, the GLIMS project uses satellite data, primarily from the Advanced Spaceborne Thermal Emission and Reflection Radiometer (ASTER) and the Landsat Enhanced Thematic Mapper Plus (ETM+) as well as historical information derived from maps and aerial photographs. Due to the very large number of glaciers worldwide, no single analysis center or group is responsible for all glaciers; rather, a series of regional centers are responsible for their region of the world (Raup et al. 2007).

Several studies have been conducted as a way to test the GLIMS database. Haritashya et al. (2009) evaluated several imagery sources, including Landsat, to perform a study over a

twenty-seven year period for the Wakhan Corridor of Afghanistan which concluded that many glaciers in the region have retreated from historic positions. Bishop et al. (2004) acknowledge that assessing glacier mass-balance with space-borne remote sensing is very challenging and the work associated with GLIMS greatly assists in developing new methods for studying glaciers and the complex relationship between glaciers and their environments. GLIMS-based research is critical to developing new methods for mapping glaciers from spatial data where glacier features might be obscured. This research is critical since it is very difficult to develop and maintain a world glacier inventory if glaciers have to be manually differentiated from their surroundings (Bishop et al., 2004). Arendt et al. (2012) describe the Randolph Glacier Inventory (RGI) as a global catalogue of glaciers that is intended to supplement the GLIMS database. The RGI used satellite imagery and other data to catalogue worldwide glaciers (Arendt et al., 2012). Arendt et al. (2012) continues to say that GLIMS data provided valuable information for glaciers in several regions of the world. In addition to GLIMS, data was ingested into RGI from the World Glacier Inventory (WGI) (Arendt et al., 2012). As of 2012; the WGI contains entries for more than 130,000 glaciers worldwide (National Snow and Ice Data Center, 2013). As of 2007, the GLIMS database contained more than 52,000 glaciers (GLIMS: Global Land Ice Measurements from Space, 2007). These values are significant considering that there is an estimated 70,000 to 200,000 glaciers worldwide (Aher et al. 2012).

The GLIMS is not a wholly original effort as it takes the World Glacier Inventory (WGI) model and expands the parameters from a single point, which represents a glacier, to an outline shapefile that accurately describes the face of a glacier (Raup et al., 2007). Raup et al. (2007) continues to describe the GLIMS as a complimentary system that allows forward and backwards

compatibility with WGI. This is an important lesson that geospatial database designers should be cognizant of in an era of declining resources and increasing expectations; leverage the work of others as often as possible. GLIMS provide online tools that allow researchers to access, download, and analyze glacier data and imagery for free. This level of transparency is critical to the longevity of GLIMS as it allows anyone to access the data and encourages diverse users to submit data to increase the coverage of GLIMS. Raup et al. (2007) describes the GLIMS as a capable toolset for recording, measuring, and assessing glaciers.

The GLIMS is more than a data repository as it contains also online tools, such as standard indices, supervised classification, and geomorphology-based methods, which allow researchers with internet access to analyze remotely sensed imagery to access glacier health (Raup et al. 2007). The online tools allow analysts to digitize the extent of a glacier after they perform image enhancement or feature extraction processes (Raup et al. 2007); results can be submitted to GLIMS for inclusion in the database. This approach allows the GLIMS to leverage the talents of potentially millions of analysts for free. This is similar to the approach that the Search for Extraterrestrial Intelligence (SETI) program uses where it allows nonscientists to process radio telescope data with their personal computers and submit results back to the SETI program administrators (Space Sciences Laboratory, 2013).

Although many people contribute to GLIMS, the task of continuously updating GLIMS is daunting. Current estimates of 70,000 to 200,000 glaciers worldwide necessitate automated or automatic methods for monitoring their health (Aher et al. 2012). Considering the exponential increase in computer processing power, software functionality, and decades of multispectral imagery, scientists should have the tools and techniques necessary to monitor every glacier

(National Aeronautics and Space Administration, 2012). However, the reality is that many of the automated tools are problematic and require much effort to ensure that the results are accurate and reliable.

It is useful to mention that Quincey and Luckman (2009) evaluated the utility of multiple types of alternative remote sensing data: synthetic aperture radar (SAR) interferometry, feature tracking, scatterometry, altimetry, and gravimetry. Traditionally, researchers have been limited to optical sensors to collect remote sensing data for studying ice sheets and glaciers. However, advances in radar altimetry, gravimetric, and microwave technologies allow researchers to analyze glacial movement, melting, swelling, and contracting (Quincy et al. 2009). This approach may provide a three-dimensional profile of a glacier to better understand if a particular glacier is shrinking or enlarging. This multitude of new data sources will continue to improve the understanding of glacial processes.

1.3 Research question and objectives

The ability to characterize the movement rates of Baird, Patterson, LeConte, and Shakes Glaciers using low resolution and cost effective remote sensing imaging data was the main research question in this study. In addition comparative analysis of the movements rates of the glaciers with respect to specific physical and environmental conditions were conducted. The investigation used GLS false color composite images enhancing ice-snow differentiation and Iterative Self-Organizing (ISO) Data Cluster Unsupervised Classification to achieve three measureable objectives:

1) movement of Baird, Patterson, LeConte, and Shakes Glaciers,
2) movement rates for glaciers that have similar terminal terrain conditions,

3) movement rates for glaciers with dissimilar terminal terrain conditions.

These measurements were compared against the GLIMS database to assess the relative glacier movements and their behavior with respect to specific glacier physical and environmental conditions.

CHAPTER TWO: STUDY AREA

2.1 Study area physical and environmental description

The project study area is located in the Southeastern region of Alaska and within the Alexander Archipelago. The Alexander Archipelago extends west of the British Columbia provincial border line and constitutes most of the land area of the Tongass National Forest (Figure 2); hereafter referred to as simply the Tongass. The Tongass is an expansive temperate rain forest with sparse human habitation. The closest town to the study area is Petersburg, Alaska; which is located several kilometers west of the study area. The two closest urban areas are Anchorage, Alaska (1,100km to the north) and Seattle, Washington (1,250km to the south). Within the study area is Baird, Patterson, LeConte, and Shakes Glaciers.

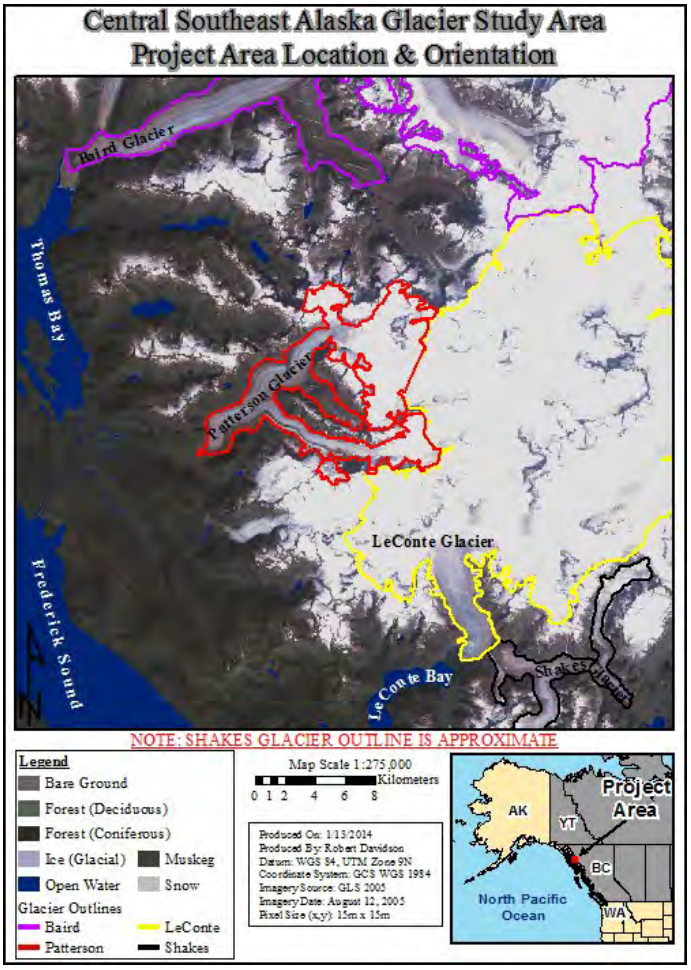

Figure 2. Central Southeast Alaska Glacier Study Project area orientation graphic. The approximate geographic center of the study area is at 57.232°N and 132.503°W. The approximate distance between the terminuses of the northernmost (Baird) and southernmost glaciers (Shakes) is 51km. Baird Glacier discharge into Thomas Bay. Patterson Glacier also discharges into Thomas Bay via the Patterson River. LeConte Glacier, the only tidewater glacier in the study, discharges into LeConte Bay. Shakes Glacier, via Shakes Slough and the Stikine River, discharges into Frederick Sound. The community of Petersburg, located on Mitkof Island, is nearby.

Approximately 25 km northeast of Petersburg, Alaska is Thomas Bay. At the head of Thomas Bay are Baird and Patterson Glaciers. Both Baird and Patterson Glaciers discharges melt water into Thomas Bay; Baird Glacier discharges directly and Patterson Glacier discharges via the Patterson River. Approximately 30km east of Petersburg, Alaska is LeConte Bay. LeConte Bay is headed by LeConte Glacier. Near LeConte Glacier is Shakes Glacier, which discharges

into the marine environment via a connected slough and river. On many occasions, I have been to LeConte Glacier, either by boat or helicopter. I have also been to Shakes Glacier by boat several times. Because of my many visits, I am intimately familiar with the area and this familiarization will be very beneficial for image classification processes.

Tongass

The Tongass extends from 54.5°N to 60.0°N; about 800km. It has an area of approximately 68,790km^2, which makes it the largest national forest in the United States and the largest intact temperate rainforest in the world (Cape Decision Lighthouse Society, 2013; United States Department of Agriculture, Forest Service, 2013). The Tongass has diverse topology, vegetation, and seasonal climate variations and according to the 2010 Census, is home to approximately 71,664 people (State of Alaska Department of Labor and Workforce Development, 2013). The highest point in the Tongass is Kates Needle, a peak on the United States and Canada border with an elevation of over 3,000m (Schweiker & Olson, 2012). The lowest elevation is sea level. Slopes range from zero slope (flat) to no slope (vertical cliff). Vegetation also ranges from the very large, like Sitka spruce, to the very small, like mosses and lichen. A very diverse range of species inhabit the lands and waters; moose, deer, humpback whales, salmon, ducks, geese, and bald eagles are numerous.

The five largest communities, which have population concentrations of over 2,000 people, are Juneau, Sitka, Ketchikan, Petersburg, and Wrangell; the combined population in 2010 was 53,523 people which represent approximately 75% of the total population of the Tongass (United States Census Bureau, 2013). Those same communities have an estimated combined area of 113km^2 as measured on IKONOS imagery, which is 0.2% of the entire area of

the Tongass (Statewide Digital Mapping Initiative, 2012; United States Department of Agriculture, Forest Service Geospatial Service and Technology Center, 2013). As a comparison, the combined land area of Massachusetts, Vermont, and New Hampshire is approximate to the size of the Tongass, but the 2010 census population of these three states is 8,489,400 people, or 12,792% of the population in the Tongass (United States Census Bureau, 2013; Environmental Systems Research Institute, 2013). The study area varies greatly in 1) topology, 2) land cover, and 3) climate. Topology, land cover, and climate data (Chapter 3-Data, and 4-Methodology) were used to characterize the study area and were assessed quantitatively and qualitatively (Chapter 5-Results) to determine their impact on glacier movement within the study area.

Survey history of Baird, Patterson, LeConte, and Shakes Glaciers

Baird, Patterson, LeConte, and Shakes Glaciers are the subject of many geophysical studies, surveys, and imagery collection events (Molnia, 2008). Many of the early surveys date back to the 1800s; which corresponds with the necessity to map and survey the Alaska territory after it had been purchased from Russia in 1867 (Billington, 2013). Molnia (2008) chronicles the earliest survey or imaging of these glaciers as follows:

- Baird Glacier: United States Coast and Geodetic Survey, 1887
- Patterson Glacier: United States Coast and Geodetic Survey, 1879
- LeConte Glacier: United States Coast and Geodetic Survey, 1887
- Shakes Glacier: Aerial Survey of Alaska, 1948

In the time since these glaciers were first surveyed or imaged, they have continued to be studied with increasingly sophisticated instruments and/or collection methods (Molnia, 2008):

- land-based and manual bathymetric surveys
- aircraft and panchromatic film cameras
- satellite-based imagery
- airborne light detection and ranging (LiDAR) surveys
- global positioning system (GPS) surveys
- remotely operated underwater vehicles

As the technology progressed, it was applied to glacier surveys. It is logical to conclude that as gravimetric, thermal, or hyperspectral imaging becomes more prevalent and available, it will be applied to studying glaciers; especially Baird, Patterson, LeConte, Shakes and the other 100,000 estimated glaciers that are located in Alaska (Molnia, 2008).

CHAPTER THREE: DATA

Data used for the physical characterization of the study was publicly available and mainly consisted of raster data and ancillary GIS datasets. The analysis of the glaciers terminus was conducted with publicly available raster data from the Global Land Survey (GLS) and Global Land Ice Measurement from Space (GLIMS) repository data sources.

3.1 Study area characterization data

Topology

Advanced Spaceborne Thermal Emission and Reflection Radiometer (http://asterweb.jpl.nasa.gov/) Global Digital Elevation Model Version 2 (http://asterweb.jpl.nasa.gov/) slope values for the study area were calculated (United States Geological Survey, 2013). The study area is on the border between two ASTER scenes (Table 3) as shown in Figure 3.

Table 3. Advanced Spaceborne Thermal Emission and Reflection Radiometer (ASTER) 30m digital elevation model (DEM) scenes which were used for this project. The project required two separate scenes (ASTGTM2_N56W133 and ASTGTM2_N57W133) to cover it entirely.

Sensor	Raster Scenes Numbers	Source	Image Collection Date	Data Type	Project Use
Advanced Spaceborne Thermal Emission and Reflection Radiometer 30m Digital elevation model	ASTGTM2_N56W133 ASTGTM2_N57W133	Alaska Statewide Digital Mapping Initiative	January 2000	Elevation data	Project study area slope graphic

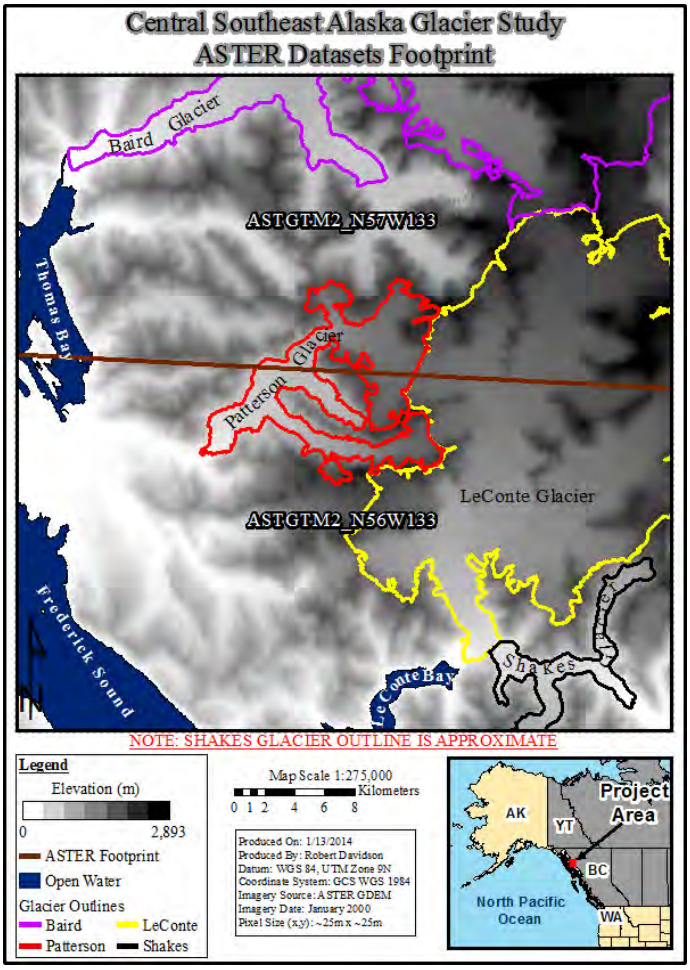

Figure 3. Central Southeast Alaska Glacier Study Project Advanced Spaceborne Thermal Emission and Reflection Radiometer (ASTER) 30m digital elevation model (DEM). The thick-brown diagonal line illustrates the border between ASTER scenes: ASTGTM2_N56W133 and ASTGTH2_N57W133. In this graphic, elevation is shown as gray-scale; the lowest elevation is 0m and the highest elevation is 2,893m. The total area encompassed for this graphic was 1,917.7km^2.

Land cover

The land cover classification for the study area was derived from the National Land Cover Dataset, 2001 (United States Geological Survey, 2013). National Land Cover Data 2001 (NCLD 2001) data was derived from Landsat imagery and therefore retains the source data's 30m spatial resolution (Table 4). In Figure 4 is shown the original NLCD coverage before a reclassification process was applied for the characterization of the study area.

Table 4. National Land Cover Data 2001 (NLCD 2001) scene that was used for this project.

Dataset	Type	Source	Date	Features	Use
National Land Cover Data 2001	Raster	United States Geological Survey	March 2008	Land cover	Project study area land cover classification graphic

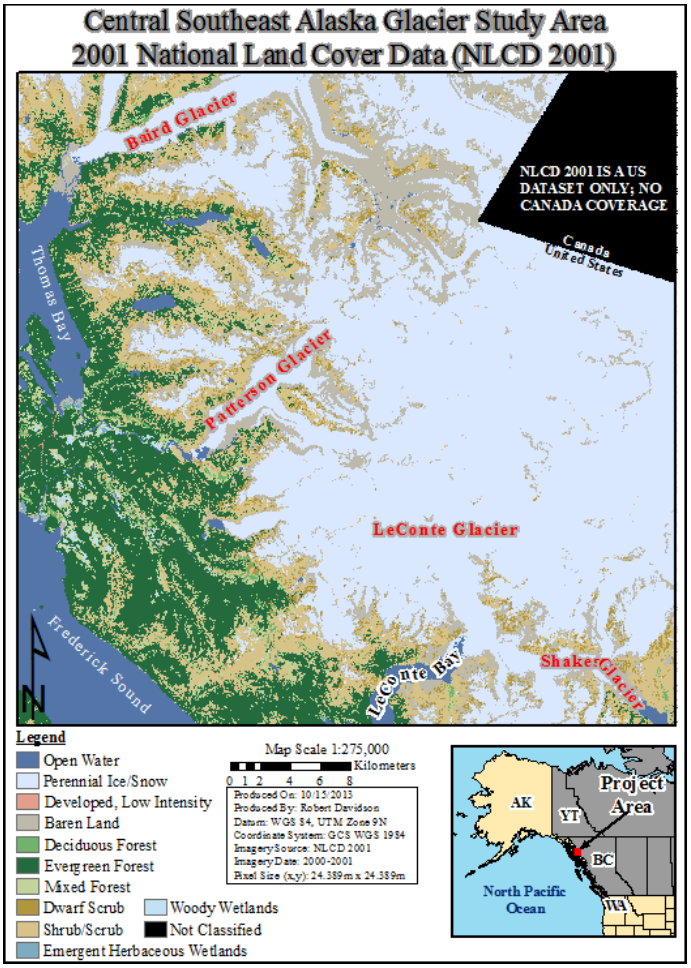

Figure 4. Central Southeast Alaska Glacier Study Project National Land Cover Data (NLCD 2001) graphic. The study area was classified into 12 distinct categories. The "Not Classified" area is located in Canada. Because NLCD 2001 is a US only dataset, areas located in Canada are not classified. The total area encompassed for this classification is 1,916.4km^2.

Climate and weather

Traditionally, climatologists classify Alaska into several distinct climate zones: arctic, continental, and maritime; which is shown in Figure 5 (Alaska Climate Research Center, 2010). In this classification, the Tongass and this project's study area were located in a maritime climate zone. The Western Regional Climate Center (2013) also characterizes the climate of the Tongass as maritime in nature with annual precipitation amounts of up to 508cm and average temperature from the -6.6s to the 15.5s (°C) depending upon season. The Alaska History and Cultural Studies (2013), as shown in Figure 6, further distinguish the climate of the Tongass as Eastern Maritime. In a climate division study of Alaska, Bieniek, Bhatt, Thoman, Angeloff, Partain, Papineau, Fritsch, Holloway, Walsh, Daly, Shulski, Hufford, Hill, Calos, and Gens (2012) consider localized temperature and precipitation amounts to further subdivide the major climate zones of Alaska into smaller, more homogenized regions. Bienieket al. (2012), as shown in Figure 7, concludes that the Tongass can be subdivided into four smaller climate zones: North Panhandle, Northeast Gulf, Central Panhandle, and South Panhandle. In this climate classification, the project study area was located within the proposed Central Panhandle climate region.

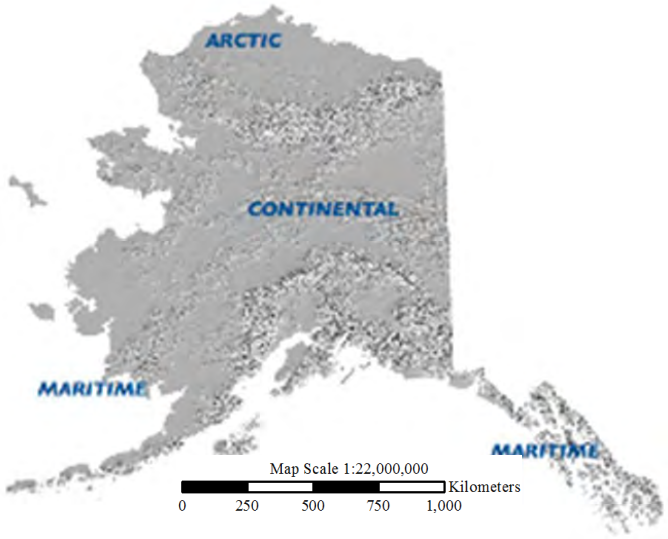

Figure 5. Alaska climate zones (traditional) graphic. The project study area is located in a "Maritime" climate zone (lower right corner of the image). Image source: Alaska Climate Research Center (2010).

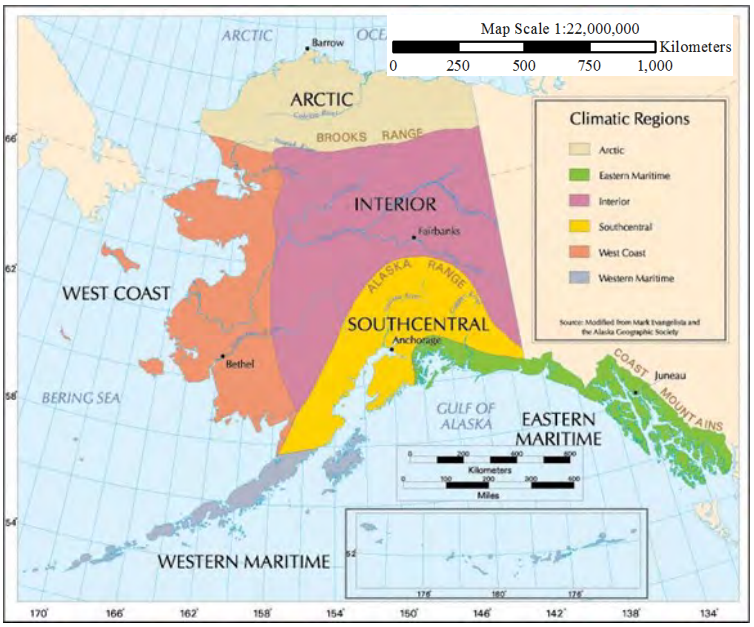

Figure 6. Alaska climate zones (revised) graphic. The project study area's climate zone is further defined as "Eastern Maritime". Image source: Alaska History and Cultural Studies (2013).

Although climate variables were not extensively considered for the analysis of glacier movements in this study, the National Oceanographic and Atmospheric Administration (NOAA) temperature data collected at the Petersburg, Alaska meteorological station from January 1, 1973

to December 31, 2009 was used to derive a general climate trend. Petersburg, Alaska is the closest meteorological data collection point to the study area. It is understood that atmospheric conditions in Petersburg, Alaska, are only close approximations for the conditions near Baird, Patterson, LeConte, and Shakes Glaciers. A summary of the characteristics of the NOAA meteorological data is provided in Table 5.

Table 5. Summary of the characteristics of the data collected at the Petersburg 1 meteorological data collection point.

NOAA Meteorological Station ID	Data Source	Data Type	Data Collection Period Start Date	Data Collection Period End Date	Observation Frequency	Number of Possible Observations *	Number of Actual Observations *
Petersburg 1	NOAA	Text	January 1, 1973	December 31, 2009	Monthly Average	444	360

* Due to the lack of available data for many of the observation collection events, especially 1978-1980 and 1996-2000, the number of possible observations is different than the number of actual observations.

The prevalent weather conditions of a maritime climate zone is rain; often hundreds of centimeters annually. Rain, and the clouds that produce rain, often obscure the surface of the earth from remote sensing satellites and aircraft. This can create a serious problem in acquiring useable data at a specific point in time. For this project, thousands of images were reviewed to select the final images that were used to complete this project.

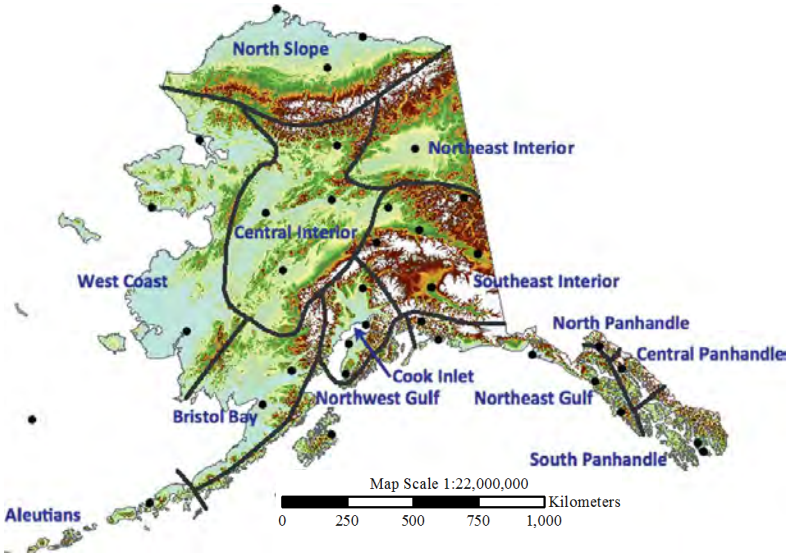

Figure 7. Alaska climate zones (expanded) graphic. The project study area's climate is further refined as "Central Panhandle". Image source: Bienieket al. (2012).

Ancillary data

These data encompass GIS data layers (Table 6) used as spatial context for the study area.

Table 6. Ancillary geospatial data that is used to create the various map graphics used in this document.

Dataset	Type	Source	Date	Features	Use
Alaska coastline	Vector	Alaska State Geo-Spatial Data Clearinghouse	February 1998	Coastal shoreline	Project study area graphics
Alaska hydrography	Vector	Alaska State Geo-Spatial Data Clearinghouse	January 2007	Linear hydrography features	Project study area graphics

3.2 Global Land Survey (GLS) data

Global Land Survey (GLS) data is a partnership between the United States Geological Survey (USGS) and the National Aeronautics and Space Administration (NASA) to create a global imagery mosaic for regular anniversary dates: 1975, 1990, 2000, 2005, and 2010 (Earth Resources Observation and Science Center, 2012). The data is collected using the latest available Landsat sensor for each collection period and provides the necessary imagery for accomplishing

this study objectives. Table 7 identifies which sensor was used to collect imagery for each dataset and the range of image collection dates that each dataset encompasses. For this study the GLS1975, GLS1990, GLS2000, GLS2005, and GLS2010 datasets containing all the imaging bands were downloaded from the United States Geological Survey Earth Explorer (2013) portal. All datasets were preprocessed at the data source to Level 1 standards. A Level 1 product corrects for either sensor detector variations, image geometry, or both (Piwowar, 2001). The GLS data acquisition is covered step-by-step in Appendix A.

For this study the panchromatic band was not used, making the images obtained by Landsat TM and ETM+ interchangeable. Table 7 summarizes the collection dates and collection sensor for each GLS dataset.

Table 7. Global Land Survey (GLS) sensor and imagery collection dates summary for Central Southeast Alaska Glacier Study Project area. Imagery from Landsats 1, 5, and 7 are used in this study.

Dataset	Sensor	Collection Dates
GLS1975	Landsat 1-5	1972-1987
GLS1990	Landsat 4*-5	1987-1997
GLS2000	Landsat 7 ETM+	1999-2003
GLS2005	Landsat 5 TM, Landsat 7 ETM+, EO-1 Ali	2003-2008
GLS2010	Landsat 5 TM, Landsat 7 ETM+	2008-2011

* Landsat 4 was not used in this work

Landsat imagery is collected in a grid pattern and each image scene has a unique row and path identification number that is referred to as the Worldwide Reference System (WRS) (Irons, 2013). Because Landsats 1-3 are flown at a different altitude than Landsats 4-7, there is a difference in the WRS identification number. The WRS for Landsats 1-3 is referred to as WRS-1 and the WRS for Landsats 4-7 is referred to as WRS-2 (United States Geological Survey, 2013). Table 8 summarizes the WRS identification numbers for the GLS data used for this study.

Table 8. World Reference System (WRS) image scene identification for central southeast Alaska glacier study area imagery.

GLS Dataset	Imagery Source Date	Landsat Satellite	WRS Version	Path ID	Row ID
GLS1975	September 3, 1974	Landsat 1	WRS-1	60	20
GLS1990	September 9, 1989	Landsat 5	WRS-2	56	20
GLS2000	August 12, 1999	Landsat 7	WRS-2	56	20
GLS2005	August 12, 2005	Landsat 7	WRS-2	56	20
GLS2010	July 30, 2009	Landsat 5	WRS-2	56	20

There are three primary reasons why GLS data was essential to this study:

1) multispectral capability;
2) temporal correlation;
3) consistent and predictable data quality.

Multispectral capability

The Landsats 5 & 7 multispectral range in the near-infrared (NIR) and shortwave-infrared (SWIR) provides the best spectral differentiation and interpretability of ice and snow; in particular, the use of SWIR (RGB: 4, 5, 7) false-color composite has proven to be very effective in differentiating ice and snow (Haq et al., 2012). Figure 8 provides a graphical illustration of the stark difference between snow and ice when this particular image composite is used. Unfortunately, this composite could not be created for the GLS1975 data. GLS1975 dataset is collected using Landsat 1 MSS sensors which only collected imagery in the visible green, visible red, and near infrared regions of the EM spectrum (refer to Table 1).

LeConte Glacier

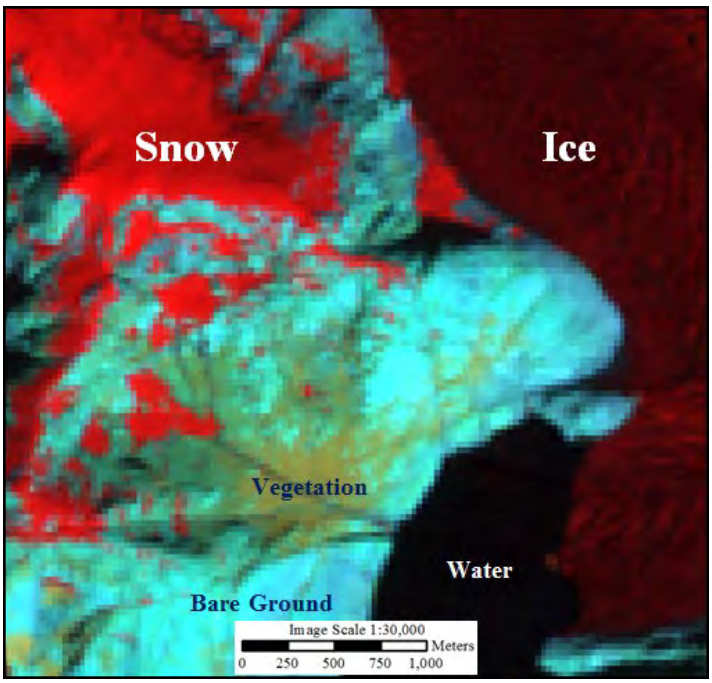

Figure 8. LeConte Glacier in GLS2010; RGB: 4, 5, 7. In this image, snow is bright red and ice is dark red; water is black; bare ground is cyan; and vegetation is shades of green. This band combination clearly distinguishes between ice and snow.

Temporal correlation

The Landsat program began in the 1970s. Although each consecutive sensor includes new capabilities, legacy capabilities are also retained. This means that while Landsat 7 ETM+ sensor has an improved panchromatic band (15m spatial resolution), the visible, near-infrared, and shortwave-infrared bands retain the same collection parameters (spectral sensitivities and ranges) as several previous Landsat sensors, like Landsat 5 TM. In addition to retaining the same collection parameters, collection areas (both size and location) are mostly identical. This sensor generational redundancy has resulted in a very large image library that can be used interchangeably. Using this multi-decadal image library, allows for cost-effective change detection of natural and man-made features; such as glaciers, deforestation, and urban sprawl.

Data quality

The atmospheric conditions in the project study area, which is located in the Tongass, are predominantly misty, rainy, and cloud covered (refer to Section 2.1). In 2009, the year that the project area was imaged for GLS2010 dataset, twenty-eight images are collected by a combination of Landsats 5 and 7. These images ranged in cloud cover percentages of 1 to 100. Statistical analysis of these cloud cover values was summarized in Table 9.

Table 9. Cloud cover descriptive statistics for Landsat images collected during 2009. During 2009 (the year that GLS 2010 data was collected), a total of 28 Landsat 5 TM and Landsat 7 ETM+ images are collected. The least amount of cloud cover present in an image is 1%, the most cloud cover is 100%. The mean cloud cover is 63.68%.

Descriptive Statistics	Value (% Cloud Cover)	Descriptive Statistics	Value (% Cloud Cover)
Mean (μ)	63.68	Standard Deviation	33.82
Median	70.00	-1 Deviation	29.86
Mode	87.00	+1 Deviation	97.50
Standard Error	6.39		

Klibanoff et al. (2005) asserts that 68.27% of all values in a population are within one standard deviation of the mean. This study required images with low cloud cover values and the analyzed population 17 (67.67% of the population) is within one standard deviation; in statistical terms, the negative outliers are the most desirable. Although the results of the statistical analysis favors Kilbanoff et al. (2005), they do not favor remote sensing; cloudy images are usually useless for most applications. Of the 28 images that were considered for 2009, there were six negative outliers (21.43% of the population) with less than 29.86% cloud cover. The unfortunate reality was that due to the infrequent cloud-free days in the Tongass, the study area was not conducive to satellite imaging.

GLS data is proving very useful for studying a variety of phenomena. More specific to this study, it has been used to previously describe the extent of Baird, Patterson, and LeConte Glaciers. In 2006, Beedle (2013) used GLS2000 data to determine the extents of Patterson and LeConte Glaciers. These extents (shapefiles) are currently included in the GLIMS database. As various processes were run during the course of this study, the shapefiles of those glaciers was used to verify results and determine validity.

3.3 Global Land Ice Measurement from Space (GLIMS) data

The Global Land Ice Measurements from Space (GLIMS) database and data access web portal is administered by the National Snow and Ice Data Center (NSIDC) in Boulder, Colorado (Raup et al. 2007). Due to the large variety of national and international projects currently managed by NSIDC, leveraging the capabilities and resources of NSIDC adds professional credibility to the GLIMS project (National Snow and Ice Data Center, 2013).

GLIMS data is stored as geographic shapefiles. The GLIMS web portal provides tools to geographically search for data. This search uses industry standard area of interest (AOI) type tools to select an area which is intersected with the GLIMS database to extract available data for download in shapefile format. The GLIMS data acquisition is covered step-by-step in Appendix B. In Figure 9 the GLIMS shapefiles for Baird Glacier, Patterson Glacier, and LeConte Glacier is shown. While Shakes Glacier is not currently in the GLIMS database, it was shown on Figure 9 in relation to the other glaciers.

One advantage of using a geographically referenced shapefile format is that it displays correctly with other georeferenced data, such as GLS data, in ArcGIS v10.2. Table 10

summarizes the GLIMS database entries for Baird Glacier, Patterson Glacier, and LeConte Glaciers.

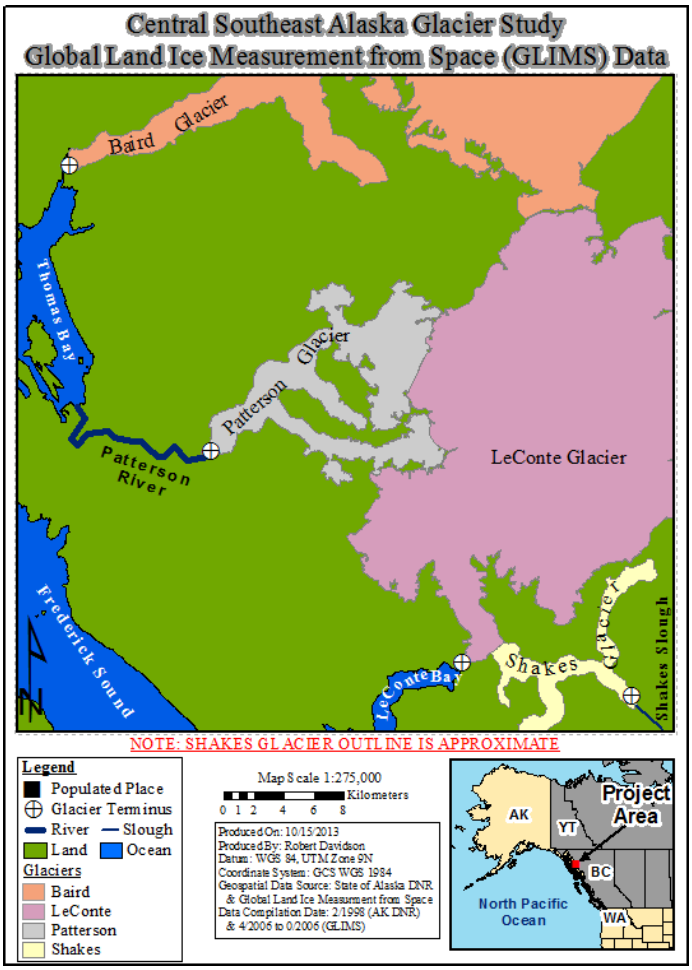

Figure 9. Central Southeast Alaska Glacier Study Project: Global Land Ice Measurements from Space data graphic. In this graphic, the extent of Baird Glacier is shown in salmon, Patterson Glacier is shown in light gray, and LeConte Glacier is shown in light pink. Shakes Glacier, shown in tan, does not currently have an entry in the GLIMS database. It is shown only to provide spatial orientation.

Table 10. Global Land Ice Measurement from Space database entries summary for Central Southeast Alaska Glacier Study Project area. Baird Glacier is the most recently analyzed glacier with imagery from 2005. Both LeConte and Patterson Glaciers were last analyzed in 1999 – almost 15 years ago.

Glacier Name	Date Last Analyzed	Source Imagery Collection Date	Source Imagery for GLS Dataset
Baird Glacier	January 1, 2007	August 13, 2005	GLS2005
LeConte Glacier	April 6, 2006	August 12, 1999	GLS2000
Patterson Glacier	April 10, 2006	August 12, 1999	GLS2000

Global Land Ice Measurements from Space (GLIMS) data was used for the imagery analysis process check as well as a metric from which to quantify glacier movement within the project study area.

CHAPTER FOUR: METHODOLOGY

Study area physical characterization: topology and land cover

Topology

Using ArcGIS version 10.2 and 1-arc second ASTER DEM mosaic a slope map was derived and thematically classified by ranges of slope percentages. From zero to 100 percent, the slope values were placed in 10 equal interval bins of 10 percent each; i.e. 0 to 10 percent was the first bin, from greater than 10 to 20 percent was in the second bin, and so forth. Slope values over 100 percent were grouped into a single bin. For reference, 100 percent slope is equivalent to 45 degrees slope. Note, by commonly accepted mathematical definition, a horizontal line has zero slope; a vertical line has no slope. The results are shown as Figure 10.

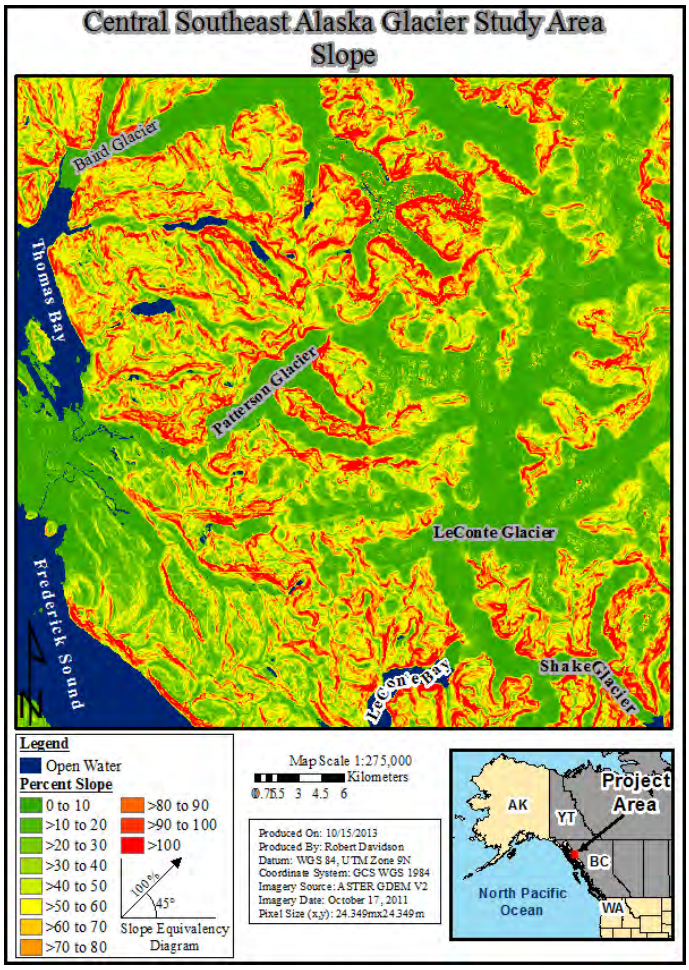

Figure 10. Central Southeast Alaska Glacier Study Project slope graphic. Slope is categorized from least to greatest; green areas have the least amount of slope and red areas have the greatest amount. The valleys surrounding the four glaciers had 100% or greater slope; the total area encompassed for this classification was 1,917.7km^2.

The examination of the slope map outlined that approximately half (47.3%) of the project study area had slope values of less than 30 percent and slopes of 10 percent or less were the most common class. Table 11 summarizes the total number of pixels and the area that they represent within the study area. It should be noted that glacier features in this study area usually had low slope values, often less than 10 percent.

Table 11. Central Southeast Alaska Glacier Study Project percent slope computation summary. Areas with 0% to 10% slope were the most common; areas >70% to 80% were the least common. Slopes values of less than 30% accounted for almost half (47.2%) of the project study area.

Class	Number of Pixels	Area of Pixels (km^2)	Percent of Total Area
0% to 10%	736,989	436.9	22.8
>10% to 20%	464,734	275.5	14.4
>20% to 30%	326,040	193.3	10.1
>30% to 40%	287,611	170.5	8.9
>40% to 50%	284,523	168.7	8.8
>50% to 60%	266,046	157.7	8.2
>60% to 70%	222,245	131.8	6.9
>70% to 80%	171,726	101.8	5.3
>80% to 90%	125,778	74.6	3.9
>90% to 100%	91,199	54.1	2.8
>100%	257,699	152.8	8.0
Total	3,234,590	1,917.7	100.0

Land Cover

Using ArcGIS 10.2, the NLCD 2001 was clipped to the study area (as shown in Figure 11). Similar feature classes were combined into a generic feature class; e.g. deciduous, evergreen, and mixed forest classes were combined into a single class: forest. In that case, image simplification improved visual interpretability. The results are shown as Figure 11. Like the slope map, feature class pixel counts, areas, and percentages of study area were determined. Based upon these calculations, several conclusions were inferred from the land cover map.

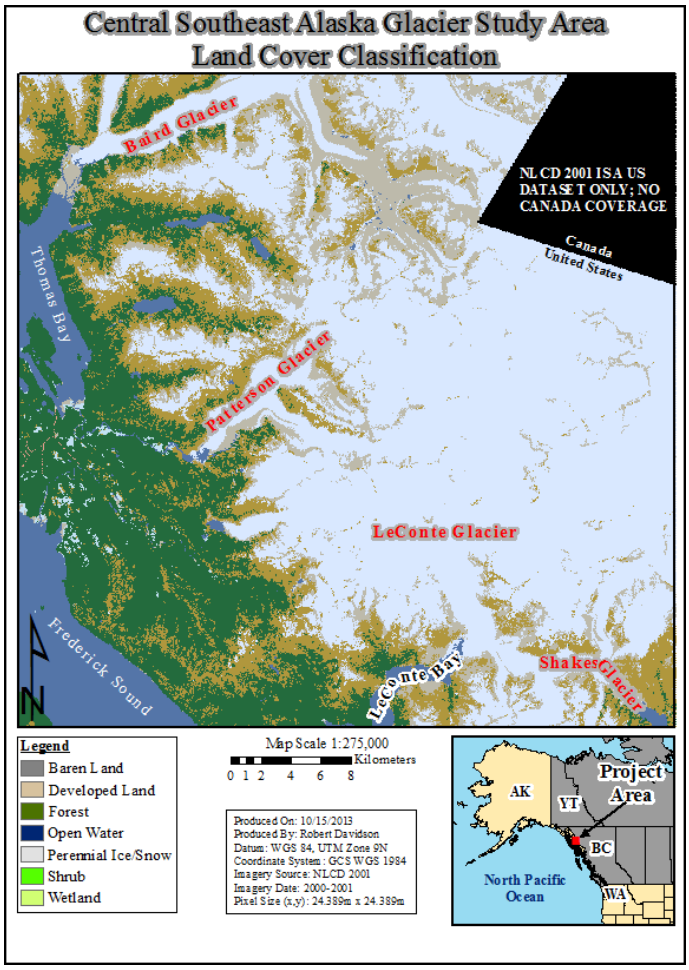

Figure 11. Central Southeast Alaska Glacier Study Project land use classification graphic. Vegetated areas dominated the western edge of the study area. The large non-vegetated area in the center and eastern edge of the study area was the Stikine Icefield. The total area encompassed for this classification is 1,916.4km^2.

Table 12 summarizes the land cover classification pixel analysis results. The most prevalent class was Perennial Ice/Snow; which covered 852.0km^2 (44.46%) of the study area. Vegetated land, a combination of forest, shrubs, and wetlands, accounted for 591.0km^2, or 30.84 percent of the study area.

Table 12. Central Southeast Alaska Glacier Study Project land use area by class computation summary. Areas with "Perennial Ice/Snow" were the most common; "Developed" areas were the least common. "Not Classified" areas are those located in Canada. Since NLCD 2001 is a US dataset, Canada is not covered. The total area encompassed for this classification is 1,916.4km^2.

Class	Number of Pixels	Area of Pixels (km^2)	Percent of Total Area
Open Water	150,301	135.3	7.06
Perennial Ice/Snow	946,661	852.0	44.46
Developed	484	0.4	0.02
Forest	366,478	329.8	17.21
Shrub	282,598	254.3	13.27
Wetlands	7,627	6.9	0.36
Barren Land	230,586	207.5	10.83
Not Classified	144,562	130.1	6.79
Total	2,129,297	1,916.4	100

Quantify the movement of Baird, Patterson, LeConte, and Shakes Glaciers

Several shortcomings were noticed in reviewing available literature. Change detection, especially the multi-decadal projects, attempted to compare imagery collected from different months. For example, imagery collected in March was compared with imagery collected in November. Change between the two images was concluded to be indicative of net glacier movement. At first glance, this approach seemed correct. However, March imagery reflected a glacier that has just come out of the coldest months of the year and has experienced its greatest potential movement. Conversely, November imagery showed a glacier that came out of the warmest months of the year and has exhibited the greatest potential for retreating by melting or

similar processes. In either situation, it was erroneous to compare glacier activity in March imagery to November imagery and draw a definitive conclusion about whether a glacier had advanced, remained the same, or retreated. The second discrepancy noticed was the creation of ground-truth data from in-scene examination. This approach did not yield valid ground-truth data. As the name implies, ground-truth means that field surveys were conducted or observations recorded. Because, it was difficult to ascertain the imagery interpretation experience (e.g. size, shape, shadow) of the analyst that produced the in scene ground-truth data, the validity of the results should be accessed.

Mitigation of the first problem was addressed by selecting imagery with similar month and day anniversary dates; for example, May 7, 2003 was compared to May 3, 2008. The Global Land Survey (GLS) datasets contained imagery with similar collection anniversary dates; e.g. all dataset imagery anniversary dates are within a month or two of each other. The potential problems of in-scene ground-truth data were addressed by using multiple classified images and false-color composite images to ensure the terminus of each glacier was accurately delineated. In addition, GLIMS data for Baird, Patterson, and LeConte Glaciers was used as a benchmark from which to measure glacier movements. Relying on multiple images with similar collection anniversary dates to delineate glacier terminus locations and using the Global Land Ice Measurement from Space (GLIMS) data as a benchmark made this glacier study project different than previous studies.

The GLS 1975, 1990, 2000, 2005, and 2010 data was used to determine the location of the terminuses of Baird, Patterson, LeConte, and Shakes Glaciers. The source imagery for these five datasets is Landsat and was collected on: September 3, 1974; September 9, 1989; August 12,

1999; August 12, 2005; and July 30, 2009 respectively. After determining the glaciers' terminus locations, these locations, with the exception of Shakes Glacier, were compared to the Global Land Ice Measurement from Space (GLIMS) database; Shakes Glacier was not listed in GLIMS. In GLIMS, Baird Glacier was last analyzed on August 13, 2005 and Patterson and LeConte Glaciers on August 12, 1999. Comparison of terminus locations in the GLS data to the GLIMS allowed for the computation of movement rates. Since Shakes Glacier was not in the GLIMS database, movement rates were calculated using only the GLS data. Completion of this objective allowed objectives two and three to be completed.

Analyze the movement rates for glaciers that have similar terminal terrain conditions

The second goal was to determine if similar terrain conditions where glacier terminuses are located induce similar glacial movement rates. During the study period (1974-2009), both Patterson Glacier and Shakes Glaciers' terminuses were located in freshwater lakes, Patterson Lake and Shakes Lake respectively. Movement rates for Patterson Glacier and Shakes Glacier were compared to determine if a significant difference in movement rates exists.

This assessment was a multi-step process. First, using Patterson and Shakes Glacier terminus locations in the various GLS datasets, which were determined for objective one, movement distances were measured between terminus locations. Second, after the movement distances were calculated for Patterson and Shakes Glaciers, the distances were compared to each other; e.g. the movement distance between the GLS2010 and GLS2005. Analysis of this data was conducted to determine if the movement rates for Patterson and Shakes Glaciers were similar.

Analyze the movement rates for glaciers with dissimilar terminal terrain conditions

The third goal was to determine if dissimilar terrain conditions of the glacier terminuses locations affected the movement rates. Baird Glacier's terminus was located on land, Patterson Glacier and Shakes Glaciers terminuses were located in fresh water lakes, and LeConte Glacier's terminus was located in LeConte Bay, which is a marine bay. While both Patterson and Shakes Glaciers had similar terminal terrain conditions, Patterson Glacier was selected for this analysis because its more conservative movement rate was closer to the movement rates of Baird and LeConte Glaciers. Shakes Glacier retreat was substantially greater than the other glaciers in this study.

This assessment process was identical to assessing the movement rates of glaciers with similar terminal terrain conditions. For this analysis, Baird Glacier's movement rate was compared to Patterson and LeConte Glaciers. Also, the movement rate for LeConte and Patterson Glaciers was compared.

Visual inspection of the GLS imagery that was used for this study reveals the difficulty in delineating the terminuses of Baird, Patterson, LeConte, and Shakes Glaciers. Because of this challenge, manual digitization from the unprocessed GLS data was problematic. Instead, unsupervised image classification methods offered the best possibility of accurately separating glacier terminuses from their surroundings (Noderer, 2010). Based on the literature review, personal experience, and a thorough exploration of the GLS data, the false-color SWIR composite image (Baolin, Zhang, and Chenghu. 2004), false-color NIR composite image, natural color composite image, Landsat NIR and SWIR image bands, and Iterative Self-Organizing (ISO) Data Cluster Unsupervised Classification (Raup et al., 2007), were used to delineate the

glacier terminuses. This process is covered in detail in Section 4.1. After assembling the various image composites, a heads-up digitization (Raup et al., 2007) of each glacier terminus was performed; the digitized terminus was recorded as a georeferenced shapefile. This process is covered in detail in Section 4.2. Figure 12 shows a schematic approach of the methodology.

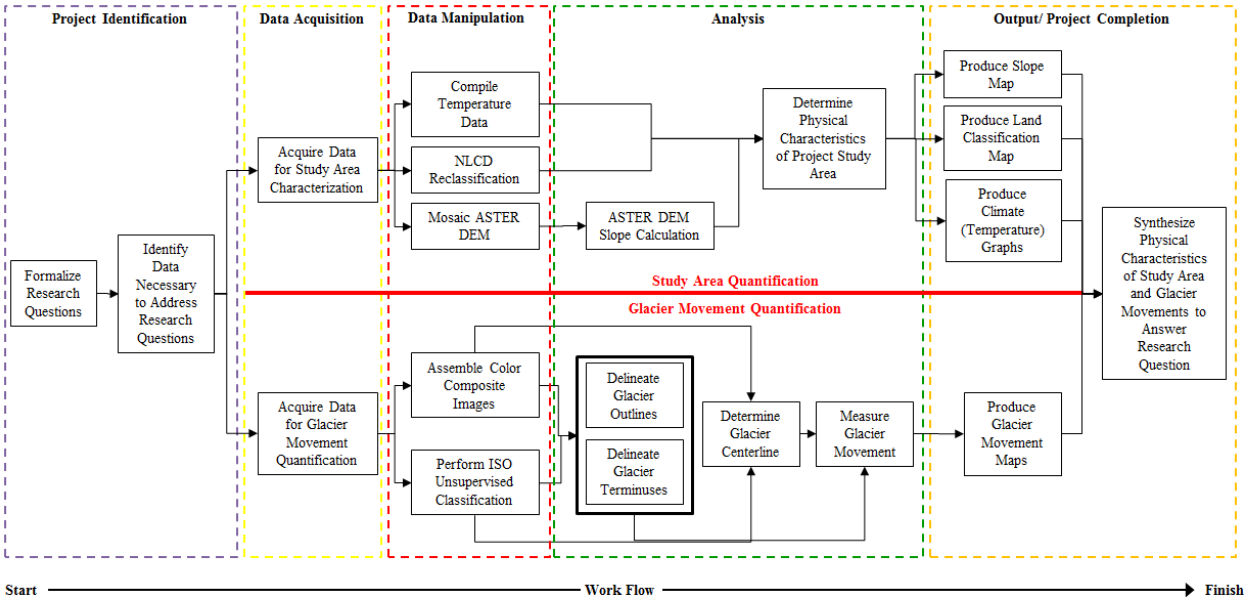

Figure 12. Glacier analysis process diagram. Reading from left to right: research questions were formalized; required data was identified, and acquired; color composites were assembled, ISO unsupervised classifications were performed, temperature data was compiled, National Land Cover Data (NLCD) reclassification was performed, and ASTER DEM data was mosaicked; glacier outlines, terminuses, and centerlines were determined, ASTER DEM slope calculations and the physical characteristics of study area were determined; slope, climate graphs, classification, and glacier movement maps were produced; and the physical characteristics of the study area and glacier movements were synthesized.

To quantify the movement of Baird, Patterson, LeConte, and Shakes Glaciers, a measurement baseline was needed. A baseline provided a geographic reference point along which all glacier movement was measured; whether a glacier move forward or backward and by how much. From Table 10 (section 3.2) note that Baird Glacier used GLS2005 data and LeConte Glacier and Patterson Glaciers both used GLS2000 data to create the most recent shapefile in

GLIMS. In this study, the original imagery GLS datasets, image composites, band images, image classifications, and GLIMS shapefiles were used. The image processing that was performed on the original GLS datasets was validated using the GLIMS shapefiles.

For each of the five GLS datasets, GLS1975, GLS1990, GLS2000, GLS2005, and GLS2010, unsupervised image classification was used to determine the terminus of Baird, Patterson, LeConte, and Shakes Glaciers. This process was often hit-or-miss and requires much refinement before adequate results were achieved. Because of this difficulty, image classification was performed using GLS2005 and GLS2000 data first. The GLIMS shapefiles for Baird, Patterson, and LeConte Glaciers were then used to check the image classification results. Results that appeared incorrect served as a basis for refining the image classification procedures. Once all image classification results were deemed satisfactory, then the glacier terminuses were delineated in each GLS dataset.

Completion of the image classification of all five GLS datasets resulted in a total of 20 shapefiles, four different glaciers at five points in time. The GLIMS shapefiles were then compared to the terminus locations of Baird, Patterson, and LeConte Glaciers in the GLS2000/2005 datasets. Based upon positional differences of each glacier's terminus in the various GLS datasets, movement rates were computed. The GLIMS dataset has been essential to this study as it was used in the validation process of the image classification results and in quantifying glacier movements over the last thirty-four years.

The Environmental Systems Research Institute (Esri) ArcGIS Desktop v10.2 software (ArcGIS, 2013) was used for all data processing and map production aspects of this study.

ArcGIS v10.2 possesses the functionality to carry on the image classification, feature extraction, feature digitization, and map production capabilities that were needed for this study.

4.1 Composite images and image processing

False-color composite image assembly

The best spectral separation of snow and ice in multispectral imagery was successfully achieved by Haq (2012) using shortwave infrared (SWIR) spectral bands, in particular a false-color composite of bands 4, 5, 7 (RGB) images. The same approach was used in this study and false-color composite of band 4, 5, 7 (RGB) images were created for GLS2010, GLS2005, GLS2000, and GLS1990 datasets. An example for Patterson Glacier in GLS2005 is shown in Figure 13.

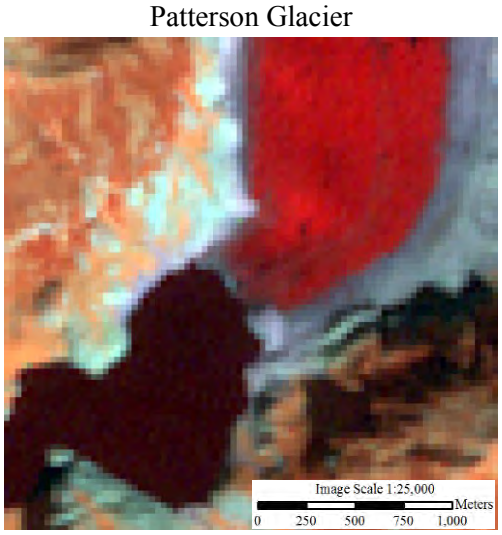

Figure 13. Landsat 7 ETM+ false-color shortwave composite image of Patterson Glacier (GLS 2005). This image is a near infrared, shortwave, shortwave composite (RGB: 4, 5, 7). In this image, ice is dark red, vegetation is shades of orange, water is black, and bare ground is shades of cyan/gray.

The GLS1975 data lacks shortwave-infrared capabilities, therefore a false-color composite of bands 7, 5, 4 (RGB) was used instead (Noderer, 2007). In this instance, Band 7 is a

near-infrared band and not a shortwave infrared band (United States Geological Survey, 2013). An example for Patterson Glacier in GLS1975 is shown in Figure 14.

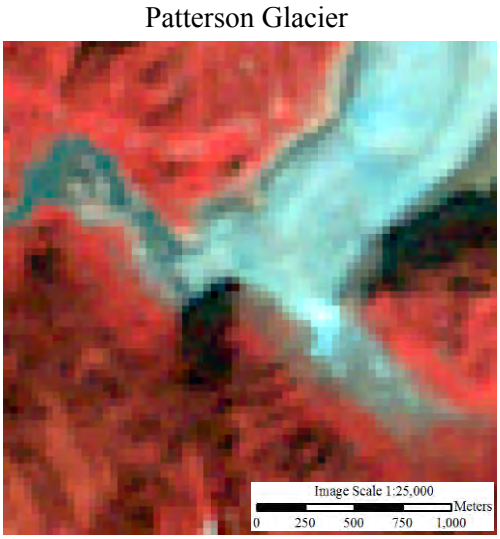

Figure 14. Landsat 1 MS false-color near infrared composite image of Patterson Glacier (GLS 1975). This image is a near infrared, visible red, visible green composite (RGB: 7, 5, 4). In this image, ice is cyan, vegetation is shades of red, water is dark blue/cyan, and bare ground is shades of gray.

The bands combination and false-color image assembly were processed in ArcGIS v10.2 using the Composite Bands tool, of the Raster Processing toolset. The tool and procedure is shown in Figure 15, which illustrates the process for the GLS2010 dataset. For the GLS2005, GLS2000, GLS1990, and GLS1975 datasets, the procedure was the same. The analysis of the false-color composite images is presented in the results section.

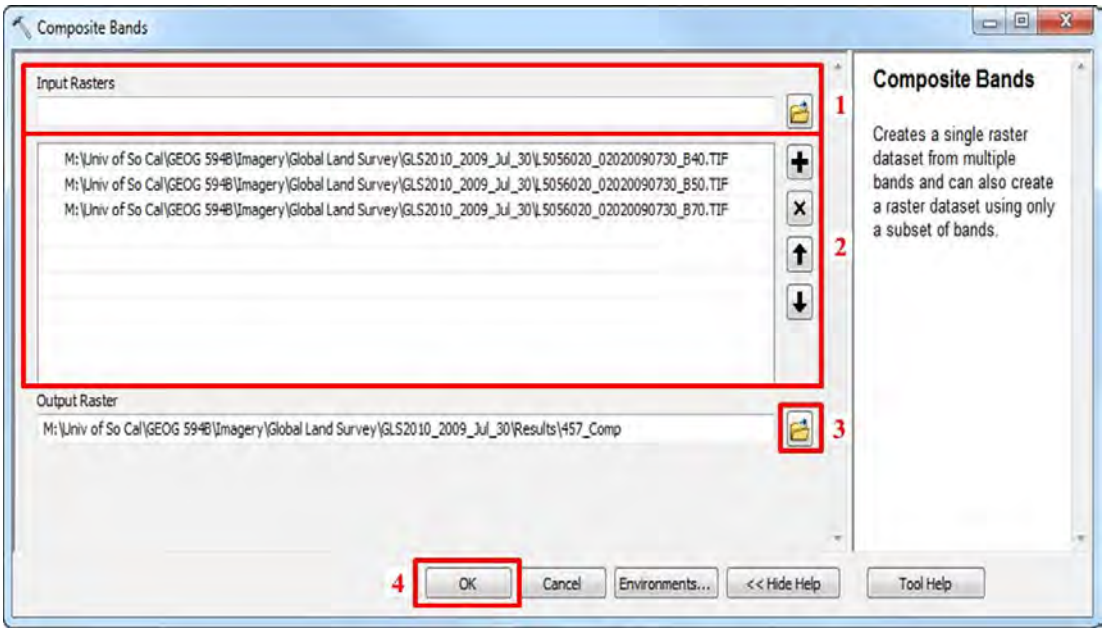

Figure 15. "Composite Bands" tool dialog window completed for GLS2010 dataset using Landsat 5 TM bands 4, 5, 7 (RGB). 1: file location of the raster images; 2: list of the selected images. It is important to note that the images were listed in the order that they will be combined to form a RGB image; 3: save output image; 4: execute the process that creates the composite band image.

Iterative Self-Organizing (ISO) Data Cluster Unsupervised Classification

An Iterative Self-Organizing (ISO) Data Cluster Unsupervised Classification is a type of unsupervised classification. It is unsupervised because the analyst does not interactively define training samples. The result of an ISO unsupervised classification is an image that is classified into classes with similar spectral properties; e.g. water, ice, etc. An additional benefit that was realized for this project was that the separation between glacier terminuses and surrounding features were better accentuated. The result of an ISO unsupervised classification is a gray scale image where each shade represents a class of pixels with similar spectral properties (Noderer, 2007). The number of resulting classes is dependent upon the variability in the input image and the number of desired output classes, which is defined a priory. This classification method is superior to the minimum distance method since it considers pixels in multidimensional data

space where more input image bands results in a more complex data space (Campbell et al., 2011). This means that as the number of input images increases, the classification results should correspondingly improve.

An ISO unsupervised classification process produces a thematically classified image. Pixels with similar brightness values are grouped together. It can be expected that since similar features are spectrally similar, they will be grouped together. However, the process simply groups pixels; it is up to an analyst to determine which features are represented by a particular grouping, e.g. water, ice, forest, etc.

The fidelity, or pureness, of each output class depends upon three factors. First, sufficient number of classes must be created; too few classes and each class will contain pixels that represent multiple classes. Likewise, too many classes introduce class redundancy. Second, more images should yield better results since each pixel is compared across *n*-dimensionality (where *n* represents the number of images). Third, the degree of image feature homogeny affects the classification results.

Each of the previously discussed three factors will have different levels of impact depending upon each image scene. Feature homogeneity, the number of input images, and the number of output classes vary considerably. For this analysis, between four and six input images were used depending upon the GLS dataset. Initial output classes were set for each dataset ranging between 20 and 40. Often, more classes produced worse results and the process had to be fine-tuned to find the optimal number of classes. Output classes were combined to produce the final output classes: ice, water, rock, sediment, and vegetation. Figure 16 shows a final classification for LeConte Glacier using GLS2010 data.

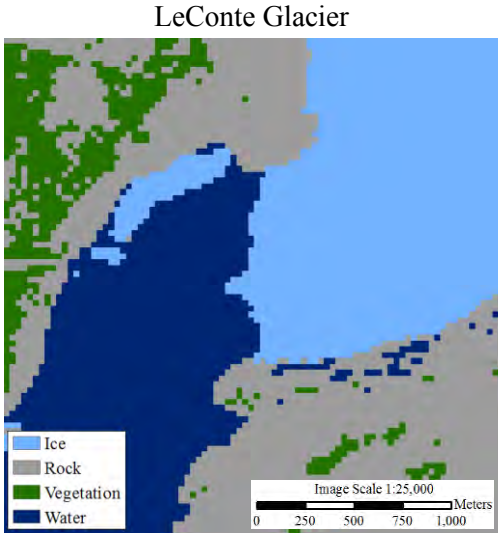

Figure 16. ISO Cluster Unsupervised Classification for LeConte Glacier (GLS2010). In this classification, ice is light blue, rock is gray, vegetation is green, and water is dark blue.

The ISO unsupervised classification process was performed in ArcGIS v10.2 using the ISO Data Cluster Unsupervised Classification tool, which is part of the Classification toolset (ArcGIS, 2012). The tool and procedure is shown in Figure 17, which illustrates the process that was used for the GLS2000 dataset. For the GLS2010, GLS2005, GLS1990, and GLS1975 datasets, the procedure was basically the same. Differences between GLS datasets and glaciers were reflected in the number of classes that were specified; which ranged between 20 and 40.

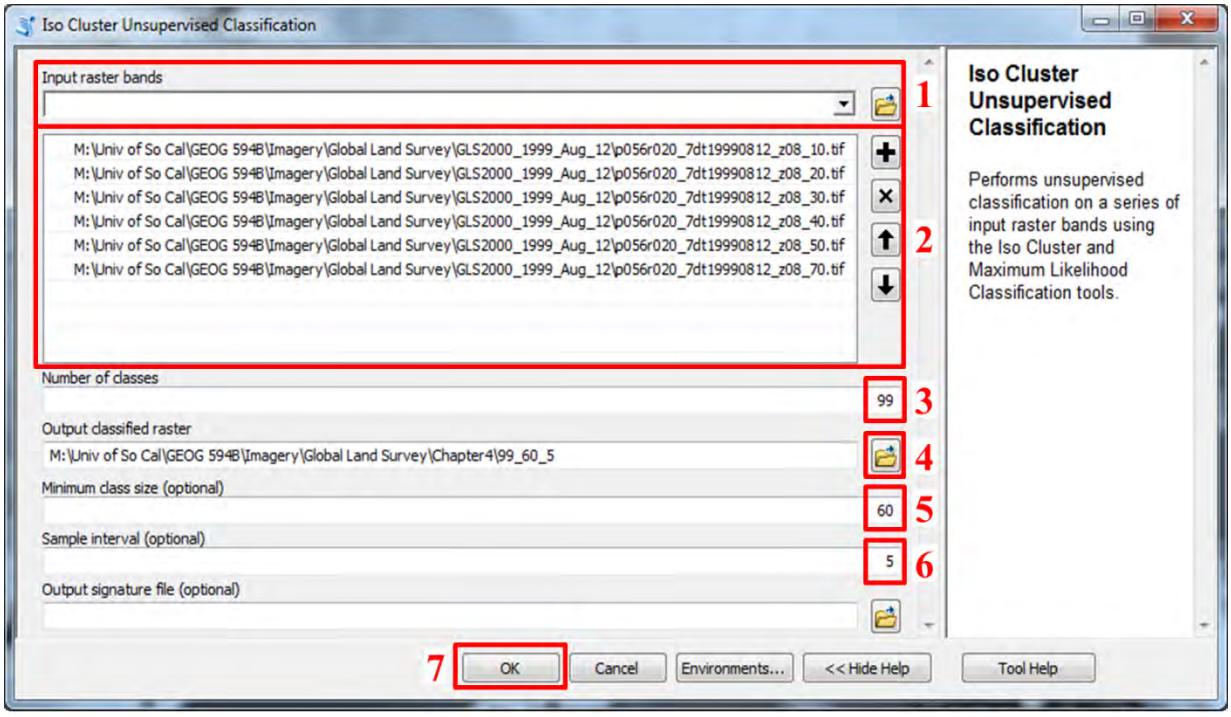

Figure 17. "ISO Data Cluster Unsupervised Classification" tool dialog window completed for GLS2000 dataset using Landsat 7 ETM+ bands 1-5 & 7. 1: file location of the raster images; 2: list of selected images; 3: number of classes for the image pixels to be placed in; 4: save output image; 5: minimum class size (number of pixels); 6: sample interval; 7: execute the process that creates and ISO Data Cluster Unsupervised Classified image.

4.2 Glacier terminus delineation

Glacier terminus location shapefile creation

The terminuses of the Baird, Patterson, LeConte, and Shakes Glaciers were delineated using the GLS dataset images (either individual images and/or image composites) and results from ISO unsupervised classifications. Visual inspection of each image clearly identified the general location of each glacier terminus. While this might have been suitable for some applications, it does not lend itself to accurate measurements. In order to determine the glacier terminuses with the available imagery, pixels were individually verified (by examining pixel brightness values) whether it was ice or something else. In the case of Baird Glacier in GLS2010, Band 4 (NIR), true color composite image, false-color SWIR composite image, and the results

from the ISO unsupervised classification were used to delineate the glacier's terminus. The resulting terminus for Baird Glacier in GLS2010 is shown in Figures 21 and 22. The images that were used for each glacier are collected in Appendix C.

The creation of a shapefile was a two-step process. First, a drawing was created that represented a glacier terminus. Pixels that were confirmed to be ice became vertices that were connected with a line feature which was subsequently stored as a geographically referenced shapefile. Second, the drawing was converted to a geographically referenced shapefile. From a software functionality standpoint, this approach was more efficient for creating many shapefiles which only contain a single feature with minimal attribution. For this study, each glacier terminus; e.g. Baird Glacier in GLS2010, was stored as a single feature shapefile and differentiation was accomplished with unique shapefile file names. ArcGIS v10.2 was used to create the shapefiles whose process is summarized in Figures 18-20.

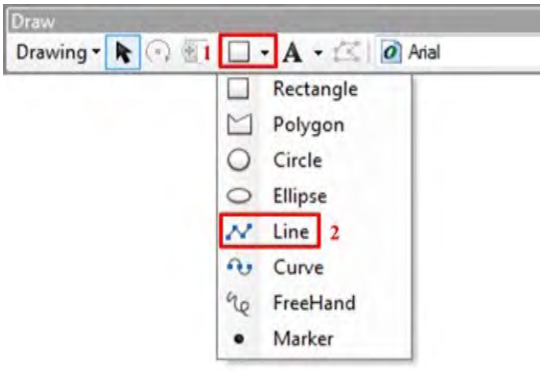

Figure 18. Draw toolbar explained. 1: allows the user to select the type of feature that they wish to draw; 2: is the "Line" tool. Because the glacier terminuses are linear features, the line tool is the best choice.

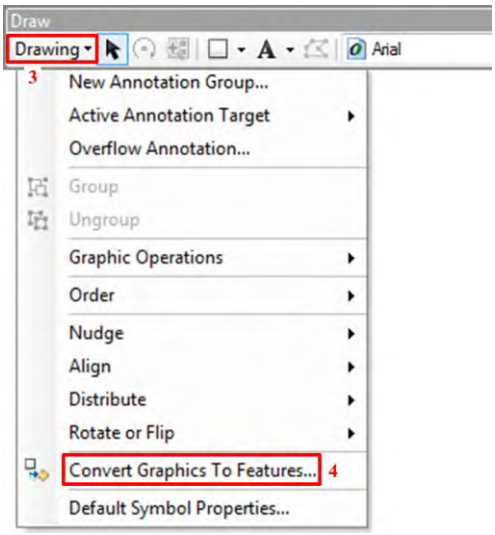

Figure 19. Draw toolbar continued. 3: contains additional drawing options; 4: allows the user to convert drawn graphics to features (shapefiles).

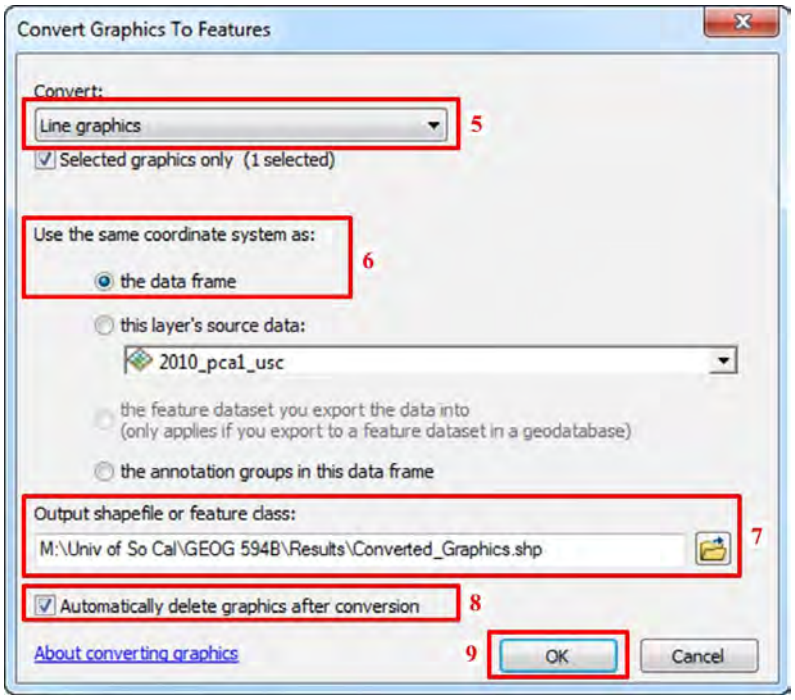

Figure 20. Convert drawn graphics to features. 5: allows the user to specify the type of features that will be contained in the output shapefile; lines, points, or polygons. Since line graphics were drawn, the output features type defaults to line graphics; 6: allows ensures that the output shapefile will possess the same coordinate system as the data upon which the graphic was drawn; 7: allows the user to specify an output image and save location; 8: is checked so that the graphics will be deleted after the shapefile is created; 9: begins the conversion process. After the graphics have been converted to shapefile, they will be loaded into the map document (user is prompted to whether or not they wish this to happen).

After the individual glacier terminus shapefiles were created (a total of 20 shapefiles), each shapefile was then attributed to include "Glacier Name" and "GLS Dataset". This was necessary so that the glacier terminuses could be differentiated in the final glacier shapefiles. Upon completion of the shapefile attribution, the shapefiles were combined to produce a final shapefile for each glacier that contains the glacier's terminus locations in the GLS2010, GLS2005, GLS2000, GLS1990, and GLS1975 datasets (a total of four final shapefiles; one for each glacier).

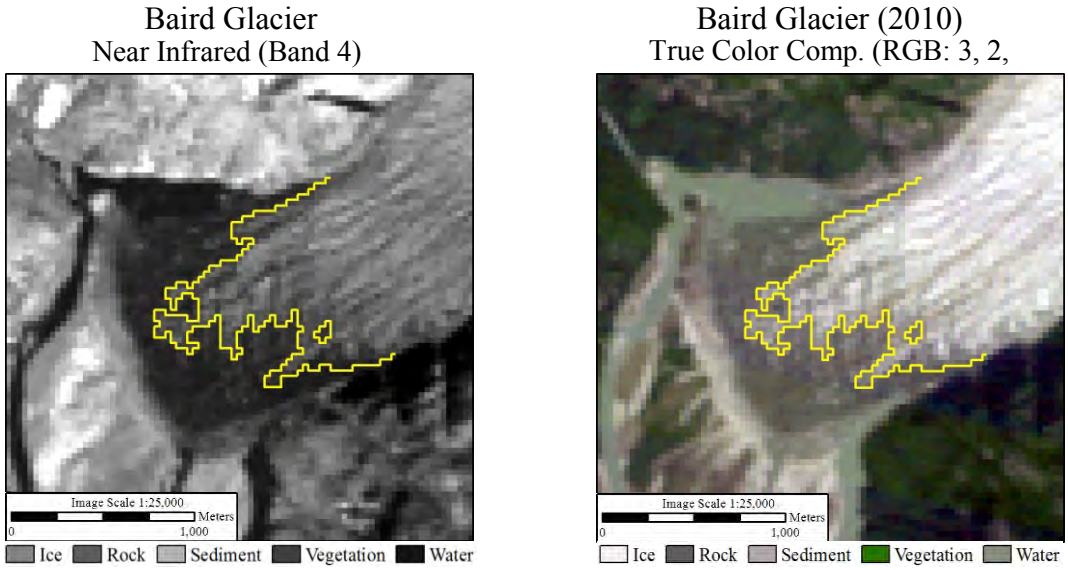

Figure 21. Baird Glacier in GLS2010: the left graphic is Landsat 7 ETM+ near infrared (Band 4) image and the right image is a natural color composite (RGB Bands 3, 2, 1). In both images, the glacier terminus was shown as a yellow line. The stair-stepped appearance of the terminus was due to the image's 30m pixels.

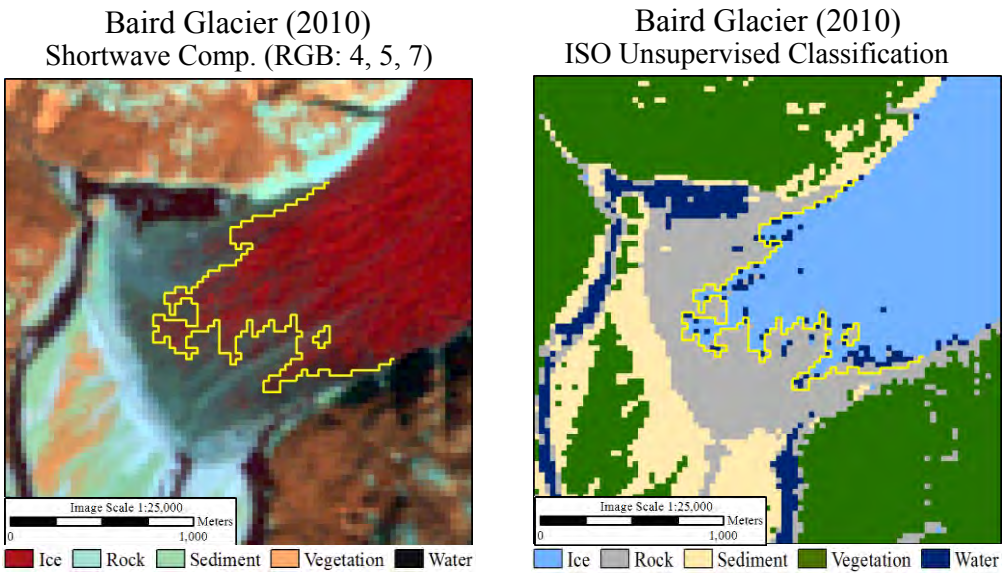

Figure 22. Baird Glacier in GLS 2010: the left graphic is Landsat 7 ETM+ shortwave infrared composite (RGB Bands 4, 5, 7) and the right image is an ISO Data Cluster Unsupervised Classification (Bands 1, 2, 3, 4, 5, & 7). In both images, the glacier terminus was shown as a yellow line. The stair-stepped appearance of the terminus was due to the image's 30m pixels.

Glacier movement quantification

Glacier terminus location shapefiles that were created from analyzing Global Land Survey (GLS) datasets were measured against the Global Land Ice Measurements from Space (GLIMS) shapefiles. The positions of Baird, Patterson, and LeConte Glaciers in the GLIMS shapefiles was used as a starting point, or zero position, from which each glacier's terminus position in the various GLS datasets was measured. These measurements indicated the movement directions and distances moved. Shakes Glacier was considered differently since it lacks an entry in the GLIMS database. For Shakes Glacier, its movement direction and distance was compared among the various GLS datasets. In addition, distances were measured for each glacier between its terminus positions in the various GLS datasets; e.g. GLS1975 to GLS1990, GLS1990 to GLS2000, and so forth.

In order to measure glacier movement over the length of the study period, approximately 1975 to 2010, a measurement method was needed. After much thought and experimentation, the following method was developed to measure glacier movement. The four-step method accounted for the shape of each glacier and the fluid nature of its movement. An explanation of each step is provided and an illustration is captured in Figures 23-26.

The first step was to determine the centerline of each glacier. Initially, this step was the most difficult to execute using the tools in ArcGIS v10.2. A line shapefile for each glacier was created where the edges of each glacier is annotated. Starting from a point several kilometers beyond the farthest advance of each glacier, the two edges of each glacier were digitized "upstream" for several kilometers beyond the most retreated glacier terminus position. Figure 23 shows the results of this process for Baird Glacier in GLS2010. Next, a multi-ring buffer process was run against each shapefile. Depending upon the distance between the edges of each glacier, the buffer distances could be considerable (1,500m-2,500m). At the center point between the sides of each glacier, the buffers would intersect, as shown in Figure 24. Finally, by connecting the "dots" created by the intersecting buffers, the centerline for each glacier was determined; as shown in Figure 25. The process was repeated for Patterson, LeConte, and Shakes Glaciers.

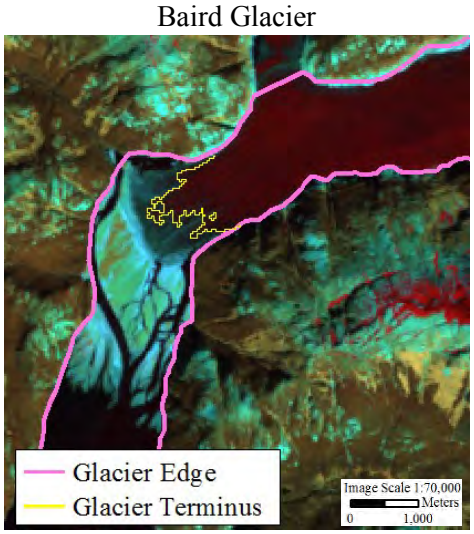

Figure 23. Glacier edge deliniation for Baird Glacier (GLS2010). The glacier's edges are shown in pink and the terminus in yellow. The glacier edges were digitized from a point several kilometers "downstream" of the terminus to a point several kilometers "upstream of the terminus. This provided an accurate understanding of the fluid nature of the glacier so that an accurate glacier centerline could be determined.

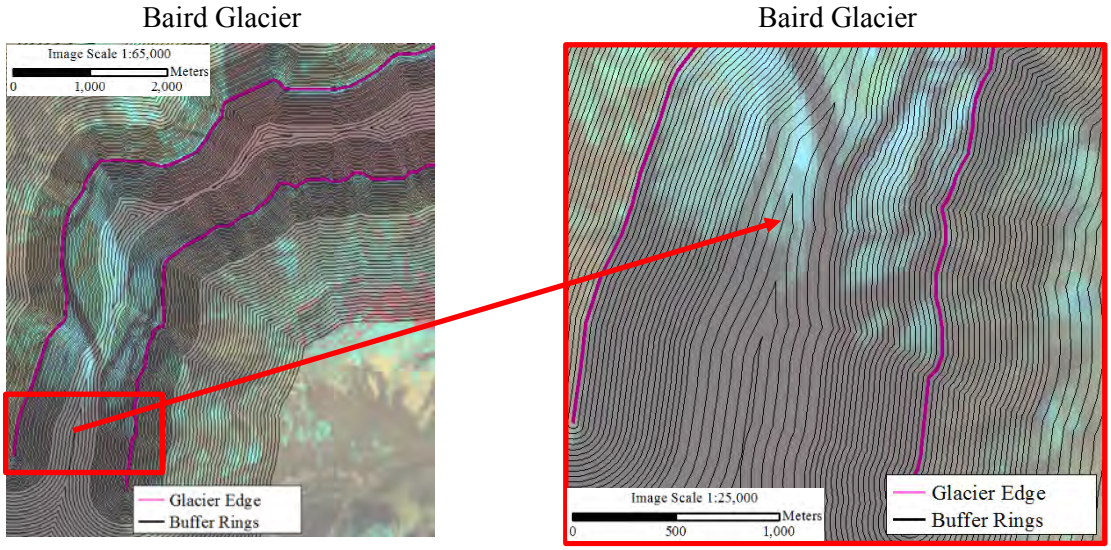

Figure 24. Glacier valley buffers for Baird Glacier (GLS2010). The glacier's edges are shown in purple and the buffers in black. The left image shows the buffers for all of Baird Glacier; while the image on the right shows an enlargement so that the buffers may be better seen.

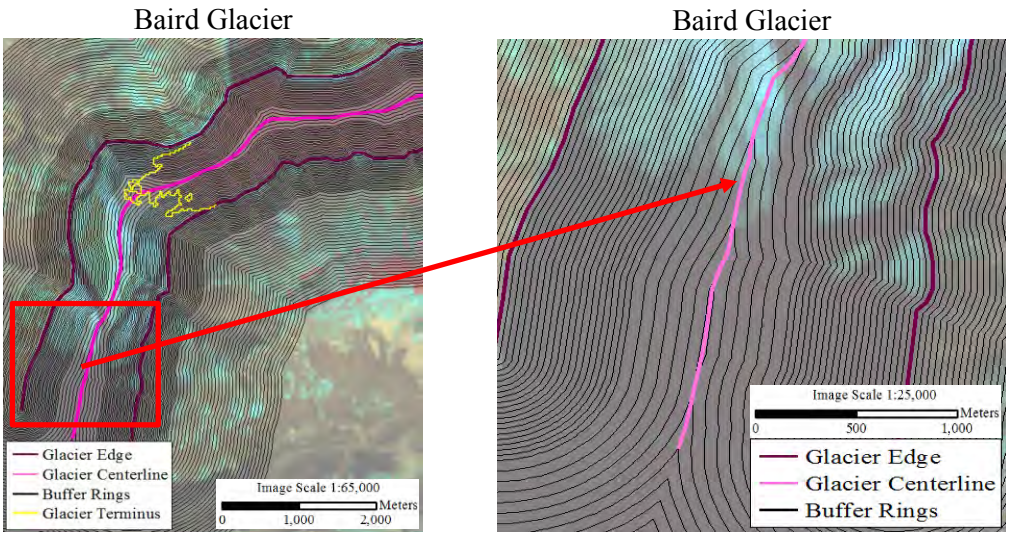

Figure 25. Glacier centerline is completed for Baird Glacier (GLS2010). The glacier's edges are shown in purple, the centerline is pink, the terminus is yellow, and buffer rings are black. The left image shows the centerline for all of Baird Glacier; while the image on the right shows an enlargement so that the centerline can be better seen.

The second step established a measuring point on each glacier centerline from which quantitative glacier movement analysis could be performed. In the previous step, a glacier centerline was established for Baird Glacier in GLS2010; which is labeled "1" on Figure 26. That centerline was critical to this step. Perpendicular lines were drawn to the glacial valley center line to identify the point on a glacier's terminus shapefile that was the most advanced point of tangency; which is labeled "2" in Figure 26. The perpendicular, intersecting both the point of tangency and the glacial valley center line, is labeled "3" on Figure 26; the point where the perpendicular intersects the glacier's centerline is labeled "4", which is the point of measurement for the terminus movement. For Baird, Patterson, and LeConte Glaciers there were a total of six perpendiculars identifying five terminus positions, one for each of the five GLS datasets, and one for the terminus position in the GLIMS dataset. For Shakes Glacier, there were no GLIMS dataset; so there were only five perpendiculars that correspond to the terminus

positions in the GLS datasets. Figures 28-31 illustrated the completed glacier valley center lines and perpendiculars for Baird, Patterson, LeConte, and Shakes Glaciers.

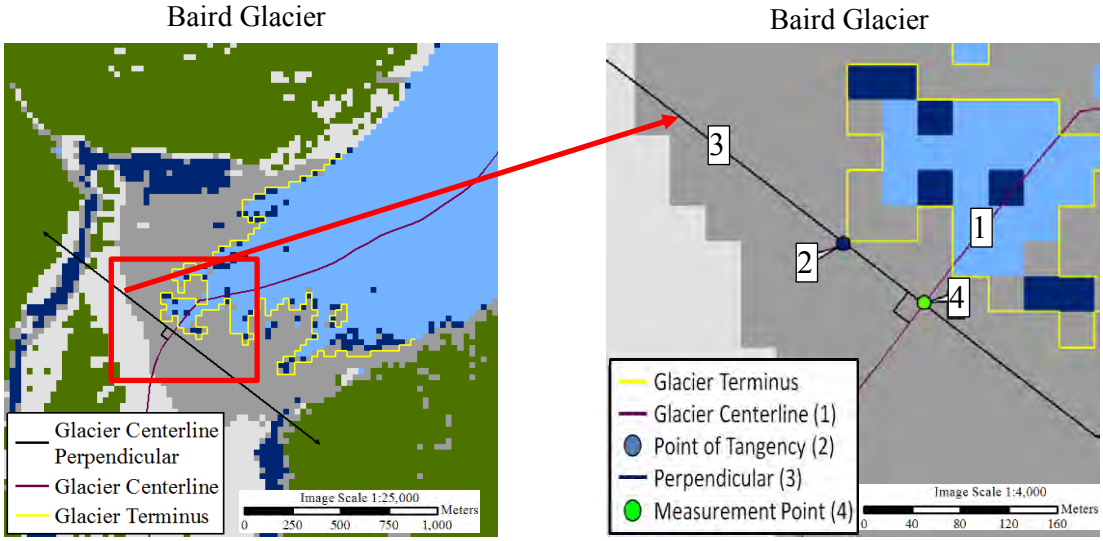

Figure 26. Glacier centerline perpendicular is completed for Baird Glacier (GLS2010 ISO Classification). The glacier's centerline is shown in purple, the perpendicular is black, and the terminus is yellow. The left image is an overview of the centerline perpendicular; while the image on the right shows an enlargement and detail of the glaciers' terminus measurement point (4).

With the origin points determined along each glacier centerline, movement and direction was then determined. Movement distance measurement was accomplished by simply conforming to the shape of each centerline and measuring between origin points. This method ensured that all measurements for Baird, Patterson, LeConte, and Shakes Glaciers were uniform and no bias was introduced favoring one glacier over another. Direction of movement (advance or retreat) was determined by comparing a glacier terminus position in one GLS dataset to its position in another GLS dataset. A partial example for Baird Glacier is shown in Figure 27.

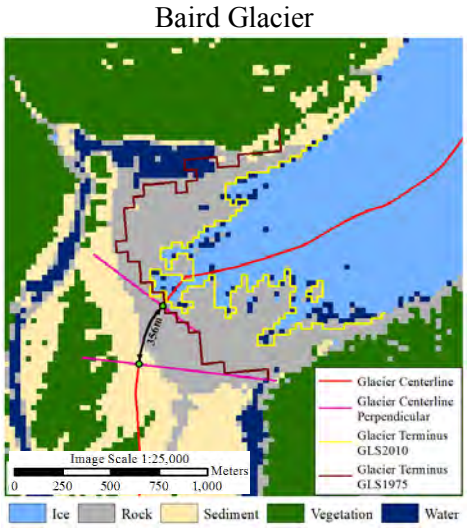

Figure 27. Baird Glacier movement measurement (partial). The glacier centerline is shown in red, the perpendiculars are magenta, GLS2010 terminus is yellow, and GLS1990 terminus is brown. The distance, as measured along the glacier centerline, between GLS1975 origin and GLS2010 origin is 356m. The image scale is 1:25,000.

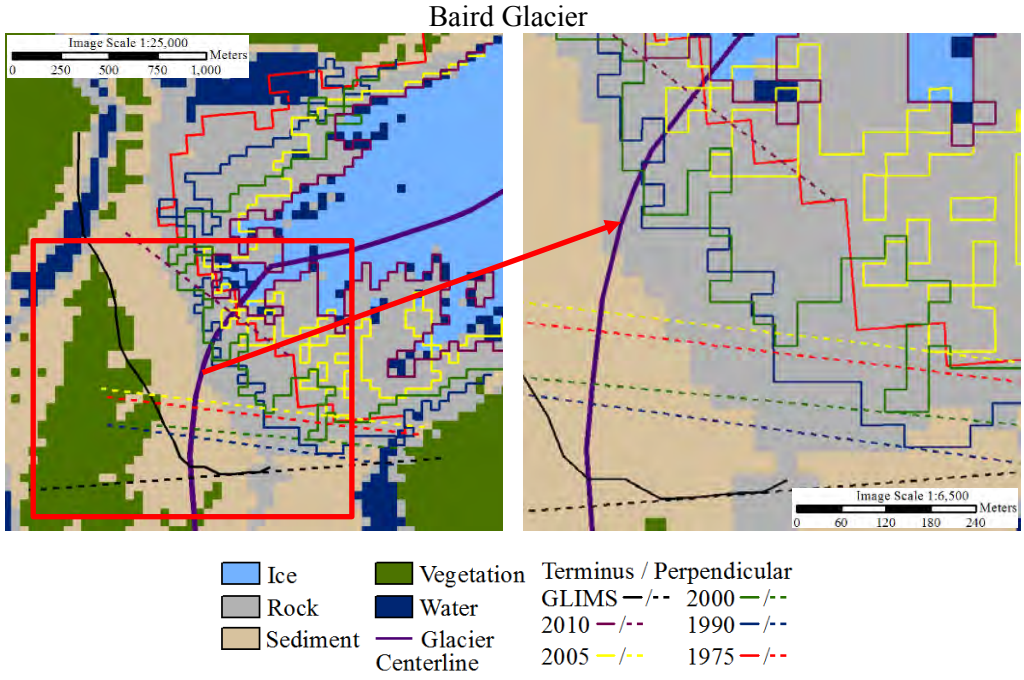

Figure 28. Baird Glacier terminuses and perpendiculars for GLS2010, 2005, 2000, 1990, and 1975 datasets. The image on the left is an overview and the image on the right is an enlargement. Terminuses are shown as solid lines and perpindiculars are dashed lines.

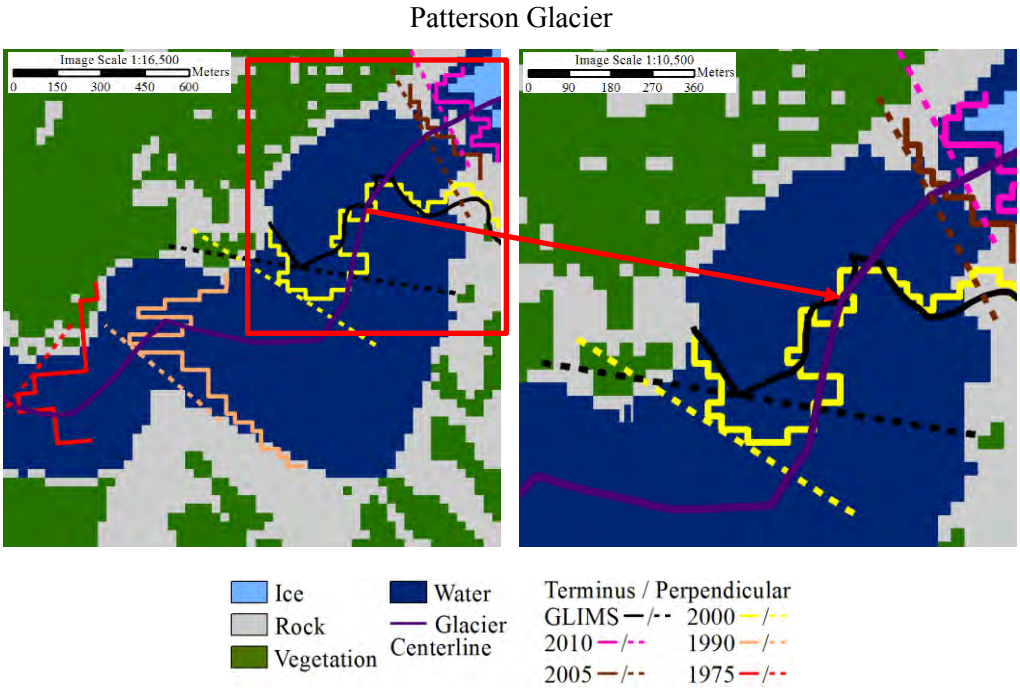

Figure 29. Patterson Glacier terminuses and perpendiculars for GLS2010, 2005, 2000, 1990, and 1975 datasets. The image on the left is an overview and the image on the right is an enlargement. Terminuses are shown as solid lines and perpindiculars are dashed lines.

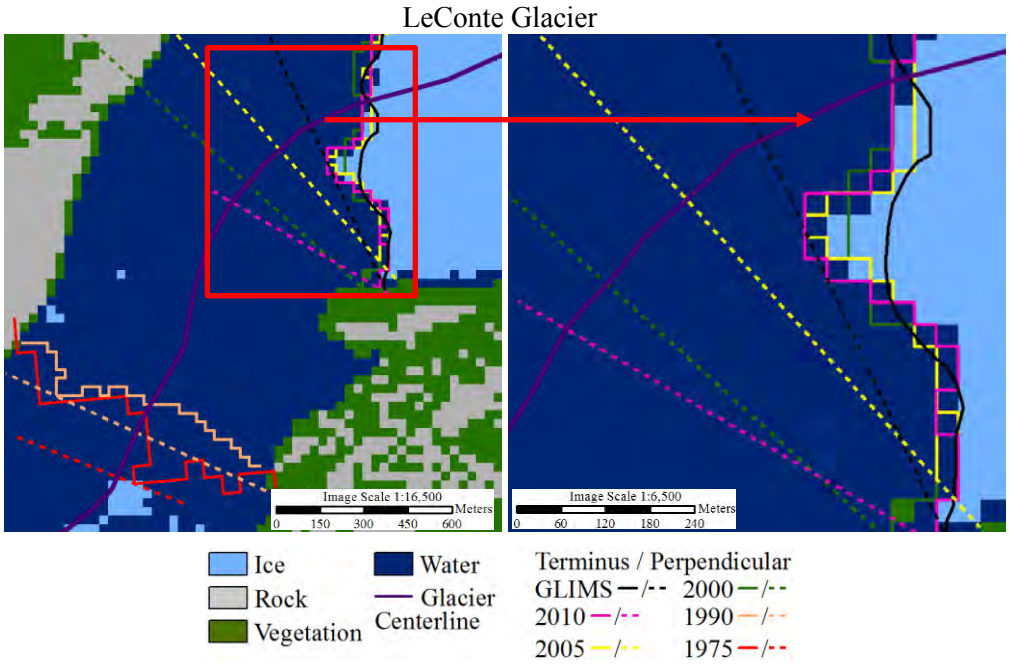

Figure 30. LeConte Glacier terminuses and perpendiculars for GLS2010, 2005, 2000, 1990, and 1975 datasets. The image on the left is an overview and the image on the right is an enlargement. Terminuses are shown as solid lines and perpindiculars are dashed lines.

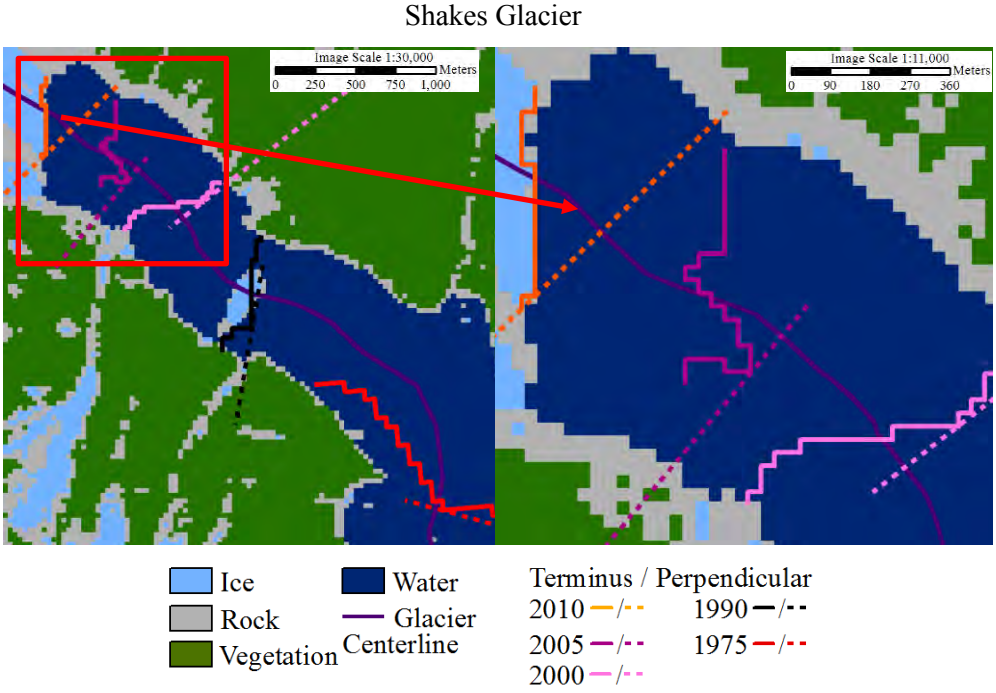

Figure 31. Shakes Glacier terminuses and perpendiculars for GLS2010, 2005, 2000, 1990, and 1975 datasets. The image on the left is an overview and the image on the right is an enlargement. Terminuses are shown as solid lines and perpindiculars are dashed lines.

Comparison of glacier movement for glaciers with similar terminus conditions

This analysis was conducted by comparing the determined movement rates for the Shakes Glacier and Patterson Glaciers, both of these glaciers' terminuses were in freshwater lakes. The results of this analysis are presented in Chapter 5.

Comparison of glacier movement for glaciers with dissimilar terminus conditions

This analysis was conducted by comparing the determined movement rates for the Baird, Patterson, and LeConte Glaciers. Baird Glacier's terminus was on dry land, Patterson Glacier's terminus was in fresh water (lake), and LeConte Glacier's terminus was in salt water (marine bay). The results of this analysis are presented in Chapter 5.

CHAPTER FIVE: RESULTS

The final combined shapefile terminus results for Baird, Patterson, LeConte, and Shakes Glaciers are shown in Figure 32. The glacier terminuses were "stair stepped" in appearance due to the usage of 30m spatial resolution Landsat imagery. No feature smoothing algorithm was applied to the terminus shapefiles.

The movement values and movement direction for Baird, Patterson, and LeConte Glaciers using the GLIMS dataset as a baseline are summarized in Table 13, while the movement distances for Baird, Patterson, LeConte, and Shakes Glaciers for the periods of time between GLS dataset collection events are summarized in Table 14 and Figure 33. Table 15 provides the average glacier movement for the periods of time between GLS dataset collection events as well as providing an average glacier movement per year for the entire breadth of the GLS datasets; which is approximately 35 years (1974-2009). The values in Table 15 were determined by dividing the movement values in Table 14 by the length of time that passed between the GLS dataset collection dates. For GLS1975 to GLS1990, the length of time is 15 years; for GLS1990 to GLS2000, the length of time is 10 years; for GLS2000 to GLS2005, the length of time is 6 years; and for GLS2005 to GLS2010 the length of time is 4 years. Refer to Table 10 for the exact collection dates for the GLS datasets.

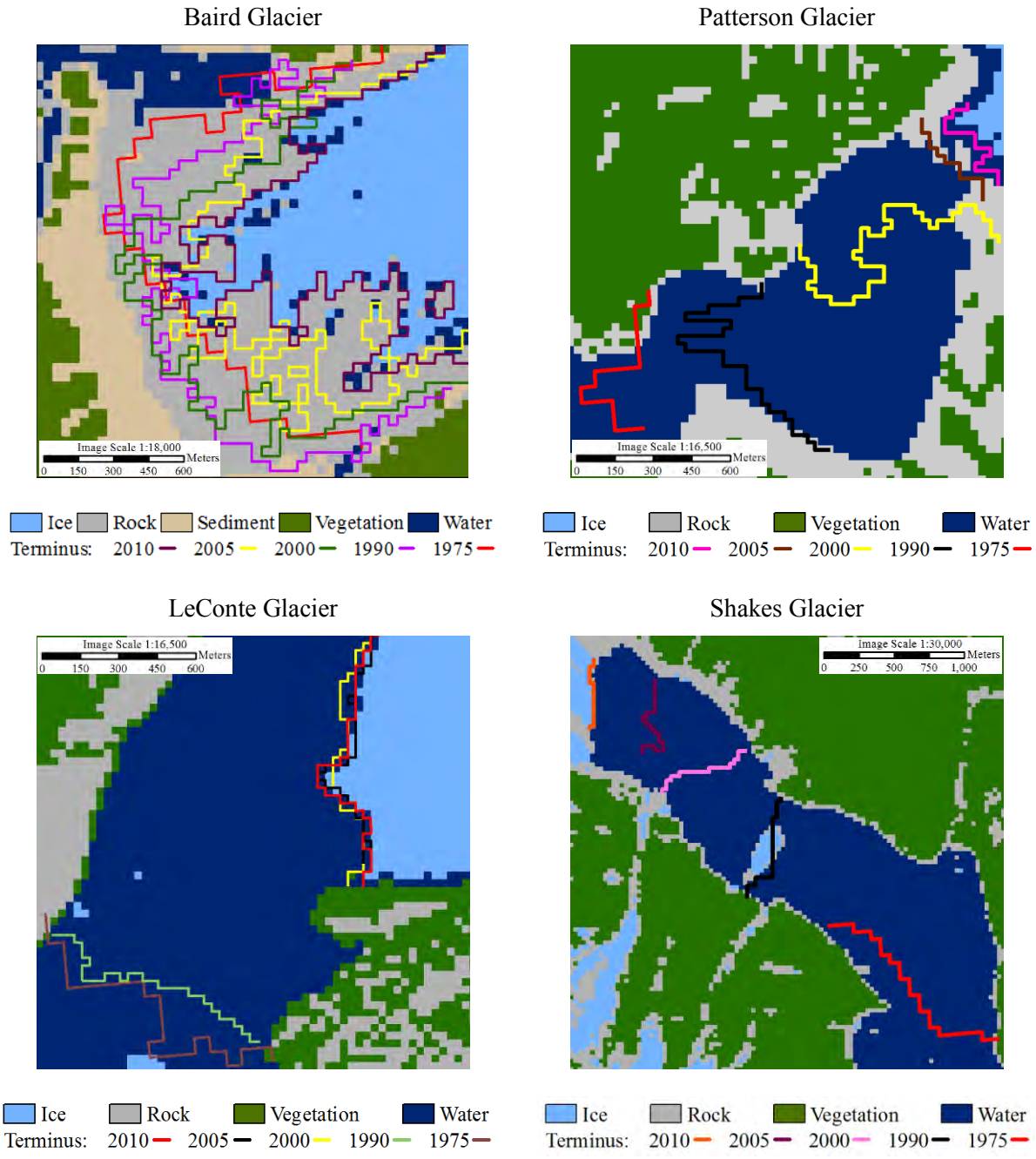

Figure 32. Glacier terminus results for the central southeast Alaska glacier GLS datasets. The top left image is Baird Glacier, the top right image is Patterson Glacier, the bottom left image is LeConte Glacier, and the bottom right image is Shakes Glacier. The background images are the ISO Cluster Unsupervised Classification results for the GLIMS 2010 dataset.

Table 13. Baird, Patterson, and LeConte Glacier terminus distance summary during the various time periods between GLS dataset collection events. Using the GLIMS perpendicular's intersection with the centerline as a starting point, distances to the intersection of each dataset's perpendicular and the centerline were measured. A positive value indicates that a glacier's terminus is in front (downstream) of the GLIMS data; a negative value indicates that a glacier terminus is behind (upstream) of the GLIMS data.

GLS Dataset	Glacier Position from GLIMS Baseline (m)		
	Baird	Patterson	LeConte
GLS1975	-242	1460	1409
GLS1990	-141	932	1242
GLS2000	-168	164	295
GLS2005	-267	-567	136
GLS2010	-597	-645	380

Table 14. Movement distance summary for each glacier from one GLS dataset collection event to the next e.g. (GLS1975 to GLS1990, GLS1990 to GLS2000, and so forth). A total amount of movement over the 35 years of data coverage is also provided at the bottom of the table. Distances were measured in meters. From approximately 1975 to 2010, Shakes Glacier experienced the greatest total movement amount; Baird Glacier experienced the least.

GLS Dataset Temporal Range	Glacier Movement per GLS Datasets (m)			
	Baird	Patterson	LeConte	Shakes
At GLS1975	0	0	0	0
GLS1975 to GLS1990	101	528	167	1942
GLS1990 to GLS2000	27	768	947	685
GLS2000 to GLS2005	99	731	159	415
GLS2005 to GLS2010	330	78	244	481
Total	557	2105	1517	3523

Table 15. Summary of the average movement rates per year for Baird, Patterson, LeConte, and Shakes Glaciers in each time period between GLS dataset collection events and average movement for entire period covered by GLS1975 to GLS2010 datasets. Distances were measured in meters. From approximately 1975 to 2010, Shakes Glacier experienced the greatest average movement; Baird Glacier experienced the least.

GLS Dataset Temporal Range	Average Glacier Movement per Year (m)			
	Baird	Patterson	LeConte	Shakes
At GLS1975	0	0	0	0
GLS1975 to GLS1990	7	35	11	129
GLS1990 to GLS2000	3	77	95	69
GLS2000 to GLS2005	17	122	27	69
GLS2005 to GLS2010	83	20	61	120
Glacier Movement per Year for GLS1975 to GLS2010	16	60	43	101

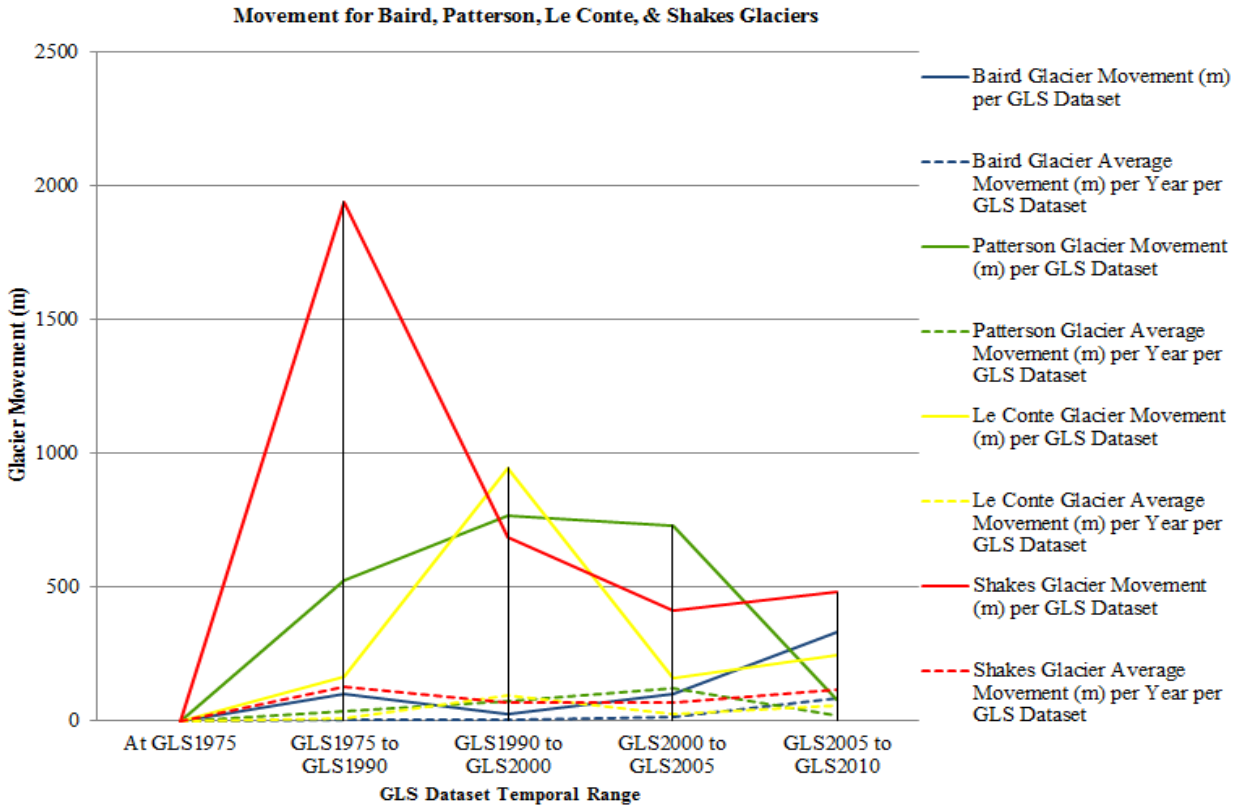

Figure 33. A summary of the movement distances for Baird, Patterson, LeConte, and Shakes Glaciers during the periods of time covered by each GLS dataset. The total movement distances for each glacier in each GLS dataset are shown as solid lines. The average movement distance per year covered by each dataset is shown as dotted lines.

5.1 Glacier movement qualification

Patterson and LeConte Glaciers steadily retreated during the time spanned by the GLS1975 to GLS2005 datasets. However, in the GLS2010 datasets, Patterson Glacier retreated and LeConte Glacier advanced from previous positions. One potential conclusion for the retreat during 1975 to 2005 is that these glaciers attempted to equalize to changing climate conditions and began retreating, as evidenced by the steady retreat exhibited in the GLS1975 to GLS2005 time period. However, they contracted too quickly and had begun to surge forward in an attempt to equalize with the environment. In the GLS2010 time period, LeConte Glacier had advanced, but Patterson Glacier continued to retreat. This oscillation movement is very similar to a weight

hanging at the end of a rubber band that is released and moves up and down until equilibrium between the rubber band's elasticity and the pull of gravity can be achieved. In this example, equilibrium is achieved when the glaciers melt rate equaled it growth rate.

There are many variables that must be considered to understand why a particular glacier flows in the manner that it exhibits. Waddington (2009) determined that glaciers flow because of two simplified principles: 1) ice deformation and 2) glacier substrate allows glacier to move over it. Waddington (2009) further explains that ice flow speed is determined by four factors: 1) ice thickness, 2) slope, 3) ice properties, and 4) bed properties. In addition, any moveable object will tend to move from an area of higher elevation to an area of lower elevation, if possible. This is typified by water moving from an area of higher elevation to an area of lower elevation, e.g. water normally runs downhill.

Glacier slope

In the case of glaciers, the high point from which they flow is a much larger collection area, like an icefield or ice cap. For Baird, Patterson, LeConte, and Shakes Glaciers, that icefield is the Stikine Icefield (Molina, 2008). To illustrate the immutable tendency of glaciers to flow from areas of higher elevation to areas of lower elevation, glacier surface elevations were determined for Baird, Patterson, LeConte, and Shakes Glaciers at the terminuses and also 5km "upstream" from the terminus. The resulting elevation values are listed in Table 16. As discussed in Section 4, the slope of the study area ranged from 0% to greater than 100%. While the slope values in the study area varied considerably, the slopes of the glaciers were comparatively slight; ranging from 3.02% to 9.20%. The glacier slopes and average movement rates are summarized in Table 15 and shown in Figure 34.

Table 16. Summary of glacier valley slopes for Baird, Patterson, LeConte, and Shakes Glaciers. Elevations were determined at terminuses and five-kilometers upstream from each terminus. Values were recorded in meters and were measured on the surface of the glacier. While this was not ideal, the lack of glacier bed elevation data at the point five-kilometers upstream necessitated surface measurements. In order to remain consistent, terminus and 5km upstream elevation values were measured on glacier surfaces. Technology, like ground penetrating radar, can provide accurate ice thicknesses which can be used to calculate glacial bedrock profiles and elevations (Geophysical Survey Systems, Inc., 2012).

Glacier	Elevation at Terminus (m)	Elevation 5km Upstream (m)	Slope (%)	Average Movement Rates Per Year (m)
Baird	27	178	3.02	16
Patterson	49	424	7.50	60
LeConte	46	506	9.20	43
Shakes	11	201	3.80	101

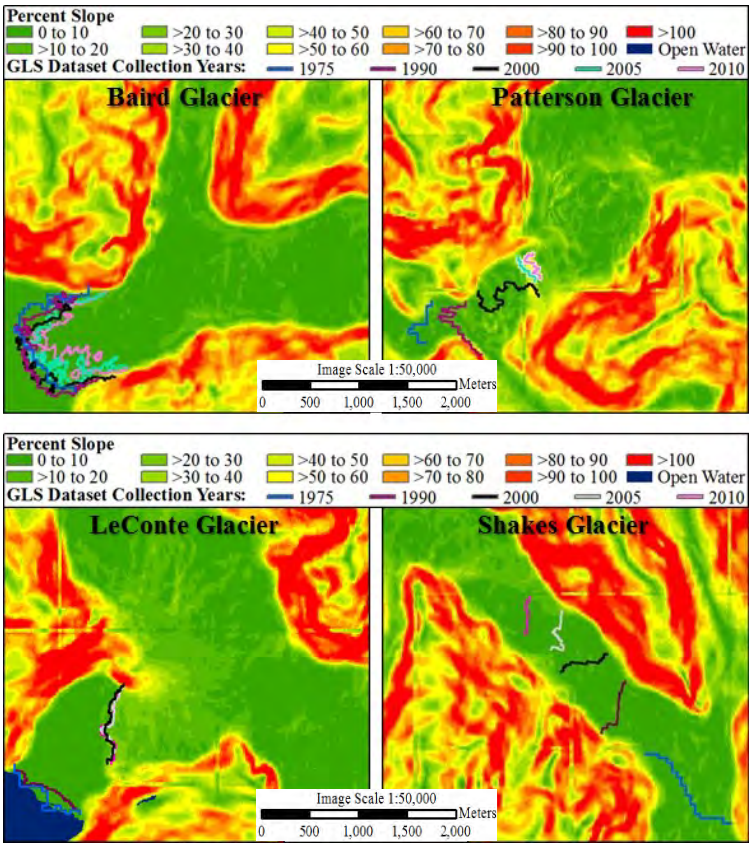

Figure 34. Slope at and within five-kilometers of Baird, Patterson, LeConte, and Shakes Glaciers. From 0 to 100 percent, slope values are divided into 10 bins; slopes greater than 100 percent are placed in a single bin. Glacier valley slopes were typically less than 10% and the surrounding terrain is much steeper.

Looking father "upstream" to the Stikine Icefield, which is the source of Baird, Patterson, LeConte, and Shakes Glaciers, elevations commonly exceeded 1,500m. Logic would indicate that glaciers with the greatest slope values should experience the greatest amount of forward movement (due to gravity assisting movement) and the least amount of backwards movement (also due to gravity retarding movement). Comparing the slope values to the average movement rates per year for GLS1975 to GLS2010 (Table 15) is contrary to this belief.

Baird Glacier had the least slope (3.02%) and the lowest average movement rate per year over the span of the GLS datasets (16m). Shakes Glacier also had low slope (3.80%), but experienced the greatest average movement rate per year over the span of the GLS datasets (101m). Patterson Glacier had greater slope (7.50%) and experienced the second greatest average movement rate per year over the span of the GLS datasets (60m). LeConte Glacier had the greatest slope (9.20%), but had experienced low average movement rate per year over the span of the GLS datasets (43m). The relationship between slope and glacier movement rates were typified in Baird and Patterson Glaciers, but LeConte and Shakes Glaciers behaved differently.

An appropriate conclusion is that other factors affect glacier movement rates, not just slope. Unfortunately, this data did not indicate what those factors may be, or the effect that they had on glacier movement rates for Baird, Patterson, LeConte, or Shakes Glaciers. Further study is warranted to identify these additional factors and the role they play on glacier movement rates.

Glacier bed properties

In addition to slope, Waddington (2009) attributed glacier flow speed to glacial bed properties. Analysis of land cover in the study area showed the areas at and near Baird,

Patterson, LeConte, and Shakes Glaciers are characterized by bare rock voided of any trees or vegetation. The lack of any vegetative cover reduced any impedance to the Glaciers' movement. Additionally, Glaciers in the study area had a historical record of advance-retreat-advance; LeConte Glacier has advanced six times since 1,600 years before present (Molina, 2008). Each time that this had occurred, the glacial bed is progressively polished and the friction between ice and rock is incrementally reduced (Michna, 2012).

Temperature dependence of ice flow

Waddington (2009) also states that there is a direct relationship between glacier flow speed and temperature; the warmer it is, the faster a glacier can flow. Figure 35 (Waddington, 2009), identifies the relationship between glacier flow speed and temperature. The temperature values are given in Kelvin (K); for reference water freezes at 273.15K and boils at 373.15K.

As temperatures increase, glacier deformation increases as does glacier flow speed (Waddington, 2009). Analyzing National Oceanographic and Atmospheric Administration (NOAA) temperature data that was collected at the Petersburg, Alaska meteorological station from January 1, 1973 to December 31, 2009 revealed a general warming trend. Petersburg, Alaska was the closest meteorological data collection point to the study area. It is understood that atmospheric conditions in Petersburg, Alaska, were only close approximations for the conditions near Baird, Patterson, LeConte, and Shakes Glaciers; i.e. large masses of ice have a noticeable effect on temperature and precipitation. As the study area is located in the Tongass, precipitation was significant (refer to Section 2.1). From January 1, 1973 to December 31, 2009, mean yearly temperatures have been increasing as shown by the positive trend line in Figure 36.

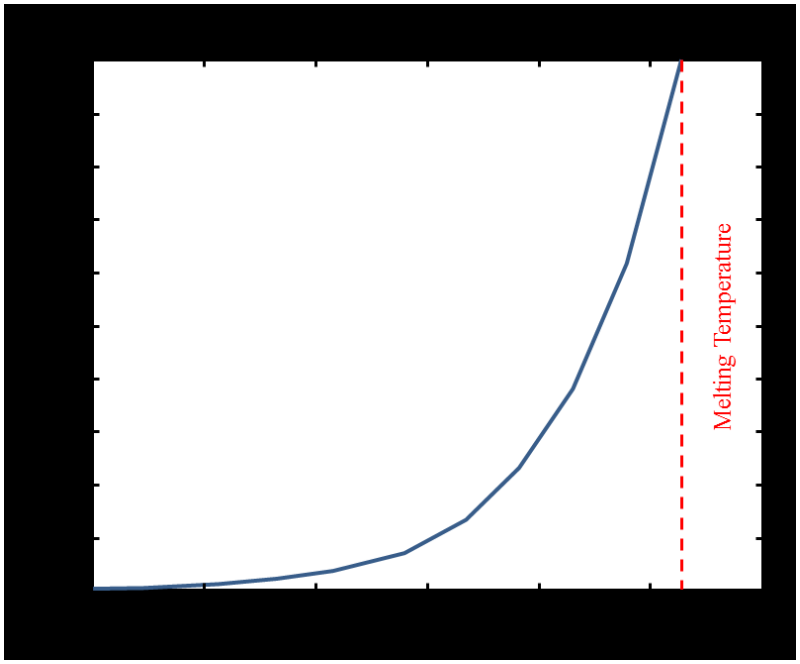

Figure 35. Relationship between ice flow rates and temperatures. As the temperature increases towards the melting point (which occurs at 273.15K), the ice deformation rate increases. Ice deformation is the ability of ice to change shape without breaking (Waddington, 2009).

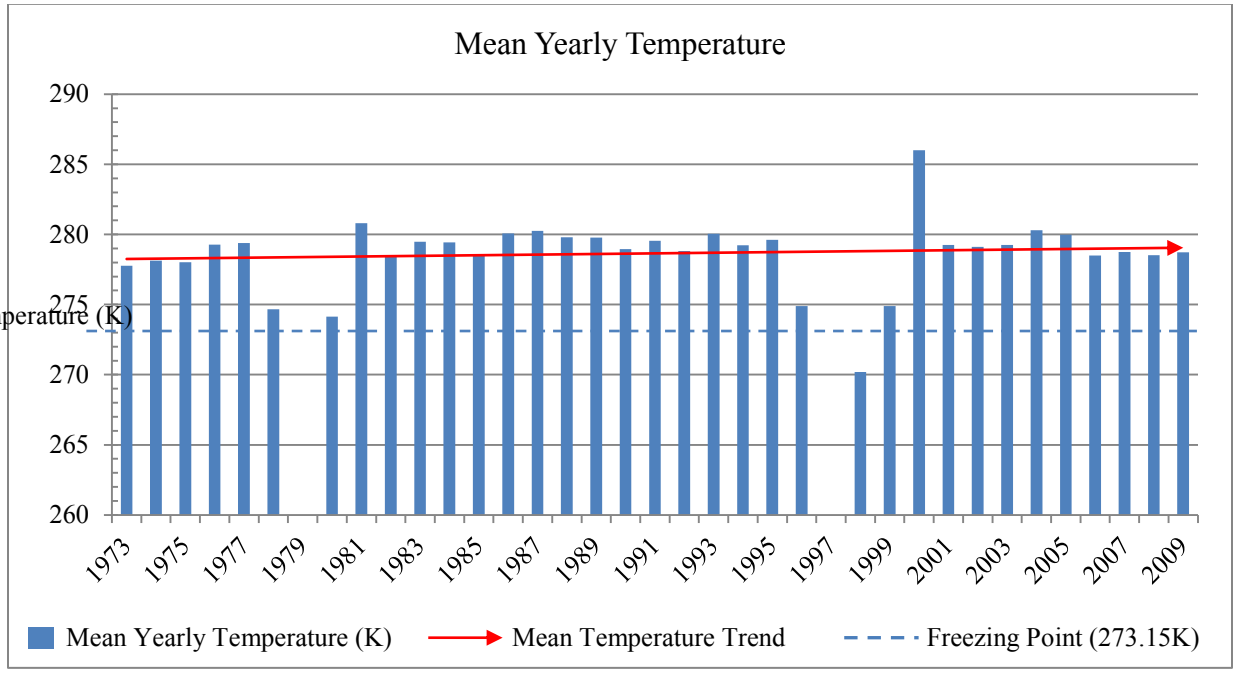

Figure 36. Mean yearly temperatures chart for 1973-2009. Years that were not represented by a data point were those years for which no data was available. The data exhibited a positive trend; suggesting that the average yearly temperature was increasing. The trend line equation is: $y = 0.0223x + 278.22$.

The increase in mean yearly temperatures can be further analyzed by examining the average monthly temperature for the same period of time. It was discovered that warming trends were experienced in the months of January, May through September, and November through December. Conversely, cooling trends were experienced in February through April, and October. Eight out of twelve months were getting warmer, while the other four months were getting colder. These trends are summarized in Table 17. It could be inferred from this data that the summers and several traditionally winter months were getting warmer. This general warming trend is detrimental to ice formation and should be leading to greater glacier melting. With the exception of Baird Glacier in the GLS1975 to GLS1990 and LeConte Glacier in GLS2005 to GLS2010 datasets, Baird, Patterson, LeConte, and Shakes Glaciers have retreated between 1975 and 2010.

Table 17. Temperature trends for average monthly temperatures from 1973 to 2009. A positive trend indicates that the particular month had gotten progressively warmer from 1973-2009; a negative trend indicates that the month had gotten colder for the same period of time. From 1973-2009, May through September and November through January have showed a positive trend; while February through April and also October have exhibited a negative trend.

Month	Season	Temperature Trend	Month	Season	Temperature Trend
March	Spring	Negative	September	Fall	Positive
April	Spring	Negative	October	Fall	Negative
May	Spring	Positive	November	Fall	Positive
June	Summer	Positive	December	Winter	Positive
July	Summer	Positive	January	Winter	Positive
August	Summer	Positive	February	Winter	Negative

In this study, it was originally suspected that slope would be a key factor in glacier movement, e.g. greater slope would yield greater glacier movement rates. However, the results fail to conclusively support this assumption. While it has been well established that glaciers are indicators of climate change, both cooling and warming, further investigation reveals that glaciers are often slow to respond to climate change and many factors influence a particular glaciers susceptibility to climate change. To further confuse the subject, each glacier's tolerance to the degree of climate change varies, for example one glacier may require a hypothetical net mass balance change of only 1°C, while another glacier requires a hypothetical net mass balance change of 3.5°C; Davies (2014) was able to force a glacier mass balance change with an increase of only 0.5°C.

Terminus conditions and response to climate change

Referring to Table 18, Baird Glacier's slope is 3.02%, its average yearly movement rate was 16m, and its terminus ended on land; Patterson Glacier's slope is 7.50%, its average yearly movement rate is 60m, and its terminus ended in a fresh water (lake); LeConte Glacier's slope is 9.20%, its average yearly movement rate is 43m, and its terminus ended in salt water (marine bay); and Shakes Glacier's slope is 3.80%, its average yearly movement rate is 101m, and its terminus ended in a fresh water (lake). If steeper slopes are expected to produce greater movement rates, the results fail to conclusively support this premise. This is especially true for the Shakes Glacier which has slight slope, but the greatest average yearly movement rate. Because of the lack of conformity to this expectation, other factors besides slope must be examined. For example, is there a time delay between glacial mass accumulation and ablation; if so, is that delay different for glaciers with different terminus conditions (land, freshwater, or

saltwater)? The terminus conditions of Baird, Patterson, LeConte and Shakes Glaciers are shown in Figure 37 and summary of conditions and rate of movement in Table 18.

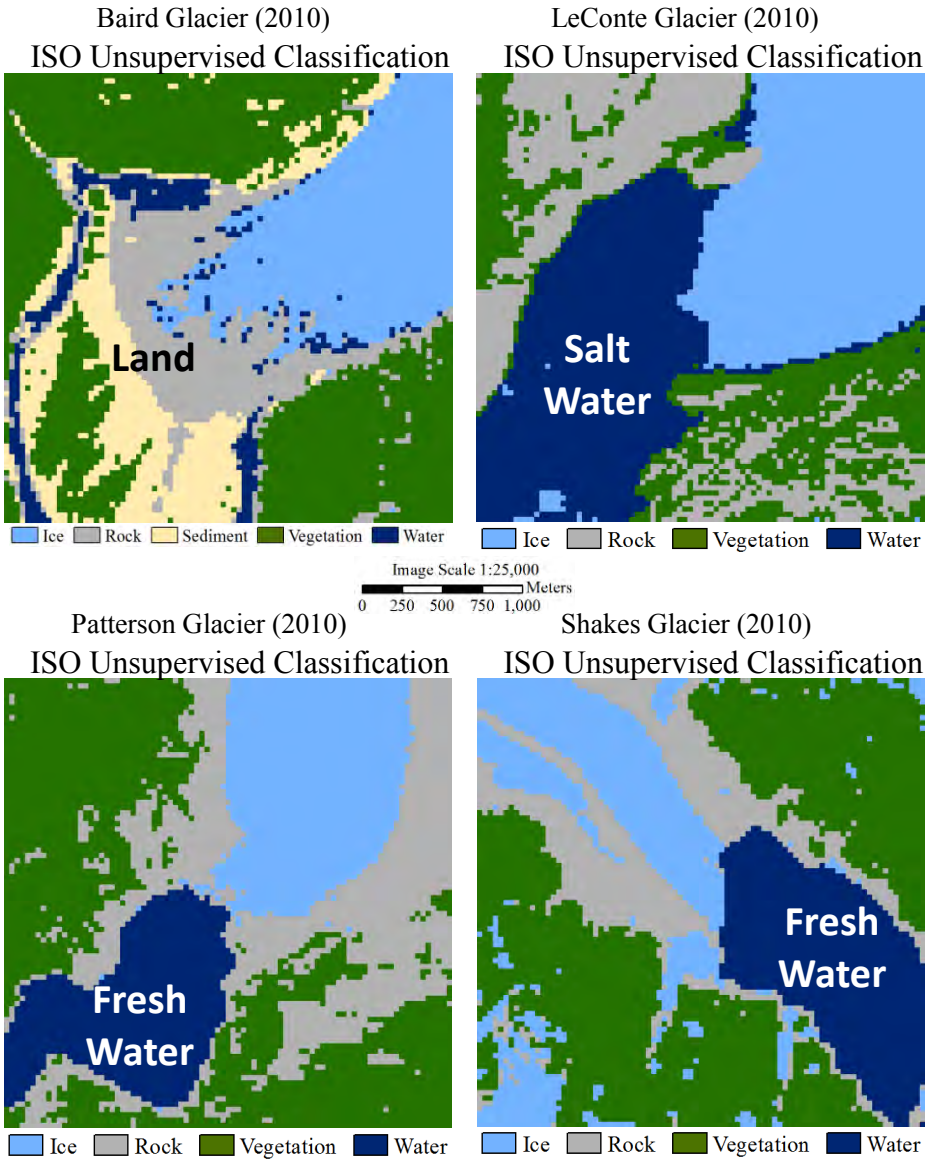

Figure 37. The terminus conditions of Baird, Patterson, LeConte and Shakes Glaciers. Baird Glacier's terminus ends on dry land, LeConte Glacier's terminus is located in salt water, and Patterson and Shakes Glaciers' terminus are located in fresh water lakes.

Table 18. Summary of glacier valley slopes for Baird, Patterson, LeConte, and Shakes Glaciers.

Glacier	Terminus Ends In/On	Slope (%)	Average Movement Rates Per Year (m)
Baird	Land	3.02	16
LeConte	Salt Water (Marine Bay)	9.20	43
Patterson	Fresh Water (Lake)	7.50	60
Shakes	Fresh Water (Lake)	3.80	101

The delay between a significant change in climate and glacier terminus response to that change is referred to as the lag time (T_s) (Pelto & Hedlund, 2001). Lag time can be thought of as the time it takes for a glacier to realize that a significant change in climate has occurred and begin to mostly respond to that change (60% conformity), either by retreating or advancing. Lag time is specific to each glacier and depends upon the glacier's mass balance history and other physical characteristics (Pelto et al., 2001). The determination of a glacier's reaction time requires a study over a lengthy period of time, during which the size and shape of the glacier are measured consistently. Once a glacier recognizes that a significant climate change had occurred, the time it takes for the glacier to approach a new steady state is referred to as response time (T_m) (Pelto et al., 2001).

A thorough literature review revealed very little information regarding lag and response times for the glaciers in this study as Baird, Patterson, LeConte, and Shakes glaciers are simply too remote and inaccessible to warrant comprehensive studies. However, lag and response times have been established for other glaciers and some similarities between these glaciers and those in this study can be expected. Harper (1993) suggests that glaciers on Mt. Baker, Washington, have a response time of approximately 20 years. Also, in a study of alpine glaciers in the North

Cascade Mountains, it was observed that the glaciers followed three general movement trends which are summarized in Table 19 (Pelto et al., 2001).

Table 19. Summary of glaciers in the North Cascades glacier study project. General characteristics, movement trends, lag time and response times are provided. Data summarized from Pelto et al., 2001.

Type	General Characteristics	1890 to 1950	1950 to 1976	1976 to Present	Lag Time (T_s)	Response Time (T_m)
I	Steeper Slopes, Higher Terminus Velocities	Continuously Retreated	Advanced	Retreated	20-30 Years	4-16 Years
II	Intermediate Slopes, Intermediate Terminus Velocities	Rapidly Retreated	Slowly Retreated/Unchanged	Rapidly Retreated	40-60 Years	4-16 Years
III	Low Slopes, Low Terminus Velocities	Retreated	Retreated	Retreated	60-100 Years	4-16 Years

This project differs from the North Cascades glacier study in three ways: (1) the study time period is comparatively short (1975-2010); (2) neither Baird, Patterson, LeConte, nor Shakes Glaciers are alpine glaciers; (3) the climate in the study area is markedly different than the climate in the northern Cascades. However, while many differences exist between the glaciers studied in this project and the glaciers studied in the Northern Cascades projects, all glaciers, regardless of location, have a specific lag time and response time to significant climate changes (Pelto et al., 2001). Additionally, Meier and Post (1986) concluded in a study of the Columbia Glacier, a tidewater glacier located in south central Alaska, that grounded tidewater glaciers rates of flow are independent of climate variables. Rather, flow rates are determined by glacier and glacial valley physical characteristics. Meier et al., 1986 believe that assigning climatic significance to grounded tidewater glacier movement is suspect.

Meier further refines his conclusions in a later study where Bahr, Pfeffer, Sassolas, and Meier (1998) summarize the traditional definition of glacier response time as a ratio of ice thickness to mass balance rate. Glacial mass balance rate is calculated by comparing measurements from glacial accumulation areas with measurement from glacial ablation areas (Krenke & Menshutin, 1987). When mass balance rate is taken into account with ice thickness, ablation, mass balance gradients, hypsometry, and ice surface slope, glacial sensitivity to climate change can be approximated (Davies, 2014).

Davies (2014) ascertains that maritime glaciers located in temperate climates, like LeConte Glacier in Central Panhandle climate region (Figure 7), have a response time of 15-60 years. While no definitive response time is available for Baird, Patterson, or Shakes Glaciers, it is available for Mendenhall Glacier, which is approximately 180km north of the project study area. Mendenhall Glacier is similar to Patterson and Shakes Glaciers in that its terminus is located in a freshwater lake. The response time of Mendenhall Glacier is currently estimated at 45 years (Motyka, O'Neel, Connor, & Echelmeyer, 2003).

It remains to be seen if the glaciers in the study area will respond to the climatic change that has occurred over the length of the study period. Examination of the mean yearly temperature, as shown in Figure 36, reveals the climate had warmed approximately 0.85°C from 1973 to 2009. This warming trend may be insufficient to force glacial responses. Additional data is needed to determine glacial mass balance rate of the glaciers in the project study area as well as relevant glacial physical characteristics. When these values are determined, it may be possible to determine response times for Baird, Patterson, and Shakes Glaciers. This data is impossible to derive from the Landsat data used in this study and would require onsite study of these glaciers.

In addition to accessing glacial ice mass balance rates, other physical forces should be analyzed to determine their effect on glacial movement rates. Referring to Table 18, LeConte, Patterson, and Shakes Glaciers, with terminuses located in water, experienced the greatest average yearly movement rates. Two hypothetical reasons for this occurrence are a heat sink effect and tidal influences. Simply stated, ice melts faster in water than in air (Helmenstine, 2014). Helmenstine (2014) further explains that molecules of water are much closer together than molecules of air which allows for greater contact between water and ice. For any given volume, it must contain more molecules of water than ice. Each molecule of water has an inherent amount of thermal energy as exhibited by the molecules' atomic motion. Thermal energy, or heat, always moves from an area of higher concentration to an area of lower concentration in an attempt to achieve equilibrium. Because there are more molecules of water than ice in any given volume, the volume of water has more energy to "share" with the ice and as a result, the molecules of ice begin to move faster and faster as they warm up and change from solid ice to liquid water (Helmenstine, 2014). Because of this natural phenomenon, LeConte, Patterson, and Shakes Glaciers, with terminuses in water, should melt faster (ablate) and exhibit greater amounts of movement (retreat) than Baird Glacier, which has its terminus located on Land.

LeConte Glacier, with its terminus located in a marine bay, is subjected to tidal influences. Tidal fluctuations in vicinity of LeConte Glacier range from 2m below mean sea level to 7m above mean sea level (Bruland, 2014). Hypothetically, this large variability in tidal levels should exert up and down forces on LeConte Glacier's terminus. In addition, as the tide moves in and out of LeConte Bay, tidal forces pull and push LeConte Glacier's terminus. In a study of a marine terminating glacier in Greenland, Walter, Box, Slawek, Brodsky, Howat, Ahn,

and Brown (2012) discovered that tidal forces do exhibit a great deal of force in both the horizontal and vertical planes, which facilitates glacial ablation. Due to the extreme tidal range, present at LeConte Glacier, calving at weak points along the terminus should contribute to glacial movement.

5.2 Comparison of glaciers with similar terminal terrain conditions

During the period of time encompassed by this project, approximately 1975 to 2010, Baird Glacier's terminus is a moraine field on land, LeConte Glacier's terminus is a marine bay, and Patterson and Shakes Glaciers' terminuses were freshwater lakes. Among these four glaciers, three different terminal terrain conditions existed: dry land, marine, and fresh water. With a diversity of terminus terrain conditions, only Shakes and Patterson glaciers were similar enough for a valid comparison.

Shakes Glacier versus Patterson Glacier

Analysis of Table 15 values revealed significant differences in the movement rates for Shakes and Patterson Glaciers for two of four GLS dataset periods. From 1975 to 1990, Shakes Glacier's average movement substantially exceeded Patterson Glacier. From 1990 to 2005, Shakes Glacier's average movement is less than Patterson Glacier. Then from 2005 to 2010, Shakes Glacier's average movement is significantly more than Patterson Glacier. Table 20 and Figure 38 summarize these findings. For the entire period covered by all GLS datasets, GLS1975 to GLS2010, Shakes Glacier's average movement rate is 1.68 times greater than Patterson Glacier (101m / 60m = 1.6833333m ~ 1.68m). While Shakes Glacier's average movement rate exceeded Patterson Glacier in two of the four study periods, it is similar enough in the other two study periods to raise the question of what other forces affect glacier movement rates. Referring

to Table 16, Patterson Glacier's slope is 7.50% and its average yearly movement rate is 60m; however, Shakes Glacier's slope is 3.80% and its average yearly movement rate is 101m. During the study period, Shakes Glacier had the greatest average movement rate and the least slope; Patterson Glacier had the greatest slope and a significantly lower average movement rate. Based upon slope, and glacier movement rates, a definitive pattern does not emerge and it cannot be conclusively determined from this data if glacier terminuses that are located in freshwater lakes within the project study area produce similar glacier movement rates.

Table 20. Movement summary for Shakes Glacier versus Patterson Glacier. Movement rate multipliers greater than 1.00 indicate that Shakes Glacier's movement rate is greater than Patterson Glacier. In addition to analyzing each GLS dataset period, an overall movement rate multiplier was determined for the entire period of time encompassed by all GLS datasets. That multiplier indicated that Shakes Glacier, on average, moved 1.68 times farther than Patterson Glacier.

Shakes Glacier versus Patterson Glacier	
GLS Dataset Temporal Range	Average Movement Rate Multiplier
GLS1975 to GLS1990	3.69
GLS1990 to GLS2000	0.90
GLS2000 to GLS2005	0.57
GLS2005 to GLS2010	6.00
GLS1975 to GLS2010	1.68

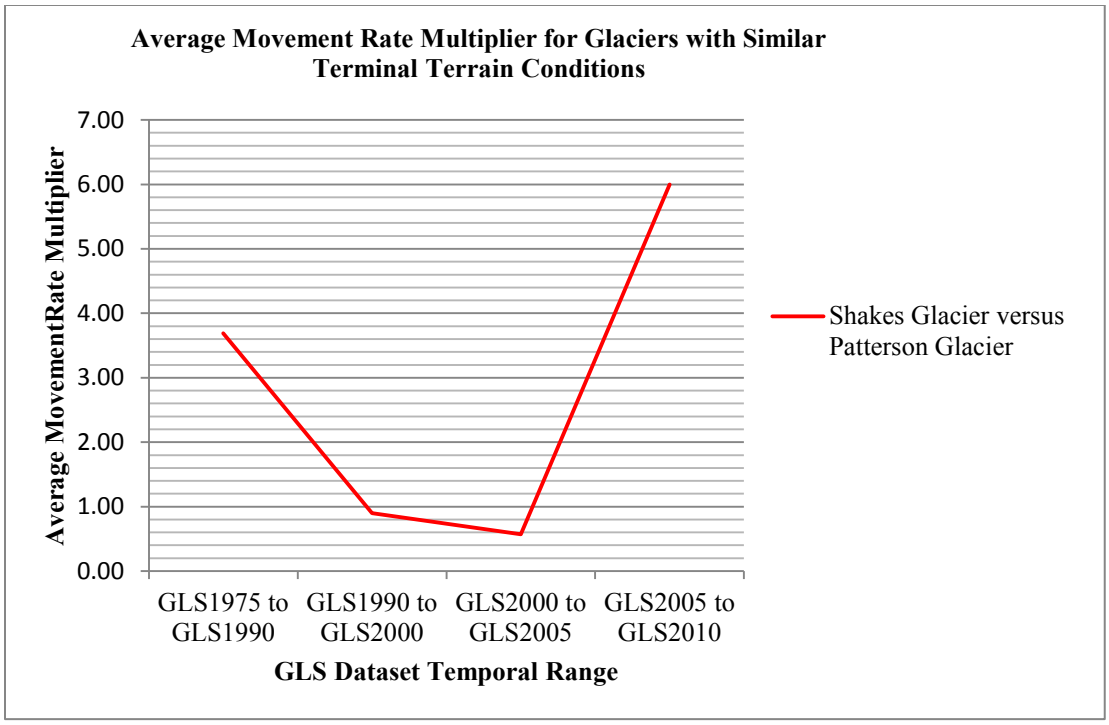

Figure 38. This graph compares the movement of Shakes Glacier to the movement of Patterson Glacier. Movement rate multipliers greater than one indicate that Shakes Glacier's movement rate is greater than Patterson Glacier. The greatest amount of movement is during the interval between GLS2005 and GLS2010 datasets where Shakes Glacier's movement is six times greater than Patterson Glacier's movement rate.

5.3 Comparison of glaciers with dissimilar terminal terrain conditions

The terminuses of Patterson and Shakes Glaciers were in freshwater lakes, LeConte Glacier is in a marine bay, and Baird Glacier is on land. Of the four glaciers, Baird Glacier had the most dissimilar terminal terrain conditions. Of the two glaciers that end in freshwater, Patterson Glacier's average movement rate is more similar to LeConte Glacier's movement rate. For this analysis, Baird Glacier is compared to Patterson and LeConte Glaciers; also, LeConte Glacier is compared to Patterson Glacier.

Baird Glacier versus Patterson Glacier

The comparison of Baird Glacier versus Patterson Glacier considered land and fresh water terminal terrain conditions, respectively. Analysis of Table 15 values revealed that in three of the four dataset periods, Baird Glacier's average movement rate is less than Patterson Glacier; from 1975 to 2005. Only from 2005 to 2010 did Baird Glacier's average movement rate exceed Patterson Glacier. For the entire period covered by all GLS datasets, GLS1975 to GLS2010, Baird Glacier had an average movement rate of only 0.27 that of Patterson Glacier (16m / 60m = 0.266667m ~ 0.27m). Table 20 and Figure 38 summarize these findings. However, when slope is considered, a different pattern emerged. Referring to Table 16, Baird Glacier's slope is 3.02% and its average yearly movement rate is 16m; conversely, Patterson Glacier's slope is 7.50% and its average yearly movement rate is 60m. Based only upon average yearly movement rates, it might be concluded that glacier terminuses which end in fresh water are more conducive to glacier movement (retreat or advance) than terminuses which were located on land. However, both Baird and Patterson Glaciers typified the relationship between slope and movement rates. When slope is considered, Patterson Glacier's greater movement rate may have less to do with glacier terminus terrain types and more to do with increased slope (7.50% versus 3.02%). More variables would need to be considered before a definitive conclusion can be reached.

Baird Glacier versus LeConte Glacier

The comparison of Baird Glacier versus LeConte Glacier considered land and marine terminal terrain conditions, respectively. Analysis of the Table 15 values revealed that in three of the four dataset periods, Baird Glacier's average movement rate is less than LeConte Glacier; from 1975 to 2005. Baird Glacier's average movement rate is greater than LeConte Glacier from 2005 to 2010. For the entire period covered by all GLS datasets, GLS1975 to GLS2010, Baird

Glacier had an average movement rate of only 0.37 that of LeConte Glacier (16m / 43m = 0.372093m ~ 0.37m). Table 20 and Figure 38 summarize these findings. However, when slope was considered, a different pattern emerged. Referring to Table 16, Baird Glacier's slope is 3.02% and its average yearly movement rate is 16m; conversely, LeConte Glacier's slope is 9.20% and its average yearly movement rate is 43m. Based only upon average yearly movement rates, it may be concluded that glacier terminuses that end in marine were more conducive to glacier movement (retreat or advance) than a terminus that were located on land. However, both Baird and LeConte Glaciers typified the relationship between slope and movement rates. When slope was considered, LeConte Glacier's greater movement rate might have less to do with glacier terminus terrain types and more to do with increased slope (7.50% versus 3.02%). More variables would need to be considered before a definitive conclusion can be reached.

LeConte Glacier versus Patterson Glacier

The comparison of LeConte Glacier versus Patterson Glacier considered marine and freshwater terminal terrain conditions, respectively. Analysis of the Table 15 values revealed that in two of the four dataset periods, LeConte Glacier's average movement rate is less than Patterson Glacier; from 1975 to 1990 and from 2000 to 2005. LeConte Glacier's average movement rate is greater than Patterson Glacier from 1990 to 2000 and 2005 to 2010. For the entire period covered by all GLS datasets, GLS1975 to GLS2010, LeConte Glacier had an average movement rate of only 0.72 that of Patterson Glacier (43m / 60m = 0.716667m ~ 0.72m). Table 21 and Figure 39 summarize these findings. Based solely upon average yearly movement rates, it might be concluded that glacier terminuses that end in fresh water are more conducive to glacier movement (retreat or advance) than a terminus which is located in marine.

However, when slope is considered, a contradiction appeared. Referring to Table 16, LeConte Glacier's slope is 9.20% and its average yearly movement rate is 43m; conversely, Patterson Glacier's slope is 7.50% and its average yearly movement rate is 60m. In this comparison, LeConte Glacier's slope is greater than Patterson Glacier's (9.20% versus 7.50%), but its average movement rate is less (43m versus 60m). Based upon average movement rates and slope, a pattern did not emerge. Move variables should be considered before a definitive conclusion can be reached regarding whether fresh water or marine is more conducive to glacier movement.

Table 21. Movement summary for Baird Glacier versus Patterson Glacier, Baird Glacier versus LeConte Glacier, and LeConte Glacier versus Patterson Glacier. Movement rate multipliers greater than 1.00 indicate that the movement rate of the first glacier in each comparison is greater than the movement rate of the second glacier. In addition to analyzing each GLS dataset period, an overall movement rate multiplier was determined for the entire length of the study area.

Average Movement Rate Multiplier			
GLS Dataset Temporal Range	Baird Glacier versus Patterson Glacier	Baird Glacier versus LeConte Glacier	LeConte Glacier versus Patterson Glacier
GLS1975 to GLS1990	0.20	0.64	0.31
GLS1990 to GLS2000	0.04	0.03	1.23
GLS2000 to GLS2005	0.14	0.63	0.22
GLS2005 to GLS2010	4.15	1.36	3.05
GLS1975 to GLS2010	0.27	0.37	0.72

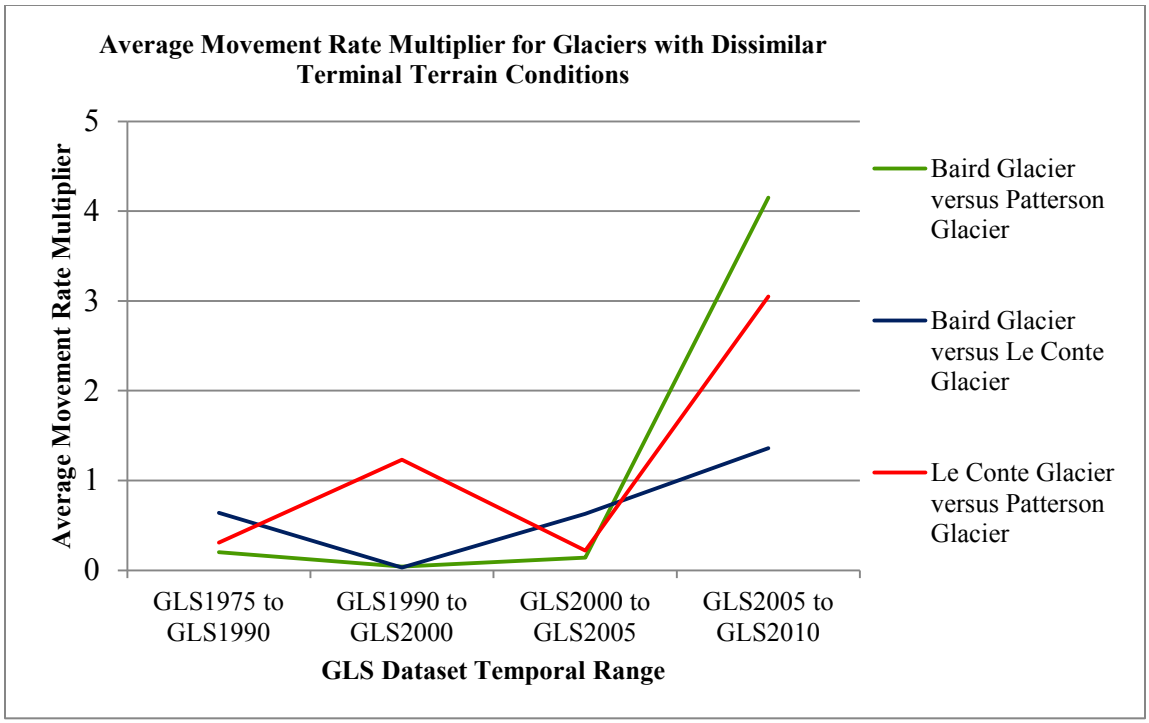

Figure 39. Movement comparison for Baird Glacier versus Patterson Glacier, Baird Glacier versus LeConte Glacier, and LeConte Glacier versus Patterson Glacier. Movement rate multipliers greater than 1.00 indicate that the movement rate of the first glacier in each comparison was greater than the movement rate of the second glacier.

Analysis of the average rates of change over the full range of GLS datasets, as summarized in Table 15, inferred that glacier terminuses that end in freshwater (Shakes and Patterson) were more conducive to movement than those that were located in a marine environment (LeConte) or on land (Baird). Likewise, terminuses located in marine environments (LeConte) were more conducive to movement than those located on land (Baird). The average movement per year for Shakes Glacier is 101m; Patterson Glacier is 60m. LeConte Glacier is 43m, and Baird Glacier is 16m. Although Shakes Glacier averaged 101m, it probably should be considered atypical for this study due to its rapid movement. Considering Baird, Patterson, and LeConte Glaciers, the difference in average movement rates between the most active glacier,

Patterson, and the least active glacier, Baird, is 44m. Analysis of Table 20 also revealed wide fluctuation in glacier movement values during the various GLS dataset periods.

When glacier slope is considered, relative glacier movement appeared to be more dependent upon glacier slope than terminal terrain conditions. Baird Glacier had the least slope and lowest average movement rates (3.02% and 16m); LeConte Glacier had the greatest slope and second lowest average movement rate (9.20% and 43m); Patterson Glacier had the second greatest slope and third greatest average movement rate (7.50% and 60m); and Shakes Glacier had the second lowest slope and the greatest average movement rate (3.80% and 101m). The most apt conclusion that may be inferred from the data presented in this project is that each glacier acted independently of other glaciers and each glacier's movement is the result of the input from many variables.

Simply considering rates of change and glacier slopes for Baird, Patterson, LeConte, and Shakes Glaciers is insufficient to determine if any particular terminal terrain condition is more conducive to glacier position change. Rather, other variables, such as glacier cross-section, glacier valley profile, and direction of flow should be considered. For example, Shakes Glacier's glacial valley is physically straighter than Baird, Patterson, or LeConte Glaciers' and contained no bottlenecks to restrict the flow of ice. While Shakes Glacier had the greatest average movement rate of 101m, it only had 3.80% slope; this relationship is contrary to what is expected (Waddington, 2009).

CHAPTER SIX: CONCLUSIONS AND SUGGESTED COMPLIMENTARY STUDIES

6.1 Conclusions

This project initially assumed that there would be a correlation between glacier movement rate and glacier slope. However, the results did not conclusively support this assumption. Shakes Glacier had the greatest average yearly movement rate of 101m, but had a very slight slope of 3.80%. Conversely, LeConte Glacier had much a smaller average yearly movement rate of 43m but had the greatest slope of 9.20%. Glacier movement rates and slope values are summarized in Table 18. Based upon these findings, it must be assumed that factors other than slope affect glacier movement.

While no definitive relationship between glacier slope and average movement rates could be established, there did appear to be a relationship between increased average movement rates and glacier terminuses that were located in water. Referring to Table 18, Baird Glacier, whose terminus is located on land, had the lowest average movement rate of 16m. LeConte Glacier, with a terminus located in salt water, had a higher yearly average movement rate of 43m. Patterson and Shakes Glaciers, which both end in fresh water, had the greatest average yearly movement rates of 60m and 101m respectively. Based upon these findings, the presence of water, especially fresh water, at the terminal end of glaciers had a greater effect on glacier movement than slope. Possible explanations for this effect might include a heat sink effect or tidal motions that hasten glacier disintegration in the ablation zone. In a heat sink scenario, it is hypothesized that the water bodies that LeConte, Patterson, and Shakes Glaciers terminus are located in act as a thermal energy transfer medium that increases glacier melting and subsequent retreat. Helmenstine (2014) proposes that the increased molecular density of water versus ice and

the nature of thermal energy to move from areas of higher concentration to areas of lower concentration are largely responsible for water induced glacial ice melting. Tidal motions hypothetically act as horizontal and vertical push/pull forces, which increase the fracturing rate, calving, and subsequent retreat of LeConte Glacier. Walter et al. (2012) discovered that tidal influences on a marine-terminating Greenland glacier significantly affected glacier ablation. Further studies are necessary to test these hypotheses to determine if a heat sink effect and tidal motions significantly affect the movement rates for the glaciers in this study. Over the length of the study period, there was 0.85°C increase in annual air temperatures. While this value may seem low, Davies (2014) was able to force a change in a glacier prediction model using only 0.5°C change in temperature. This temperature increase of 0.85°C may prove important when determining glacial mass balance rates.

A significant result of this study is the creation of shapefiles delineating the positions of Shakes Glaciers in the Global Land Survey (GLS) dataset time periods. These shapefiles can be submitted to the Global Land Ice Measurements from Space (GLIMS) program for inclusion in their master worldwide glacier database, which currently does not include Shakes Glacier. Although the submission process for the shapefile is not included in the thesis, it is ongoing, and general information is deferred to the GLIMS site and possibly available within six months from the time of this writing. This information should be useful to other researchers and its inclusion in GLIMS would insure that they could readily access information about Shakes Glacier.

6.2 Lessons learned

This project was analytically challenging. The self-imposed constraint of using the GLS datasets was both beneficial and problematic. From a historical perspective, the GLS datasets

provided an un-parallel source of multispectral imagery. The disadvantage to this dataset is the 30m spatial resolution (60m for GLS°975). Although the false-color shortwave infrared composite (RGB 4, 5, 7) was invaluable for determining the extent of clean glacial ice, it had difficulty in determining the extent of dirty ice. Dirty ice, with its large concentration of rock and soil, exhibited spectral properties similar to the bare ground and soil that surrounds the periphery of the glacier terminus. Differentiating the extent of glacial ice with this visual analysis alone was often insufficient.

Image band combinations, like the false-color shortwave infrared composite (RGB: 4, 5, 7), and the true color composite (RGB: 3, 2, 1); unsupervised classifications; and individual image bands, like the near infrared (Band 4), were often difficult to interpret and could not be used exclusively to delineate glacier terminuses. Often, the line between glacial ice and surrounding terrain was indistinct. Determining each terminus required constantly switching between the various composite images and image bands to verify whether each pixel at a glacier's terminus represents a point on a glacier's terminus. This method was time consuming and each glacier terminus was revised several times before the results were acceptable.

The Global Land Ice Measurements from Space (GLIMS) data did not match the GLS dataset very well, as discussed in Section 5.3. For example, the GLIMS data for LeConte Glacier was determined from the GLS2005 dataset. When the GLIMS data was overlaid on the GLS2005 imagery, the difference between the terminuses of LeConte Glacier was off in several places by hundreds of meters. Areas that GLIMS indicates as ice was in fact bare ground and vice-versa. It is important to note, that an authoritative data source, like GLIMS, can also potentially have errors and should be used cautiously.

Iterative Self-Organizing (ISO) Data Cluster Unsupervised Classification methods were useful but were often difficult to interpret. Often, the process resulted in misclassified image pixels which required traditional image interpretation skills to assess the validity. It was often the case that a particular pixel was examined in multiple images to determine if it was glacial ice. This was tedious and required a considerable investment in time to accomplish. More often than not, resulting classes were not pure and had to be labeled based upon the most prevalent feature in that class. Despite the many challenges that were presented during the course of this project, it should be noted that all imagery and other geospatially enabled data was free.

6.3 Suggested complimentary studies

There are large differences in glacier movement values that resulted from this project, as summarized in Table 14. Although the goal of the project was not seeking to specifically determine why there was such high rate of variability, considerations were made based on terrain conditions and slope. It is clear that considering only terminal terrain conditions and slope is insufficient to determine whether one terminal terrain condition is more conducive to glacier movement than another. Additional studies should be attempted to determine other variables that could affect glacier movement in this area, for which suggestions are provided below.

For example, it is well established that glaciers respond to changes in climate conditions. Glacier lag and response times are unique to each glacier (Pelto et al., 2001). Establishing a particular glacier's lag and response time requires a thorough understanding of its mass balance change rate (Davies, 2014). Research suggests that mass balance change rates have yet to be established definitively for Baird, Patterson, LeConte or Shakes Glaciers. If lag and response

times were determined for these Glaciers, it might offer some insight into the movement patterns for these glaciers.

This study considered air temperature in the context that warming trends could explain the movement patterns of the glaciers in the study (Waddington, 2009). This historical data was collected from a weather station in Petersburg, Alaska, which is approximately 30km to the west of the study area. Establishing on-site meteorological collection equipment would provide more useful data. In addition to weather data, collecting water temperature data for Patterson, LeConte, and Shakes Glaciers would be useful to test for any heat-sink effect.

Another factor that contributes to glacier movement rates is subsurface bed composition and profile (Michna, 2012). Technologies like ground penetrating radar can be used to examine these characteristics. Understanding the physical characteristics of the channel that each glacier flows through may help to explain movement patterns.

Glaciers change shape and size simultaneously in three dimensions: length, width, and thickness. This study only considered length; additional studies should consider change in all dimensions. Newer technologies, like Light Detection and Ranging (LiDAR), would be very useful for determining the three-dimensional shape of each glacier. A limiting factor of LiDAR surveys is that the sensors must be able to "see" the ground to sense it. The study area, located in the Tongass, was often obscured from satellite observation due to overcast, misty, or rainy weather conditions (Sections 2.1 and 3.1). These same weather conditions precluded high flying aircraft for LiDAR surveys. The steep terrain (Section 2.1) also precluded low flying survey aircraft due to the operational risk for aircraft operating in steep, often ascending terrain. Because

of these difficulties, it may be necessary to identify a new type of aerial platform that is capable of cost-effectively surveying glaciers in remote settings and with minimal risk to human life.

REFERENCES

Aher, Sainath P. and Sanjaykumar Dalvi. 2012. "Remote Sensing Techniques for Monitoring the Glacier Retreating Process and Climatic Changes Study." *Indian Streams Research Journal* 2 (8). Accessed October 1, 2012. http://www.isrj.net/PublishArticles/1200.pdf.

Alaska Climate Research Center. 2010. "Alaska Climatology." Fairbanks: Alaska Climate Research Center. Accessed January 31, 2013. http://climate.gi.alaska.edu/Climate/index.html.

Alaska Department of Fish and Game. 2012. "Commercial Fisheries." Juneau: Alaska Department of Fish and Game. Accessed November 22, 2012. http://www.adfg.alaska.gov/index.cfm?adfg=fishingcommercial.main.

Alaska Department of Fish and Game. 2012. "Southcentral." Juneau: Alaska Department of Fish and Game. Accessed November 22, 2012. http://www.adfg.alaska.gov/index.cfm?adfg=fishingCommercialByArea.southcentral.

Alaska Humanities Forum. 2013. "The Geography of Alaska: Places and Regions." Anchorage: Alaska Humanities. Accessed February 15, 2013. http://www.akhistorycourse.org/articles/article.php?artID=122.

Alesheikh, A. A., A. Ghorbanali, and N. Nouri. 2007. "Coastline Change Detection using Remote Sensing." *International Journal of Environmental Science and Technology: (IJEST)* 4 (1): 61-66. Accessed October 1, 2012. http://search.proquest.com/docview/199331137?accountid=14749.

ArcGIS (Version 10.2) [Software]. (2013). Redlands: Environmental Systems Research Institute, Inc. Retrieved from http://www.esri.com/.

Arendt, A., T. Bolch, J.G. Cogley, A. Gardner, J.-O. Hagen, R. Hock, G. Kaser, W.T. Pfeffer, G. Moholdt, F. Paul, V. Radić, L. Andreassen, S. Bajracharya, M. Beedle, E. Berthier, R. Bhambri, A. Bliss, I. Brown, E. Burgess, D. Burgess, F. Cawkwell, T. Chinn, L. Copland, B. Davies, H. De Angelis, E. Dolgova, K. Filbert, R. Forester, A. Fountain, H. Frey, B. Giffen, N. Glasser, S. Gurney, W. Hagg, D. Hall, U.K. Haritashya, G. Hartmann, C. Helm, S. Herreid, I. Howat, G. Kapustin, T. Khromova, C. Kienholz, M. Koenig, J. Kohler, D. Kriegel, S. Kutuzov, I. Lavrentiev, R. LeBris, J. Lund, W. Manley, C. Mayer, E. Miles, X. Li, B. Menounos, A. Mercer, N. Moelg, P. Mool, G. Nosenko, A. Negrete, C. Nuth, R. Pettersson, A. Racoviteanu, R. Ranzi, P. Rastner, F. Rau, B.H. Raup, J. Rich, H. Rott, C. Schneider, Y. Seliverstov, M. Sharp, O. Sigurðsson, C. Stokes, R. Wheate, S. Winsvold, G. Wolken, F. Wyatt, and N. Zheltyhina. 2012. "Randolph Glacier Inventory [v2.0]: A Dataset of Global Glacier Outlines." Boulder: Global Land Ice Measurements

from Space. Accessed February 26, 2011. http://www.glims.org/RGI/RGI_Tech_Report_V2.0.pdf.

Bahr, David B., W. Tad Pfeffer, Christophe Sassolas, and Mark F. Meier. 1998. "Response Time of Glaciers as a Function of Size and Mass Balance." *Journal of Geophysical Research* 103 (B5): 9777-9782.

Baolin, Li, Zhang Yichi, and Zhou Chenghu. 2004. "Remote Sensing Detection of Glacier Changes in Tianshan Mountains for the Past 40 Years." *Journal of Geographical Sciences* 14 (3): 296-302.

Beuchle, Rene, Hugh D. Eva, Hans-Jürgen Stibig, Catherine Bodar, Andereas Brink, Philippe Mayaux, Desiree Johansson, Frederic Achard, and Alan Belward. 2011. "A Satellite Dataset for Tropical Forest Area Change Assessment." *International Journal of Remote Sensing* 32 (22): 7009-7031. doi:10.1080/01431161.2011.611186.

Bieniek, Peter A., Uma S. Bhatt, Richard L. Thoman, Heather Angeloff, James Partain, John Papineau, Frederick Fritsch, Eric Holloway, John E. Walsh, Christopher Daly, Martha Shulski, Gary Hufford, David F. Hill, Stavros Carlos, and Rudiger Gens. 2012. "Climate Zones of Alaska." *Journal of Applied Meteorology and Climatology* 51: 1276-1289.

Billington, James H. 2013. "America's Story." Washington: Library of Congress. Accessed March 6, 2013. http://www.americaslibrary.gov/jb/recon/jb_recon_alaska_1.html.

Bishop, Michael P., Jeffrey A. Olsenholler, John F. Shroder, Roger G. Barry, Bruce H. Raup, Andrew B. G. Bush, Luke Copland, John L. Dwyer, Andrew G. Fountain, Wilfried Haeberli, Andreas Kääb, Frank Paul, Dorothy K. Hall, Jeffrey S. Kargel, Bruce F. Molnia, Dennis C. Trabant, and Rick Wessels. 2004. "Global Land Ice Measurements from Space (GLIMS): Remote Sensing and GIS Investigations of the Earth's Cryosphere." *Geocarto International* 19 (2): 57-74. Accessed February 26, 2013. http://www.geocarto.com.hk/cgi-bin/pages1/june04/bishop.pdf.

Boyce, Eleanor S., Roman J. Motyka, and Martin Truffer. 2007. "Flotation and Retreat of a Lake-Calving Terminus, Mendenhall Glacier, Southeast Alaska, USA." *Journal of Glaciology* 53 (181): 211-224. doi: 10.3189/172756507782202928.

Bruland, Kris. 2014. "Petersburg, Alaska Tides." Coupeville: Admiralty Software, LLC. Accessed March 14, 2014. http://www.americantides.com/tide-predictions/petersburg-alaska.

Campbell, James B. and Randolph H. Wynne. 2011. “Introduction to Remote Sensing.” 5th Edition. New York & London: The Guilford Press.

Canadian Space Agency. 2013. “RADARSAT-1.” Saint-Hubert: Canadian Space Agency. Accessed November 30, 2013. http://www.asc-csa.gc.ca/eng/satellites/radarsat1/components.asp.

Cape Decision Lighthouse Society. 2013. “Tongass Facts.” Sitka: Cape Decision Lighthouse Society. Accessed February 11, 2013. http://capedecisionlight.org/Tongass-facts.html.

Davies, Bethan. 2014. “Glacier Response Time.” Antarctic Glaciers.org. Accessed February 12, 2013. http:// antarcticglaciers.org/glaciers-and-climate/glacier-response-time/.

Earth Resources Observation and Science Center. 2012. “Global Land Survey (GLS).” Washington: United States Geological Survey. Accessed February 22, 2013. http://eros.usgs.gov/#/Find_Data/Products_and_Data_Available/GLS.

Environmental Systems Research Institute, Inc. 2013. “Online base map data.” Redlands: Environmental Systems Research Institute. Accessed February 11, 2013. http://www.esri.com/.

Frery, Alejandro C., Susana Ferrero, and Oscar H. Bustos. 2009. "The Influence of Training Errors, Context and Number of Bands in the Accuracy of Image Classification." *International Journal of Remote Sensing* 30 (6): 1425-1440. Accessed October 1, 2012. doi:10.1080/01431160802448919.

Geophysical Survey Systems, Inc. 2012. “Ground Penetrating Radar for Ice and Snow Profiling”. Salem: Geophysical Survey Systems, Inc. Accessed December 2, 2013. http://www.geophysical.com/directionstogssi.htm.

GLIMS: Global Land Ice Measurements from Space. 2007. “GLIMS Impacts.” Boulder: National Snow and Ice Data Center. Accessed February 26, 2013. http://www.glims.org/About/impacts.html.

GLIMS: Global Land Ice Measurements from Space. 2013. “Home Page.” Boulder: National Snow and Ice Data Center. Accessed February 28, 2013. http://www.glims.org/.

Gutman G, R. Byrnes, J. Masek, S. Covington, C. Justice, S. Franks, and R. Headley. 2008. “Towards monitoring land cover and land use changes at a global scale: the global land survey 2005.” Photogrammetric Engineering & Remote Sensing 74 (1): 6–10. Accessed March 10, 2013. http://gls.umd.edu/documents/GLS_2005_PERS_Jan2008_Gutman.pdf.

Haq, NM Anul, Kamal Jain, and KPR Menon. 2012. "Change Monitoring of Gangotri Glacier using Remote Sensing." *International Journal of Soft Computing & Engineering* 1 (6): 259-261.

Haritashya, Umesh K., Michael P. Bishop, John F. Shroder, Andrew B. Bush, G., Henry N. Bulley, and N. 2009. "Space-Based Assessment of Glacier Fluctuations in the Wakhan Pamir, Afghanistan." *Climatic Change* 94 (1-2): 5-18. doi:10.1007/s10584-009-9555-9.

Harper, Joel T. 1993. "Glacier Terminus Fluctuations on Mount Baker, Washington, U.S.A., 1940-1990, and Climatic Variations." *Arctic and Alpine Research* 25 (4) 332-340. Accessed February 13, 2014. http://www.jstor.org/stable/1551916.

Hekkers, Michael. 2010. "Mendenhall Glacier Science." Juneau: University of Alaska Southeast. Accessed November 19, 2012. http://www.uas.alaska.edu/arts_sciences/naturalsciences/envs/links.html.

Helmenstine, Anne Marie. 2014. "Does Ice Melt Faster in Water or Air." About.Com Chemistry. Accessed March 14, 2014. http://chemistry.about.com/od/howthingswork/f/ice-melt-faster-water-air.htm.

Hood, Eran., Jason Fellman, Robert G. M. Spencer, Peter J. Hernes, Rick Edwards, David D'Amore, and Durelle Scott. 2009. "Glaciers as a Source of Ancient and Labile Organic Matter to the Marine Environment." *Nature* 462 (24): 1044-7. Accessed October 1, 2012. doi:10.1038/nature08580.

Irons, James R. 2013. "The Worldwide Reference System." Washington: National Aeronautics and Space Administration. Accessed February 23, 2013. http://landsat.gsfc.nasa.gov/about/wrs.html.

Jet Propulsion Laboratory. 2013. "ASTER Advanced Spaceborne Thermal Emission and Reflection Radiometer." Pasadena: Jet Propulsion Laboratory at California Institute of Technology. Accessed November 30, 2013. http://asterweb.jpl.nasa.gov/.

Justice, Chris. 2013. "Global Land Survey." College Park: National Aeronautics and Space Administration: Land-Cover and Land-Use Change. Accessed February 23, 2013. http://gls.umd.edu/index.html.

Kim, Yonl-Il, Yang-Dam Eo, and Byoung-Kil Lee. 1999. "Analyzing the Spatial Distribution Pattern of Image Classification Error." *Journal of the Japan Society of Photogrammetry and Remote Sensing* 38 (2): 53-60.

Klibanoff, Peter, Alvaro Sandroni, Boaz Moselle, and Brett Saraniti. 2005. "Managerial Statistics: A Case-Based Approach." 1st Edition. Cincinnati: South-Western College Pub.

Krenke, A. N. and V.M. Menshutin. 1987. "Calculation of Mass Balance of Glaciers by Remote-Sensing Imagery Using Similarity of Accumulation and Ablation Isoline Patterns." *Journal of Glaciology* 33 (115): 363-368.

Lillesand, Thomas M., Ralph W. Kiefer, and Jonathan W. Chipman. 2008. "Remote Sensing and Image Interpretation." 6th Edition. New York: John Wiley & Sons, Inc.

Lindquist, E. J., M. C. Hansen, D. P. Roy, and C. O. Justice. 2008. "The Suitability of Decadal Image Datasets for Mapping Tropical Forest Cover Change in The Democratic Republic of Congo: Implications for the Global Land Survey." *International Journal of Remote Sensing*." 29 (24): 7269-7275. doi: 10.1080/01431160802275890.

Masek, Jeff. 2011. "LEDAPS." Washington: National Aeronautics and Space Administration. Accessed February 24, 2013. http://ledaps.nascom.nasa.gov/.

Meier, M. F., and Austin Post. 1986. "Fast Tidewater Glaciers." *Journal of Geophysical Research*. 92 (B9): 9051-9058. Accessed February 12, 2014. doi: 10.1029/JB092iB09p09051.

Michna, Paul. 2012. "Glaciers." Earth Science Australia. Accessed March 21, 2013. http://earthsci.org/education/teacher/basicgeol/glacier/glacier.html#MovementofGlaciers.

Microsoft Excel (Version 10) [Software]. (2010). Redmond: Microsoft Corporation, Inc. Retrieved from http://www.microsoft.com/en-us/default.aspx.

Molnia, B.F., 2008. Glaciers of North America -- Glaciers of Alaska, *in* Williams, R.S., Jr., and Ferrigno, J.G., eds., Satellite image atlas of glaciers of the world: U.S. Geological Survey Professional Paper 1386-K, 525 p. Accessed March 1, 2013. http://pubs.usgs.gov/pp/p1386k/.

Motyka, Roman J., Shad O'Neel, Cathy L. Connot, and Keith A. Echelmeyer. 2003. "Twentieth Century Thinning of Mendenhall Glacier, Alaska, and its Relationship to Climate, Lake Calving, and Glacier Run-off." *Global and Planetary Change.* 35 (1-2): 93-112. doi: 10.1016/S0921-8181(02)00138-8.

Muralidhar, Ashwini. 2011. "Augmented Image Classification using Image Registration Techniques." M.S., Arizona State University. Accessed October 1, 2012.

National Aeronautics and Space Administration. 2012. “From the Beginning.” Washington: National Aeronautics and Space Administration. Accessed November 19, 2012. http://landsat.gsfc.nasa.gov/history.html.

National Ocean Service. 2013. “LIDAR-Light Detection and Ranging-is a Method to Examine the Surface of the Earth.” Silver Spring: National Oceanic and Atmospheric Administration’s National Ocean Service. Accessed November 30, 2013. http://oceanservice.noaa.gov/facts/lidar.html.

National Snow and Ice Data Center. 2013. “Programs and Projects ant NSIDC.” Boulder: National Snow and Ice Data Center. Accessed February 25, 2013. http://nsidc.org/programs/.

National Snow and Ice Data Center. 2013. “Submit Data.” Boulder: National Snow and Ice Data Center. Accessed February 25, 2013. http://nsidc.org/data/submit.html.

Noderer, Michael. 2010. *Intermediate Spectral Exploitation and Analysis Course II (ISEA-II)*. Springfield: National Geospatial-Intelligence Agency, National Geospatial-Intelligence College.

Noderer, Michael. 2007. *Remotely Sensed Imagery Course (RSI)*. Fort Belvoir: National Geospatial-Intelligence Agency, National Geospatial-Intelligence College.

Patra, Swarnajyoti, Susmita Ghosh, and Ashish Ghosh. 2011. "Histogram Thresholding for Unsupervised Change Detection of Remote Sensing Images." *International Journal of Remote Sensing* 32 (21): 6071-6089. Accessed October 1, 2012. doi:10.1080/01431161.2010.507793.

Pelto, Mauri S. and Cliff Hedlund. 2001. “Terminus Behavior and Response Time of North Cascade Glaciers, Washington, U.S.A.” *Journal of Glaciology* 47 (158): 497-506. Accessed February 12, 2014. doi: 10.3189/172756501781832098.

Pidwirny, Michael and Scott Jones. 2010. “Physical Geography.net: Glossary of Terms.” Okanagan: University of British Columbia. Accessed March 6, 2013. http://www.physicalgeography.net/physgeoglos/i.html.

Quincey, D. J. and A. Luckman. 2009. "Progress in Satellite Remote Sensing of Ice Sheets." *Progress in Physical Geography* 33 (4): 547-567.

Raper, Sarah C. B. and Roger J. Braithwaite. 2006. "Low Sea Level Rise Projections from Mountain Glaciers and Icecaps Under Global Warming." *Nature* 439 (7074): 311-3.

doi:http://dx.doi.org/10.1038/nature04448. http://search.proquest.com/docview/204516467?accountid=14749. Raup, Bruce, Andreas Kääb, Jeffrey S. Kargel, Michael P. Bishop, Gordon Hamilton, Ella Lee, Frank Paul, Frank Rau, Deborah Soltesz, Siri Jodha Singh Khalsa, Mathew Beedle, and Christopher Helm. 2007. "Remote Sensing and GIS Technology in the Global Land Ice Measurements from Space (GLIMS) Project." *Computers & Geosciences* 33 (1): 104-125. Accessed October 1, 2012. doi:10.1016/j.cageo.2006.05.015.

Raup, Bruce, Andreas Kääb, Jeffrey S. Kargel, Michael P. Bishop, Gordon Hamilton, Ella Lee, Frank Paul, Frank Rau, Deborah Soltesz, Siri Jodha, Singh Khalsa, Mathew Beedle, and Christopher Helm. 2007. "Remote Sensing and GIS Technology in the Global Land Ice Measurements from Space (GLIMS) Project." *Computers and Science* 33(2007): 104-125. doi: 10.1016/j.cageo.2006.05.015.

Schweiker, Roy and David Olson. 2012. "U.S. National Forest High Point." Accessed February 20, 2013. http://www.peakbagger.com/list.aspx?lid=1825.

Sharma, Bharat R., Upali A. Amarasinghe, and Alok Sikka. 2008. "Indo-Gangetic River Basins: Summary Situation Analysis." *International Water Management Institute*. New Delhi Office, New Delhi, India.

Shukla, A., M. K. Arora, and R. P. Gupta. 2010. "Synergistic Approach for Mapping Debris-Covered Glaciers using optical–thermal Remote Sensing Data with Inputs from Geomorphometric Parameters." *Remote Sensing of Environment* 114 (7): 1378-1387. Accessed October 1, 2012. doi:10.1016/j.rse.2010.01.015.

Space Sciences Laboratory. 2013. "SETI@Home." Berkley: University of California. Accessed February 1, 2013. http://setiathome.ssl.berkley.edu/.

State of Alaska Department of Labor and Workforce Development. 2013. "Research and Analysis." Juneau: State of Alaska Department of Labor and Workforce Development. Accessed February 11, 2013. http://labor.alaska.gov/research/census/maps.htm.

State of Alaska Department of Natural Resources. 2012. "ASGDC: Alaska State Geo-Spatial Data Clearinghouse." Anchorage: State of Alaska Department of Natural Resources. Accessed February 28, 2013. http://www.asgdc.state.ak.us/.

Tappan, Ray and Matthew Cushing. 2004. Use of SLC-Off Landsat Image Data for Monitoring Land use / Land Cover Trends in West Africa. Sioux Falls, SD: United States Geological Survey.

Théau, Jérôme. 2012. "Change Detection." In *Springer Handbook of Geographic Information*, 75-94. Berlin, Heidelberg: Springer Berlin Heidelberg.

United States Census Bureau. 2013. “American Fact Finder.” Washington: United States Census Bureau. Accessed February 11, 2013. http://factfinder2.census.gov/faces/nav/jsf/pages/index.xhtml.

United States Department of Agriculture, Forest Service. 2013. “About the Forest.” Washington: United States Department of Agriculture, Forest Service. Accessed January 31, 2012. http://www.fs.usda.gov/main/tongass/about-forest.

United States Department of Agriculture, Forest Service Geospatial Service and Technology Center. 2013. “FSGeoData Clearing House.” Salt Lake City, United States Department of Agriculture Forest Service Geospatial Service and Technology Center. Accessed February 10, 2013.

United States Geological Survey. 2013. “Earth Explorer Data Portal.” Washington: United States Geological Survey. Accessed February 23, 2013. http://earthexplorer.usgs.gov/.

United States Geological Survey. 2012. “Glaciers and Icecaps: Storehouses of Freshwater.” Washington: United States Department of the Interior, United States Geological Survey. Accessed October 1, 2012. http://ga.water.usgs.gov/edu/earthglacier.html.

United States Geological Survey. 2013. “Global Land Survey.” Washington: United States Geological Survey. Accessed February 20, 2013 with Earth Explorer Data Portal. http://earthexplorer.usgs.gov/.

United States Geological Survey. 2012. “Landsat: A Global Land-Imaging Mission.” Sioux Falls: United States Geological Survey. Accessed February 23, 2013. http://pubs.usgs.gov/fs/2012/3072/fs2012-3072.pdf.

United States Geological Survey. 2013. “Landsat Missions.” Reston: United States Geological Survey. Accessed November 30, 2013. http://landsat.usgs.gov/.

United States Geological Survey. 2013. “The USGS Land Cover Institute (LCI).” Washington: U.S. Department of the Interior, U.S. Geological Service. Accessed February 28, 2013. http://landcover.usgs.gov/.

University of Alaska Fairbanks. 2012. “Alaska Mapped and the Statewide Digital Mapping Initiative.” Fairbanks: University of Alaska Fairbanks. Accessed February 15, 2013. http://www.alaskamapped.org/.

Waddington, Ed. 2009. “Principles of Glaciology ESS 431.” Seattle: University of Washington. Accessed March 20, 2013. http://courses.washington.edu/ess431/Lectures/lecture_2009/Lect_07_Glacier_flow_2009.pdf.

Walter, Jacob I., Jason E. Box, Slawek Tulaczyk, Emily E. Brodsky, Ian M. Howat, Yushin Ahn, and Abel Brown. 2012. “Oceanic Mechanical Forcing of a Marine-Terminating Greenland Glacier.” *Annals of Glaciology* 53(60): 1-12. Accessed March 14, 2014. doi: 10.3189/2012AoG60A083.

Western Regional Climate Center. 2013. “Climate Zones of Alaska.” Reno: Western Regional Climate Center. Accessed January 31, 2013. http://www.wrcc.dri.edu/narratives/ALASKA.htm.

Wolfe, Robert, Jeffrey Masek, Nazmi Saleous, and Forest Hall. 2004. “LEDAPS: Mapping North American Disturbance from the Landsat Record.” Greenbelt: National Aeronautics and Space Administration: Goddard Space Flight Center. Accessed February 24, 2013. http://ledaps.nascom.nasa.gov/docs/pdf/ledaps_igarss04.pdf.

APPENDIX A: GLOBAL LAND SURVEY (GLS) DATA SOURCING AND DOWNLOAD

This appendix provides a step-by-step process flow for locating and downloading GLS datasets.

Locating Global Land Survey (GLS) data

Data source: The GLS data was downloaded using the United States Geological Survey's Earth Explorer web portal (United States Geological Survey, 2013). The uniform resource locator (URL) for Earth Explorer is http://earthexplorer.usgs.gov/.

Cost: There is no cost to download data from this service. However, I could not do it anonymously; rather I had to create a user profile that identified 1) who I am and 2) why I am using this data. This type of information usually allows the site administrator to generate site statistics that can be used to justify future funding or service improvements.

Downloading GLS data

Downloading GLS data is a twelve-step process. Refer to Figures 39-44 for step-by-step instructions on accomplishing this.

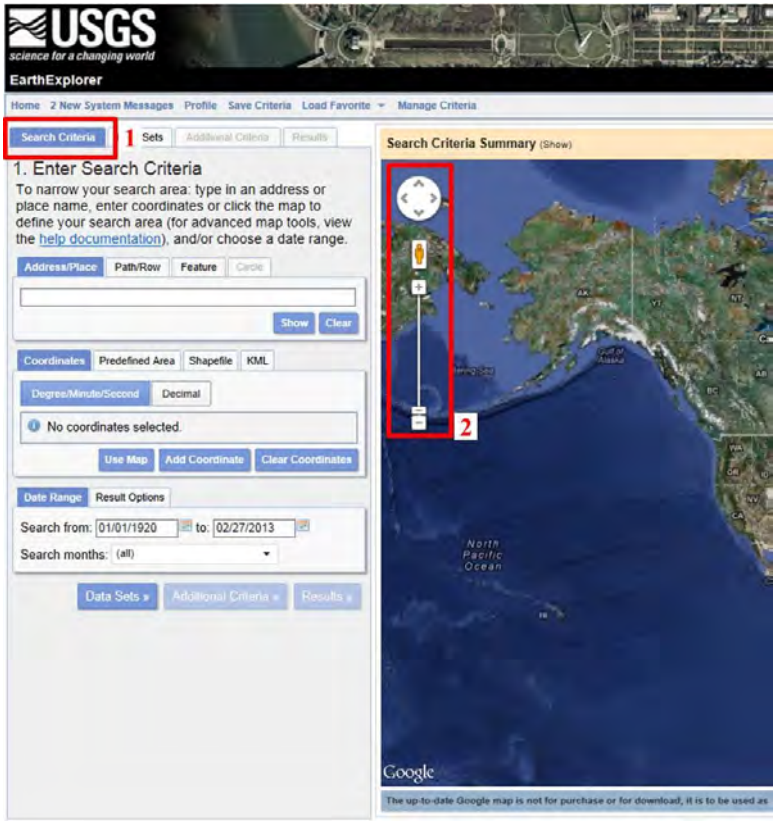

Figure 40. United States Geological Survey (USGS) Earth Explorer home page is the starting point for downloading GLS datasets. 1: select the "Search Criteria" tab; 2: scale the display map into the study area using the pan and zoom tools.

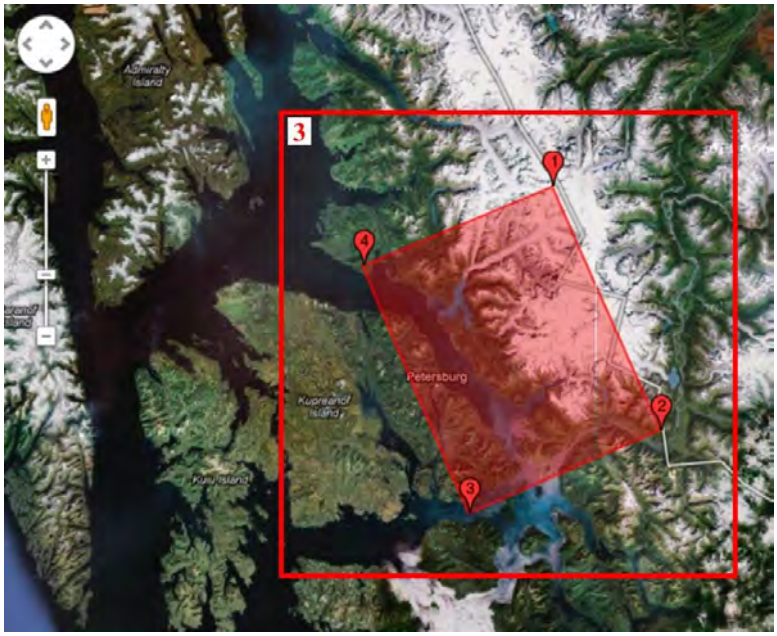

Figure 41. Define the area of interest for GLS image searches. 1: loosely bound the project study area by left-clicking to form a polygon area of interest (AOI); outlined by the red box labeled. The labels for each of the vertices correspond to the order in which the AOI is defined.

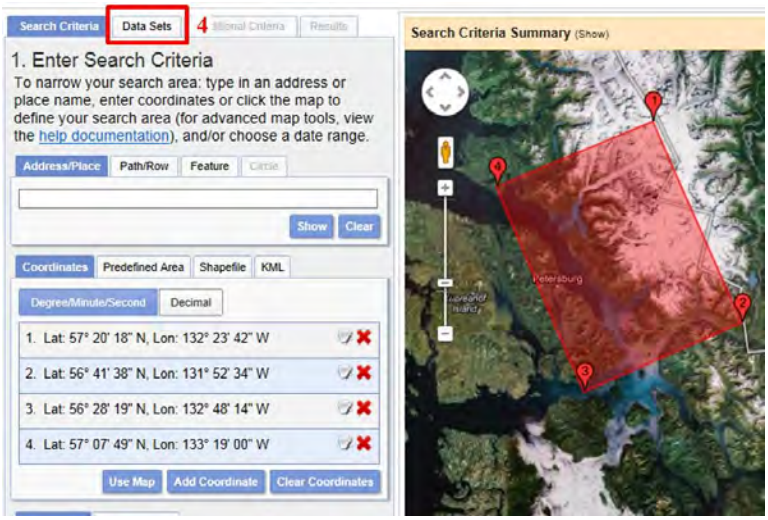

Figure 42. Switch from AOD definition to dataset(s) selection. 4: select the "Data Sets" tab.

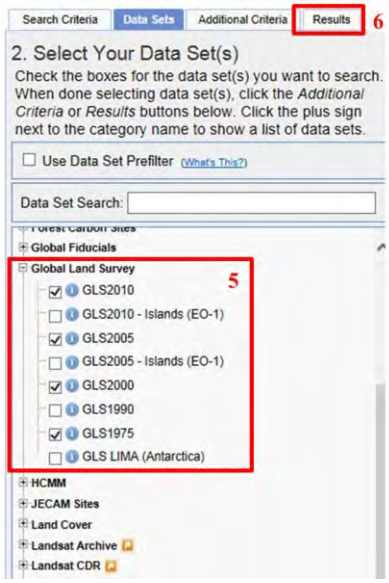

Figure 43. Specify the datasets for downloading. 5: in the dataset list, expand the "Global Land Survey" data list and select the desired datasets; 6: select the "Results" tab.

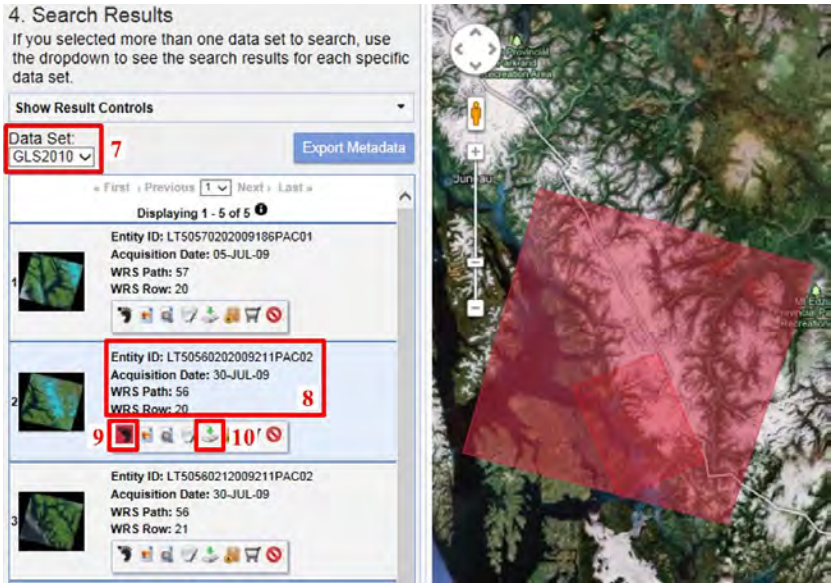

Figure 44. Earth Explorer search results page. This page displays the available data for the area of interest. If multiple datasets were specified in Step 5 (Figure 53), then only one may be displayed at a time. 7: select a dataset to view images for; 8: image metadata summary with WRS path and row address and date of image collection; 9: image footprint allows for visual confirmation of image location; 10: image download button. Table 22 summarizes relevant image information for the various GLS datasets used for this study.

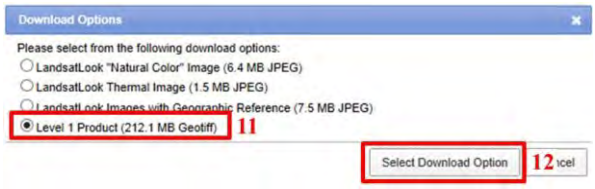

Figure 45. GLS data download options. 11: Level 1 Product is selected. For this dataset, the file size is 212.1 MB and is in Geotiff format. 12: "Select Download Option" button will begin the download process.

The GLS data files are very large, in the case of GLS2010 data, that size is approximately 212 MB (Figure 44). The data file is compressed in a **T**ape **AR**chive (.**tar**) format. WinRAR software was used to un-compress the data. For the GLS2010 data, the un-compressed size is 481MB. Large datasets like the GLS data can quickly use computer resources and may require careful planning to ensure that these datasets can be used. As a comparison, a digital video disk (DVD) can only store approximately eight GLS data scenes. Table 22 summarizes the image details for all five GLS datasets. After downloading the GLS2010 dataset, GLS2005, GLS2000, GLS1990, and GLS1975 datasets were downloaded in a similar manner by simply changing the "Dataset" choice (Figure 43, Step "7") and following all subsequent steps.

Table 22. Image details for Global Land Survey (GLS) datasets summary for Central Southeast Alaska Glacier Study Project area.

GLS Dataset	Entity ID	Acquisition Date	WRS Path	WRS Row	Download Option	Un-compressed Size (MB)
GLS2010	LT50570202009186PAC01	July 30, 2009	56	20	Level 1 Product	481
GLS2005	LE70560202005224EDC00	August 12, 2005	56	20	Level 1 Product	636
GLS2000	P056R020_7X19990812	August 12, 1999	56	20	Level 1 Product	656
GLS1990	P056R020_5X19890909	September 9, 1989	56	20	Level 1 Product	391
GLS1975	P060R020_1X19740903	September 3, 1974	60	20	Level 1 Product	70
					Total	2234

APPENDIX B: GLOBAL LAND ICE MEASUREMENTS FROM SPACE (GLIMS) DATA SOURCING AND DOWNLOAD

This appendix provides a step-by-step process flow for locating and downloading GLIMS datasets.

Locating Global Land Ice Measurements from Space (GLIMS) data

Data source: The GLIMS data was downloaded using the National Snow and Ice Data Center's (NSIDC) GLIMS Glacier Viewer web portal (GLIMS: Global land Ice Measurements from Space, 2013). The uniform resource locator (URL) for GLIMS: Global Land Ice Measurements from Space is http://glims.org/.

Cost: There is no cost to download data from this service. Unlike Earth Explorer, no login is required.

Downloading GLIMS data

Downloading GLIMS data is an eight-step process. Refer to Figures 45-49 for step-by-step instructions on accomplishing this.

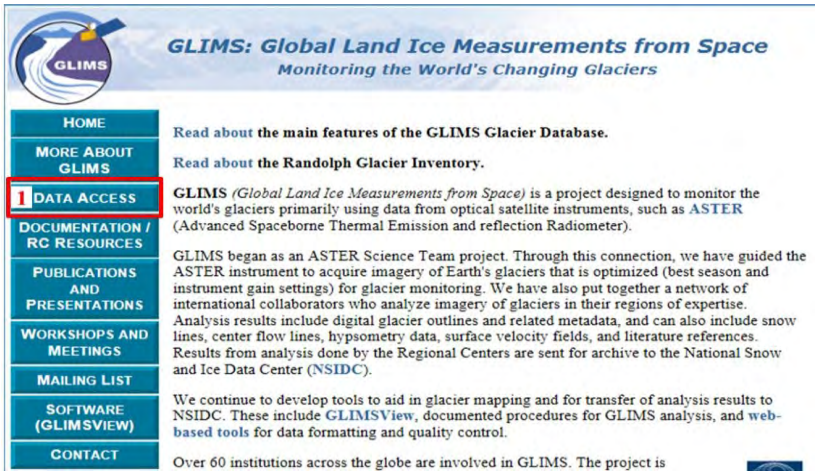

Figure 46. Global Land Ice Measurements from Space (GLIMS) home page. 1: select "Data Access" button that will take the user to a screen where GLIMS data can be downloaded.

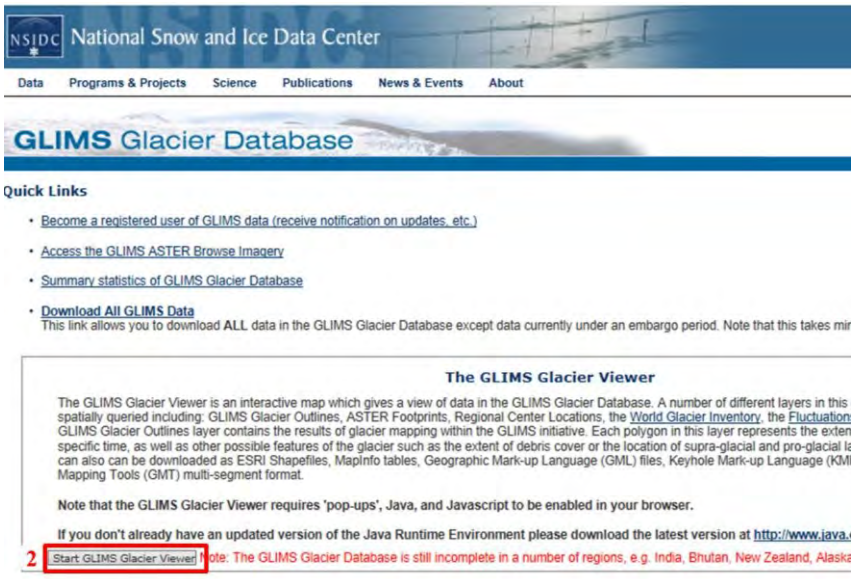

Figure 47. GLIMS glacier database home page. 2: select "Start GLIMS Glacier Viewer" to proceed to the online data search portal.

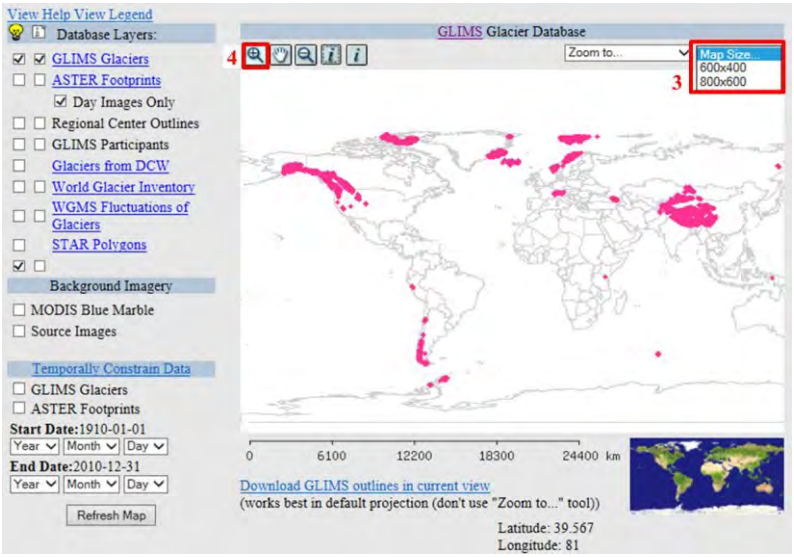

Figure 48. GLIMS glacier database graphical summary page for the entire world. 3: change the map size to "800x600"; 4: use the zoom tool to go to area of interest.

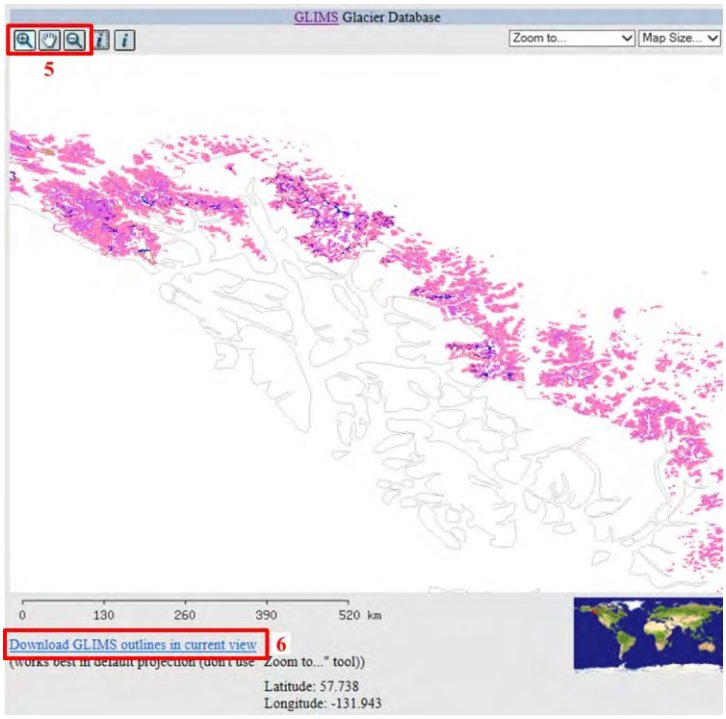

Figure 49. GLIMS glacier database graphical summary for display window. Glaciers are shown as magenta outlines. 5: pan and zoom tools to refine area of interest; 6: download button to download all glaciers in current extent.

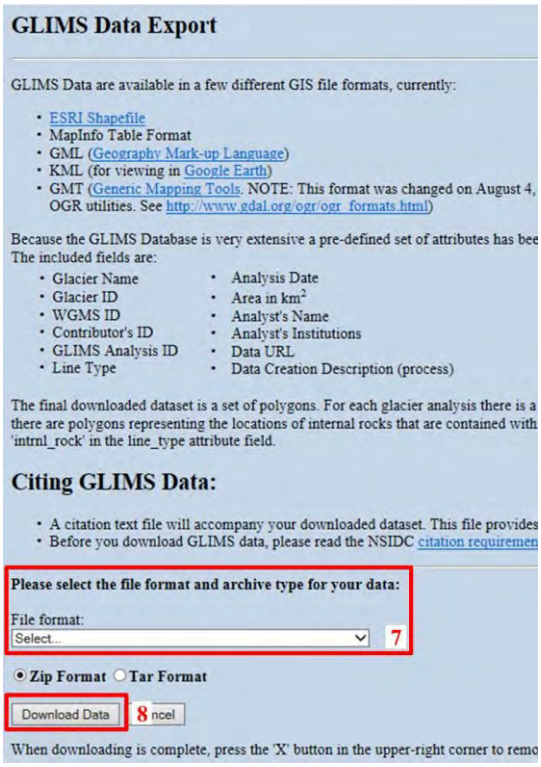

Figure 50. GLIMS data download page. 7: select the type of file that the export will be stored as; 8: select the "Download Data" button to download GLIMS data. For this step, select an ESRI Shapefile for easy data viewing in ArcGIS 10.2. Note: if the extent is too large, the download process may crash. Also, the GLIMS portal does not provide a download progress bar, so have patience and assume that the data request is going to work. Once the data is fully downloaded, the user is notified.

APPENDIX C: GLACIER IMAGES USED TO CREATE THE GLACIER TERMINUSES SHAPEFILES

Collection of the GLS datasets used as either stand-alone images or to create true color and false color image composites and Iterative Self-Organizing (ISO) Data Unsupervised Classifications to delineate the glacier terminuses. These images are displayed in Figures 50-69. Images are grouped by GLS dataset and arranged in order of Baird, Patterson, LeConte, and Shakes Glaciers. Table 23 is provided as a means to locate a particular glacier/GLS dataset combination.

Table 23. Glacier images page number summary. The page numbers are given for all images used for glacier terminus delineation.

Glacier Name	GLS2010 Page #	GLS2005 Page #	GLS2000 Page #	GLS1990 Page #	GLS1975 Page #
Baird	113	117	121	125	129
Patterson	114	118	122	126	129
LeConte	115	119	123	127	130
Shakes	116	120	124	128	130

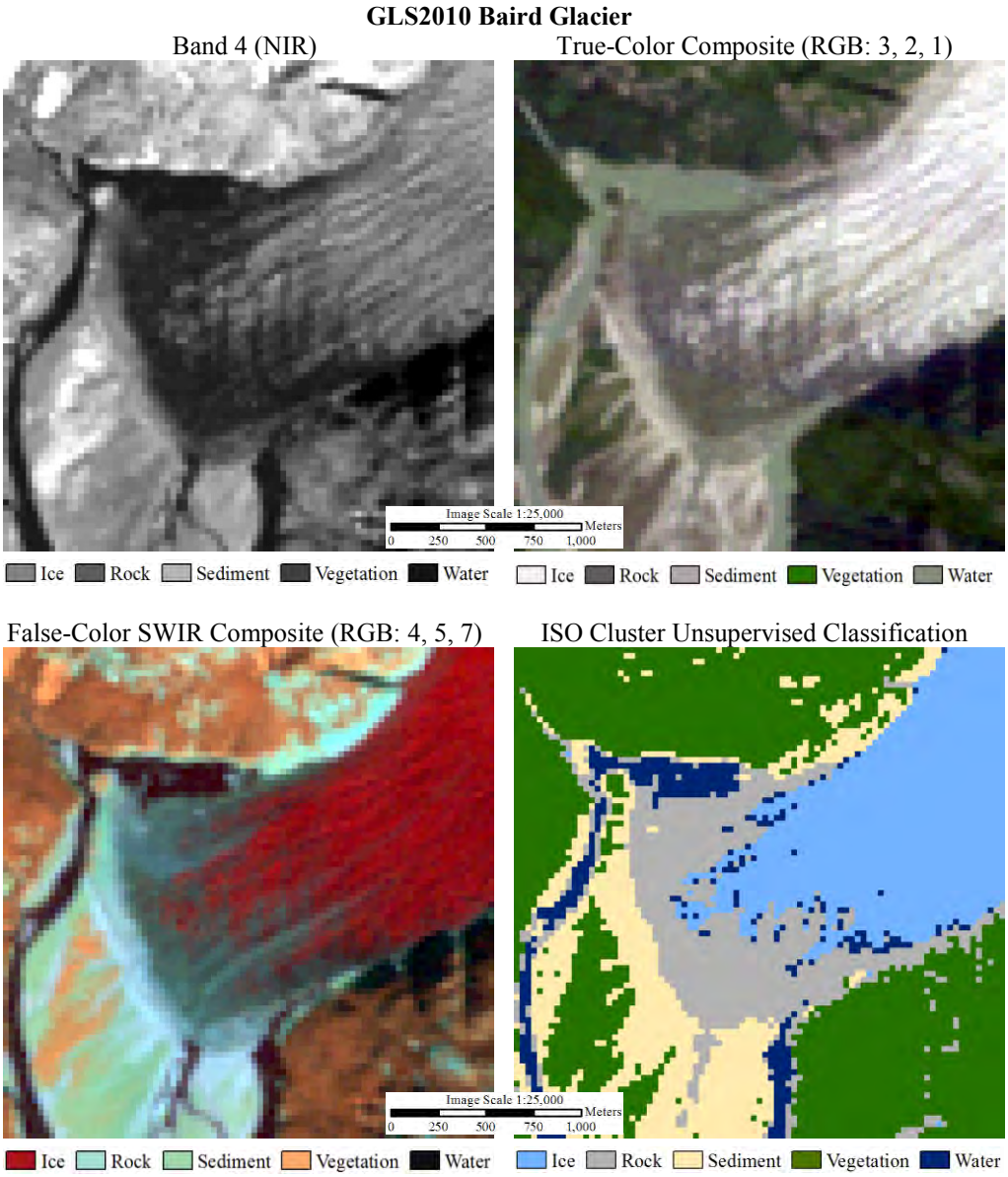

Figure 51. Baird Glacier in GLS2010 images used for glacier terminus delineation. The collecting sensor was Landsat 5 TM. The upper left image is Band 4 (NIR) image. The upper right image is a true-color composite image (RGB: 3, 2, 1). The lower left image is a false-color shortwave infrared composite (RGB: 4, 5, 7). The lower right image is an ISO Data Cluster Unsupervised Classification. Legends for each image are displayed below their respective images.

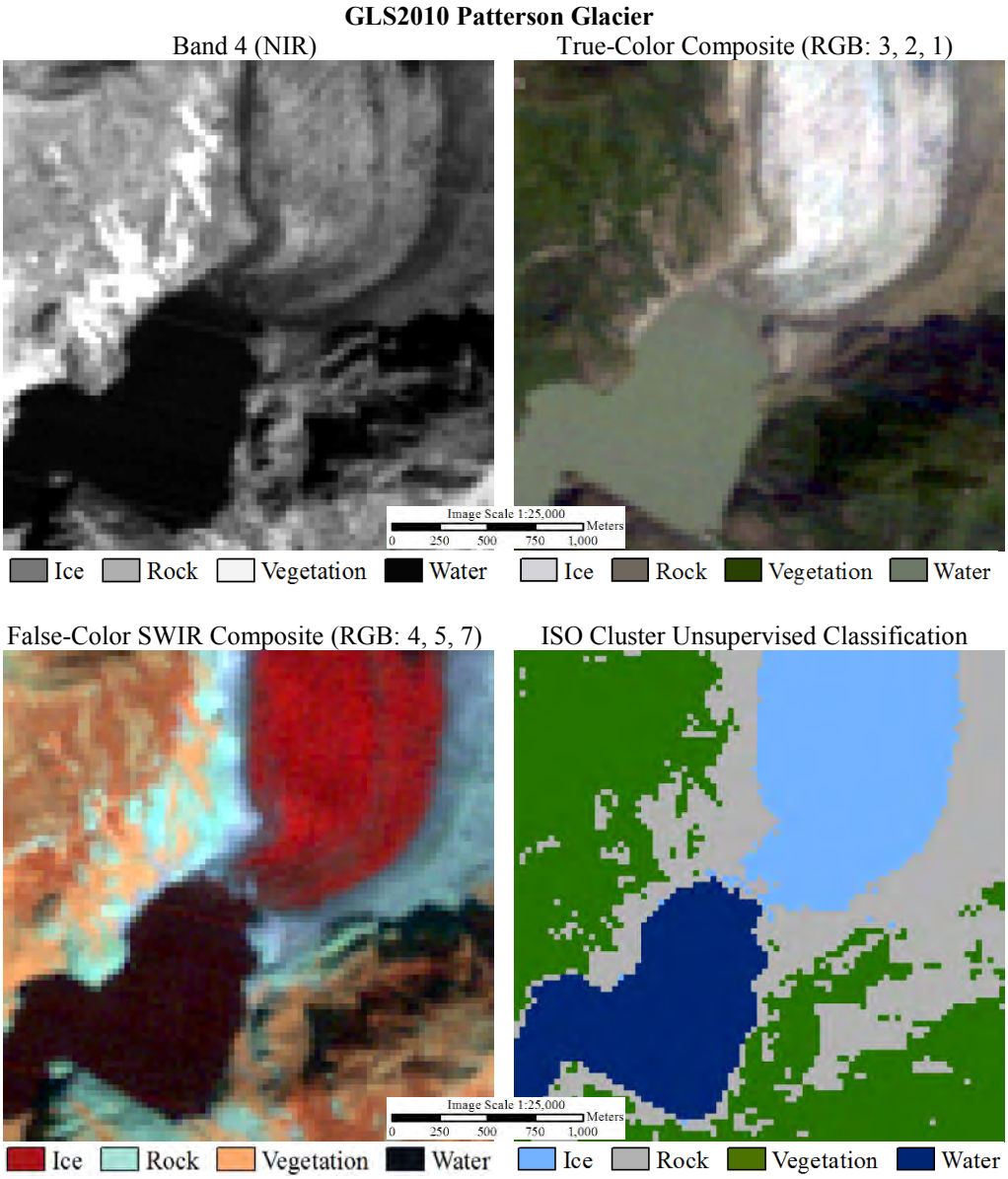

Figure 52. Patterson Glacier in GLS2010 images used for glacier terminus delineation. The collecting sensor was Landsat 5 TM. The upper left image is Band 4 (NIR) image. The upper right image is a true-color composite image (RGB: 3, 2, 1). The lower left image is a false-color shortwave infrared composite (RGB: 4, 5, 7). The lower right image is an ISO Data Cluster Unsupervised Classification. Legends for each image are displayed below their respective images.

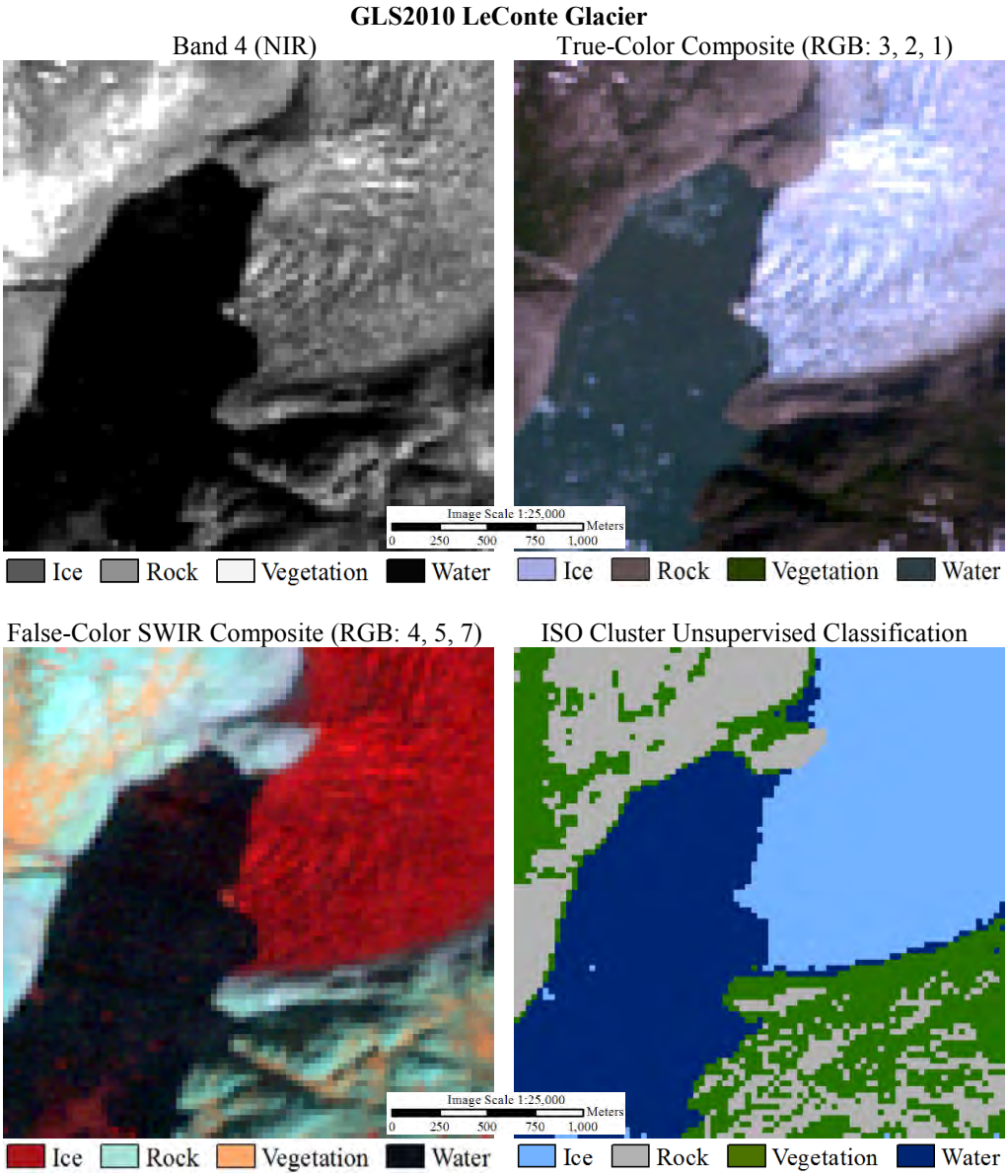

Figure 53. LeConte Glacier in GLS2010 images used for glacier terminus delineation. The collecting sensor was Landsat 5 TM. The upper left image is Band 4 (NIR) image. The upper right image is a true-color composite image (RGB: 3, 2, 1). The lower left image is a false-color shortwave infrared composite (RGB: 4, 5, 7). The lower right image is an ISO Data Cluster Unsupervised Classification. Legends for each image are displayed below their respective images.

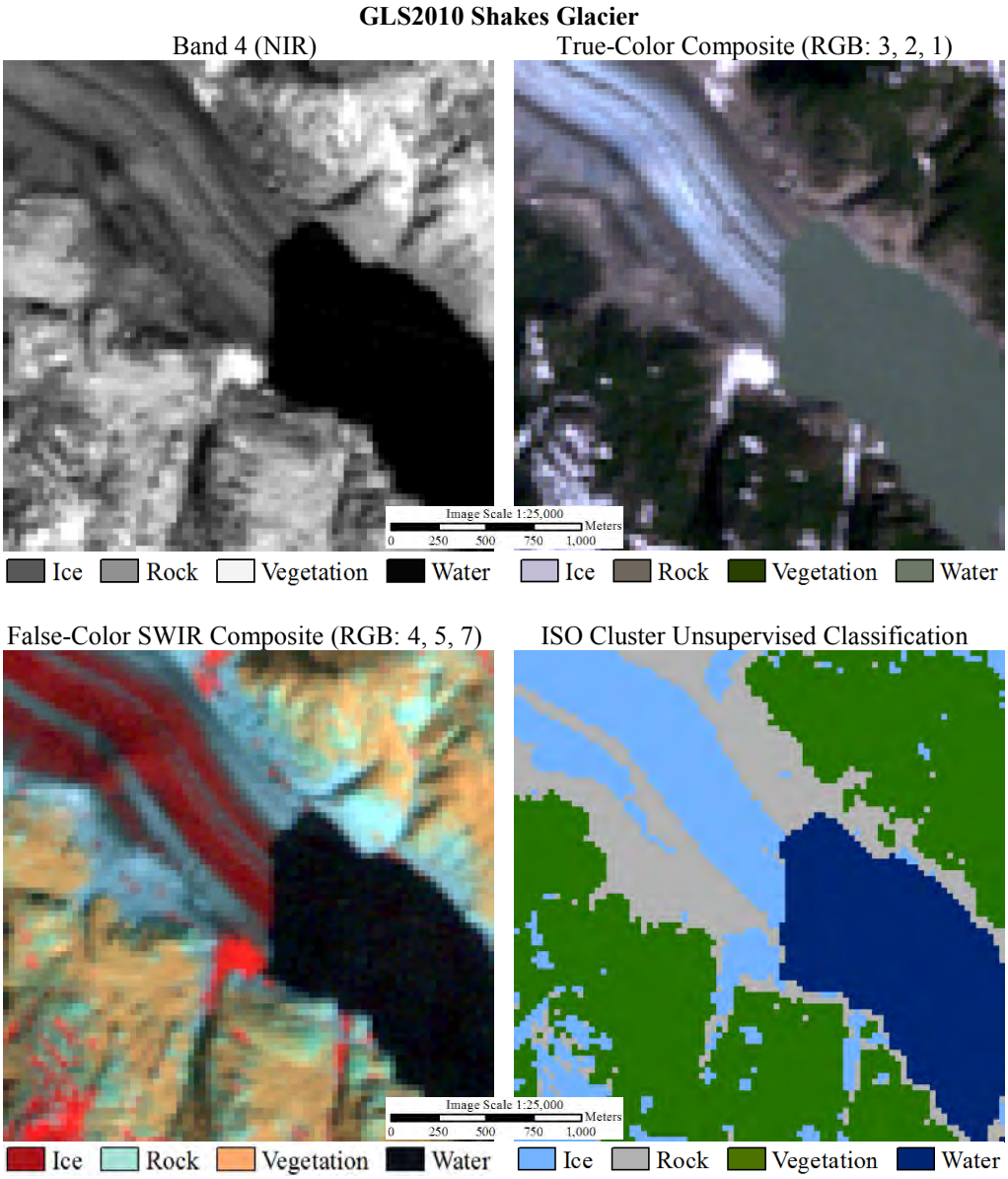

Figure 54. Shakes Glacier in GLS2010 images used for glacier terminus delineation. The collecting sensor was Landsat 5 TM. The upper left image is Band 4 (NIR) image. The upper right image is a true-color composite image (RGB: 3, 2, 1). The lower left image is a false-color shortwave infrared composite (RGB: 4, 5, 7). The lower right image is an ISO Data Cluster Unsupervised Classification. Legends for each image are displayed below their respective images.

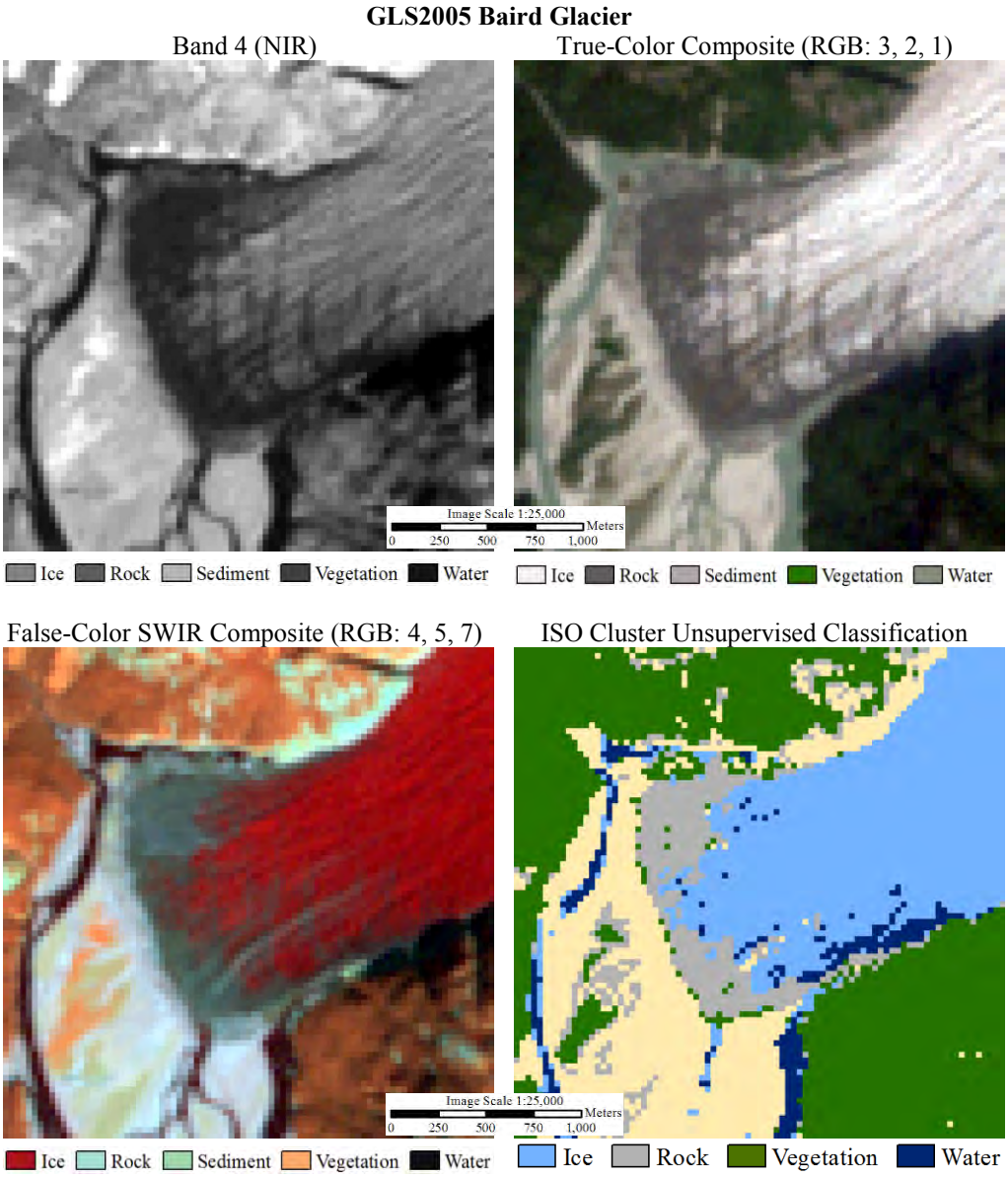

Figure 55. Baird Glacier in GLS2005 images used for glacier terminus delineation. The collecting sensor was Landsat 7 ETM+. The upper left image is Band 4 (NIR) image. The upper right image is a true-color composite image (RGB: 3, 2, 1). The lower left image is a false-color shortwave infrared composite (RGB: 4, 5, 7). The lower right image is an ISO Data Cluster Unsupervised Classification. Legends for each image are displayed below their respective images.

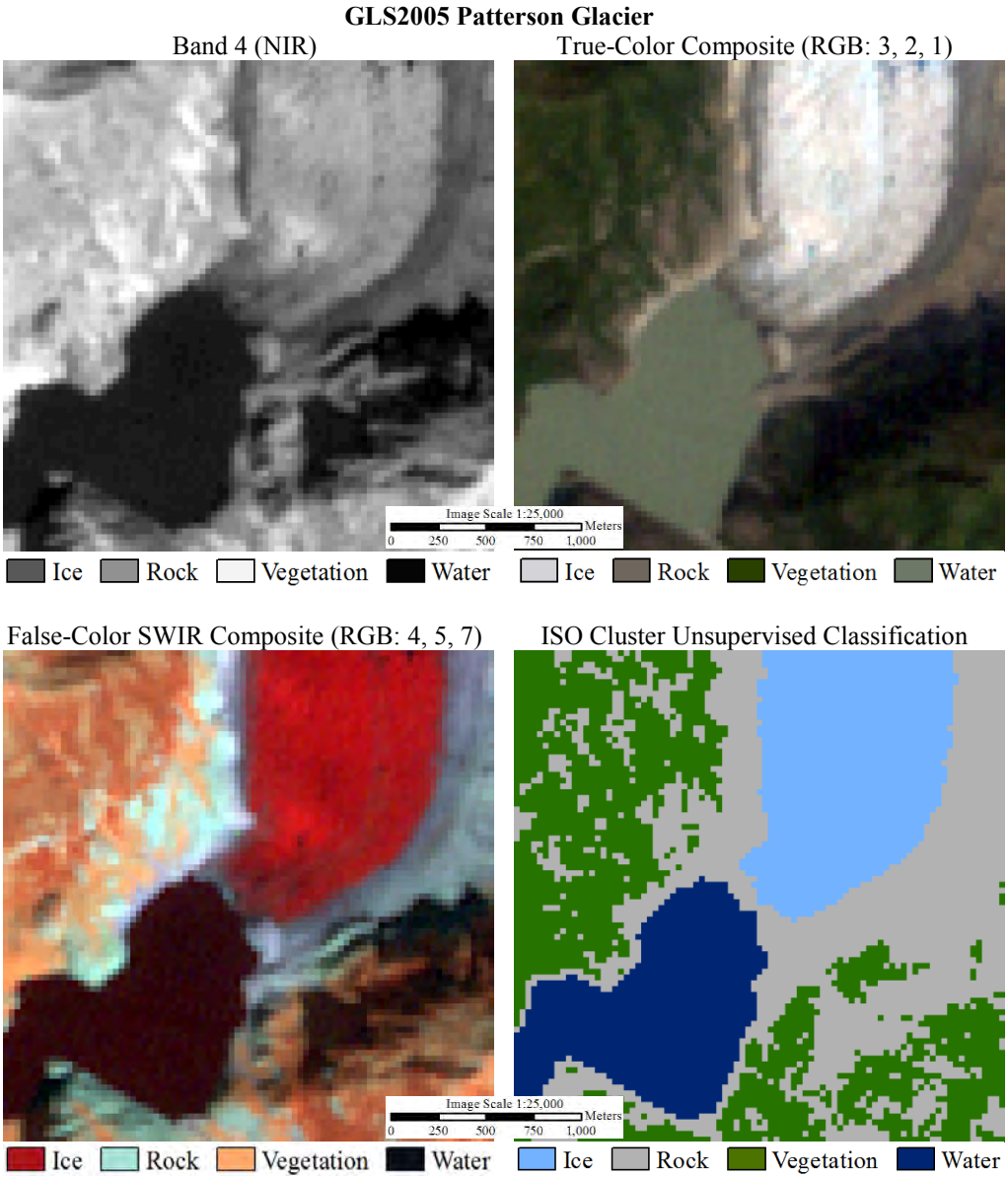

Figure 56. Patterson Glacier in GLS2005 images used for glacier terminus delineation. The collecting sensor was Landsat 7 ETM+. The upper left image is Band 4 (NIR) image. The upper right image is a true-color composite image (RGB: 3, 2, 1). The lower left image is a false-color shortwave infrared composite (RGB: 4, 5, 7). The lower right image is an ISO Data Cluster Unsupervised Classification. Legends for each image are displayed below their respective images.

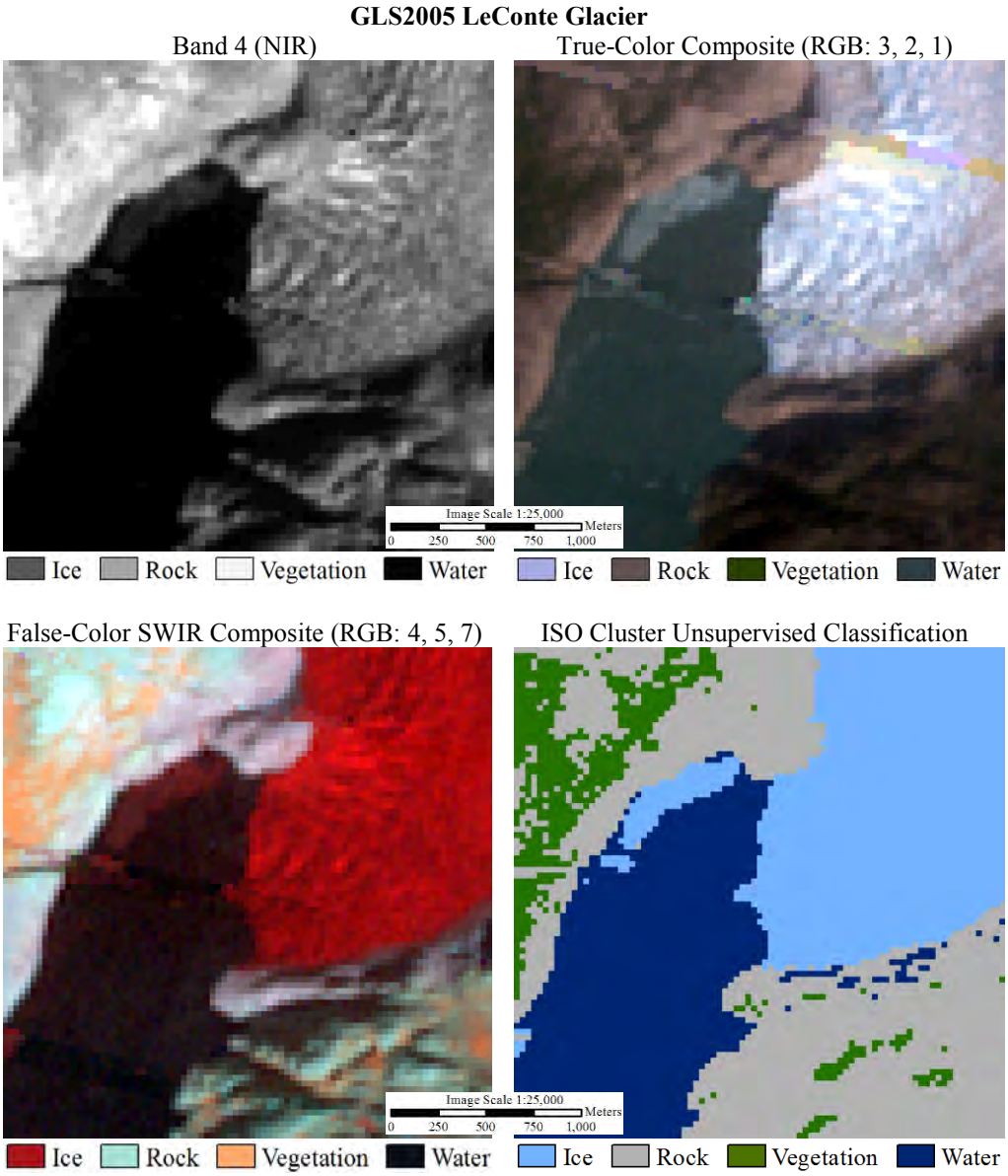

Figure 57. LeConte Glacier in GLS2005 images used for glacier terminus delineation. The collecting sensor was Landsat 7 ETM+. The upper left image is Band 4 (NIR) image. The upper right image is a true-color composite image (RGB: 3, 2, 1). The lower left image is a false-color shortwave infrared composite (RGB: 4, 5, 7). The lower right image is an ISO Data Cluster Unsupervised Classification. Legends for each image are displayed below their respective images.

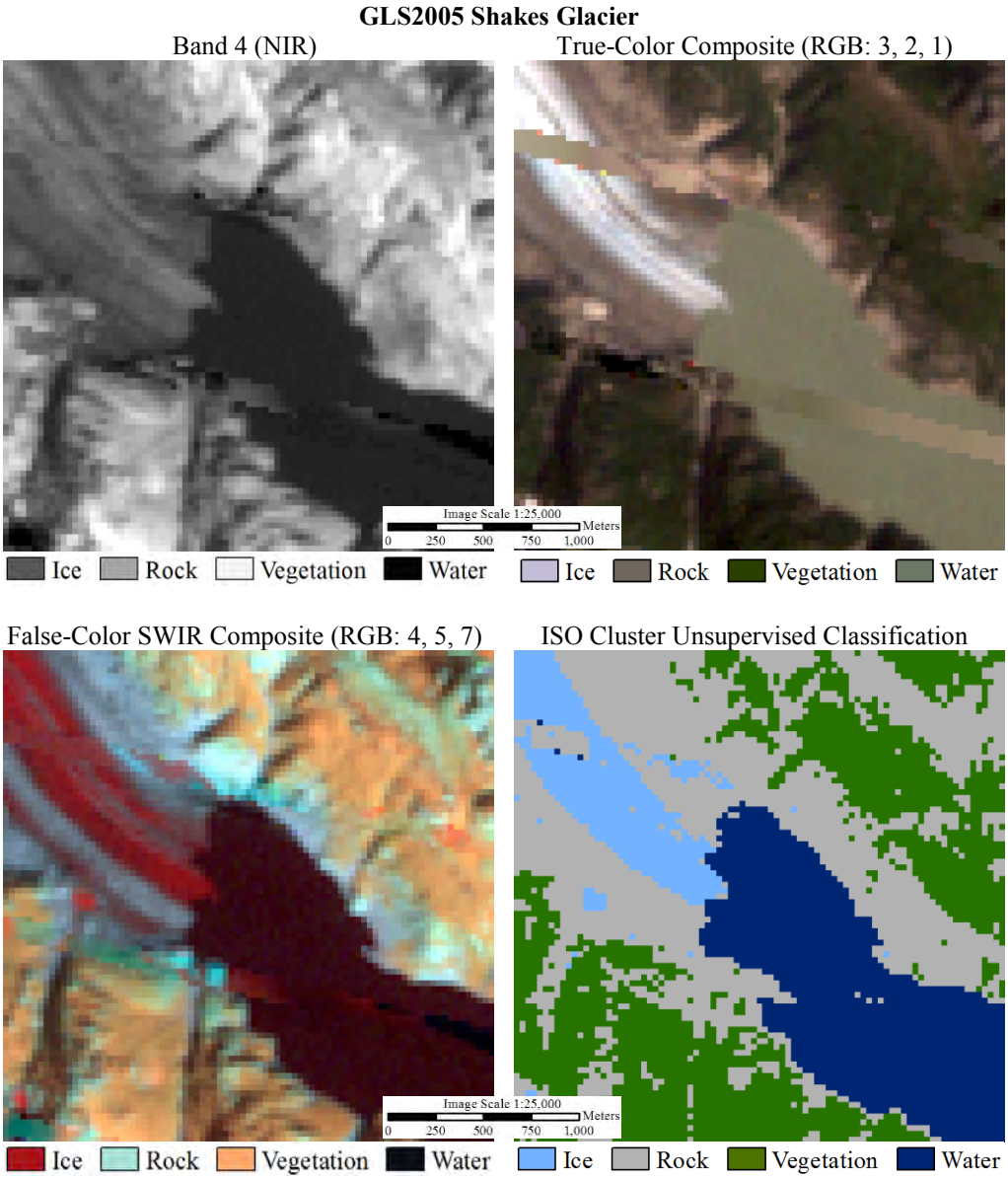

Figure 58. Shakes Glacier in GLS2005 images used for glacier terminus delineation. The collecting sensor was Landsat 7 ETM+. The upper left image is Band 4 (NIR) image. The upper right image is a true-color composite image (RGB: 3, 2, 1). The lower left image is a false-color shortwave infrared composite (RGB: 4, 5, 7). The lower right image is an ISO Data Cluster Unsupervised Classification. Legends for each image are displayed below their respective images.

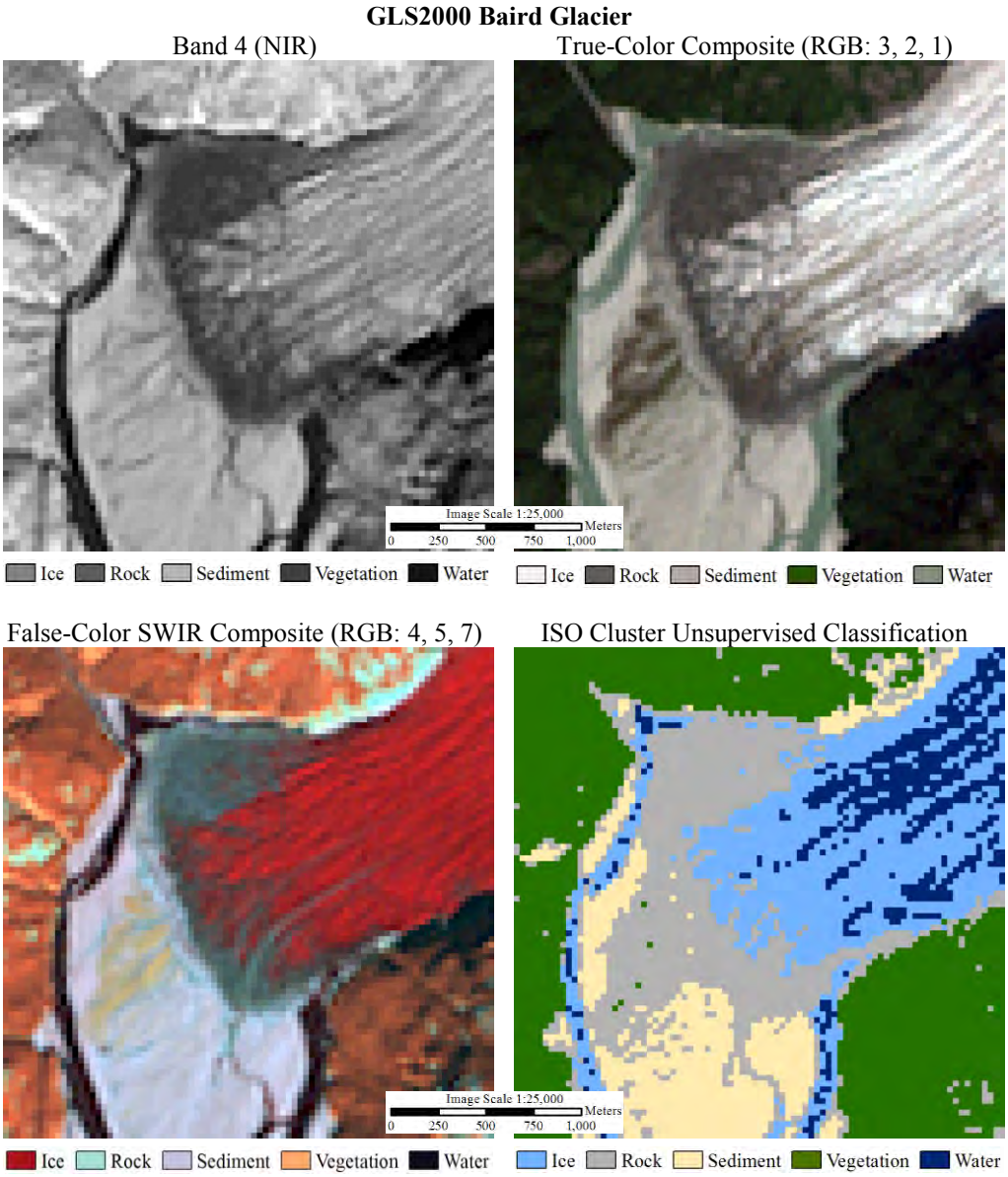

Figure 59. Baird Glacier in GLS2000 images used for glacier terminus delineation. The collecting sensor was Landsat 7 ETM+. The upper left image is Band 4 (NIR) image. The upper right image is a true-color composite image (RGB: 3, 2, 1). The lower left image is a false-color shortwave infrared composite (RGB: 4, 5, 7). The lower right image is an ISO Data Cluster Unsupervised Classification. Legends for each image are displayed below their respective images.

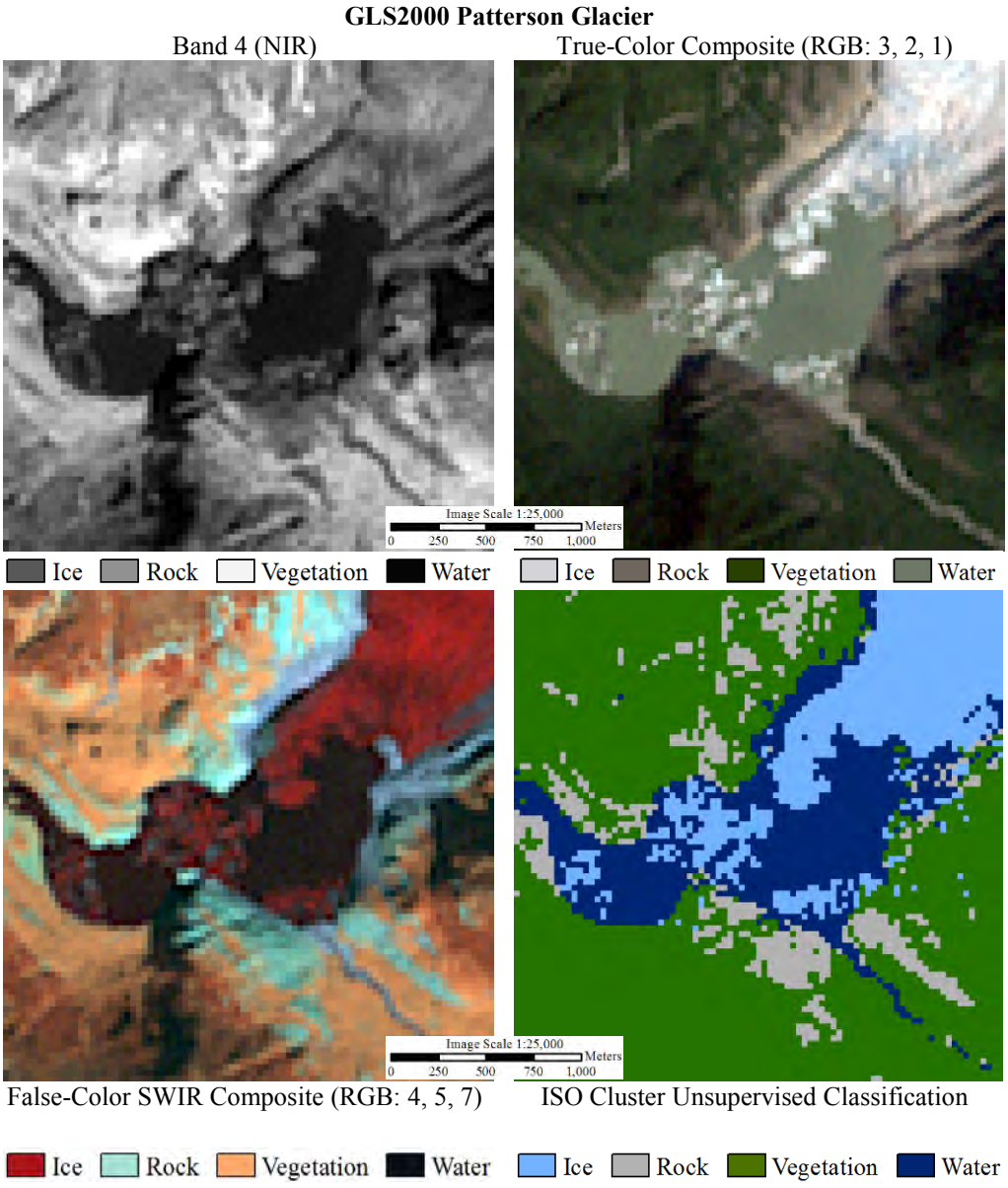

Figure 60. Patterson Glacier in GLS2000 images used for glacier terminus delineation. The collecting sensor was Landsat 7 ETM+. The upper left image is Band 4 (NIR) image. The upper right image is a true-color composite image (RGB: 3, 2, 1). The lower left image is a false-color shortwave infrared composite (RGB: 4, 5, 7). The lower right image is an ISO Data Cluster Unsupervised Classification. Legends for each image are displayed below their respective images.

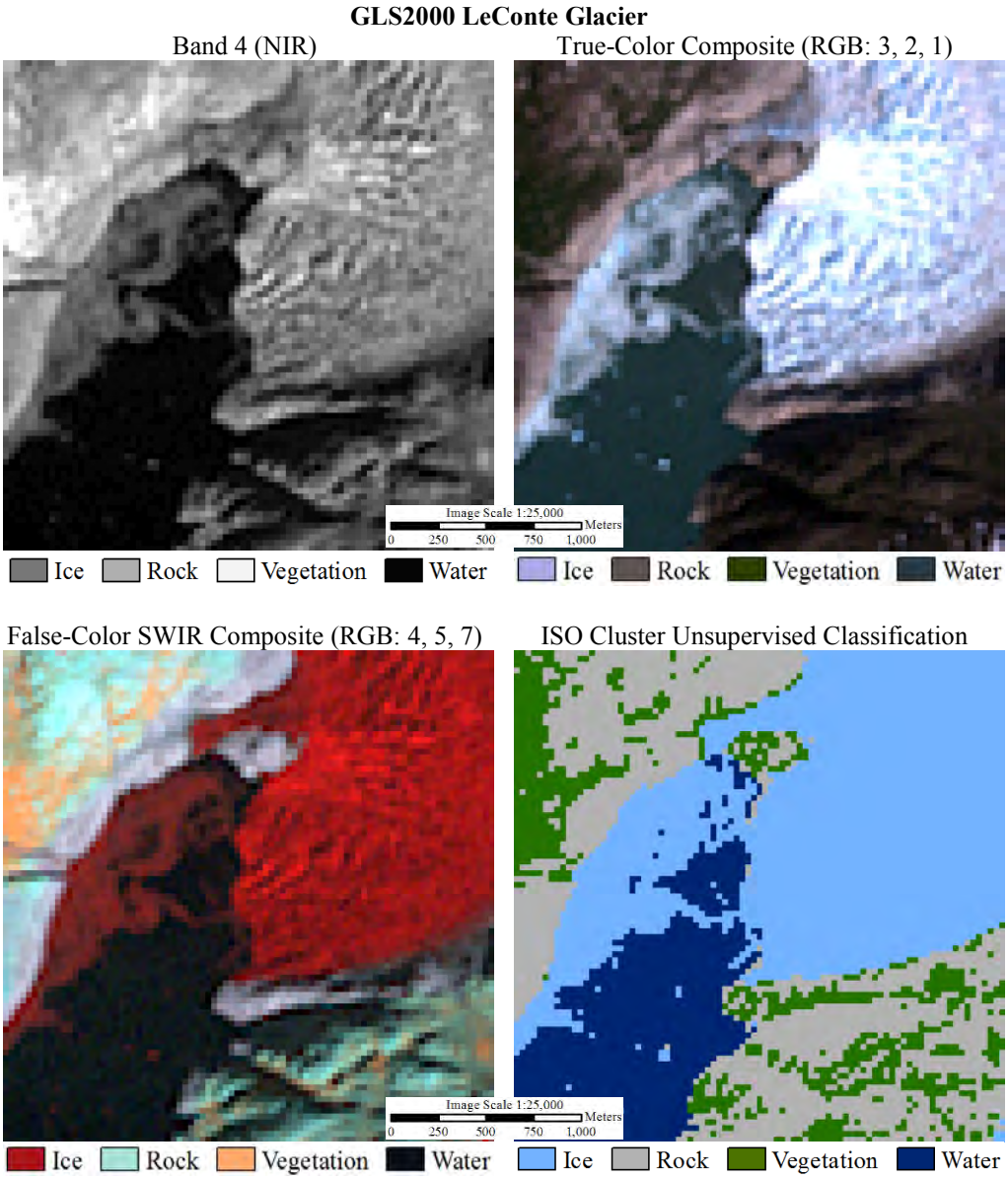

Figure 61. LeConte Glacier in GLS2000 images used for glacier terminus delineation. The collecting sensor was Landsat 7 ETM+. The upper left image is Band 4 (NIR) image. The upper right image is a true-color composite image (RGB: 3, 2, 1). The lower left image is a false-color shortwave infrared composite (RGB: 4, 5, 7). The lower right image is an ISO Data Cluster Unsupervised Classification. Legends for each image are displayed below their respective images.

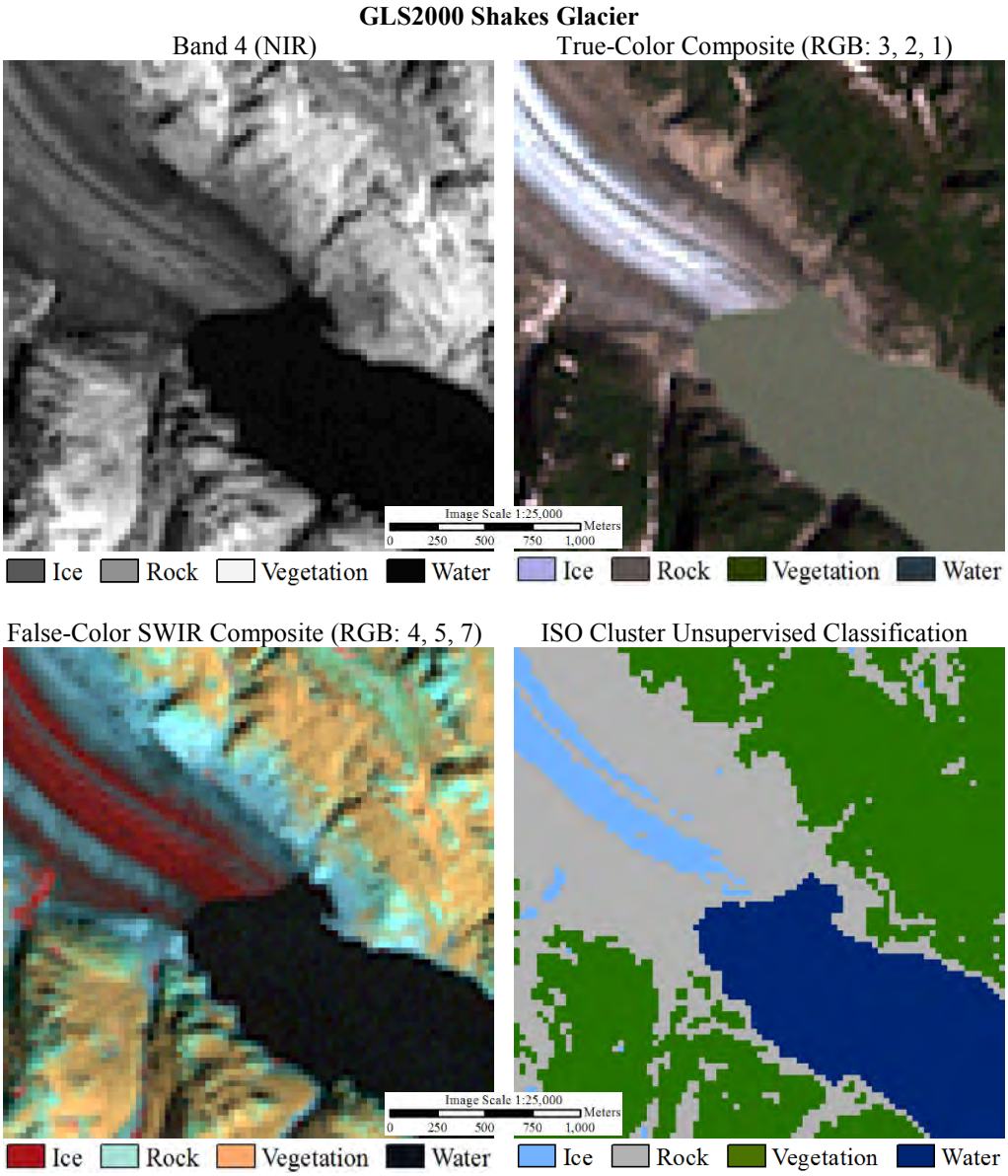

Figure 62. Shakes Glacier in GLS2000 images used for glacier terminus delineation. The collecting sensor was Landsat 7 ETM+. The upper left image is Band 4 (NIR) image. The upper right image is a true-color composite image (RGB: 3, 2, 1). The lower left image is a false-color shortwave infrared composite (RGB: 4, 5, 7). The lower right image is an ISO Data Cluster Unsupervised Classification. Legends for each image are displayed below their respective images.

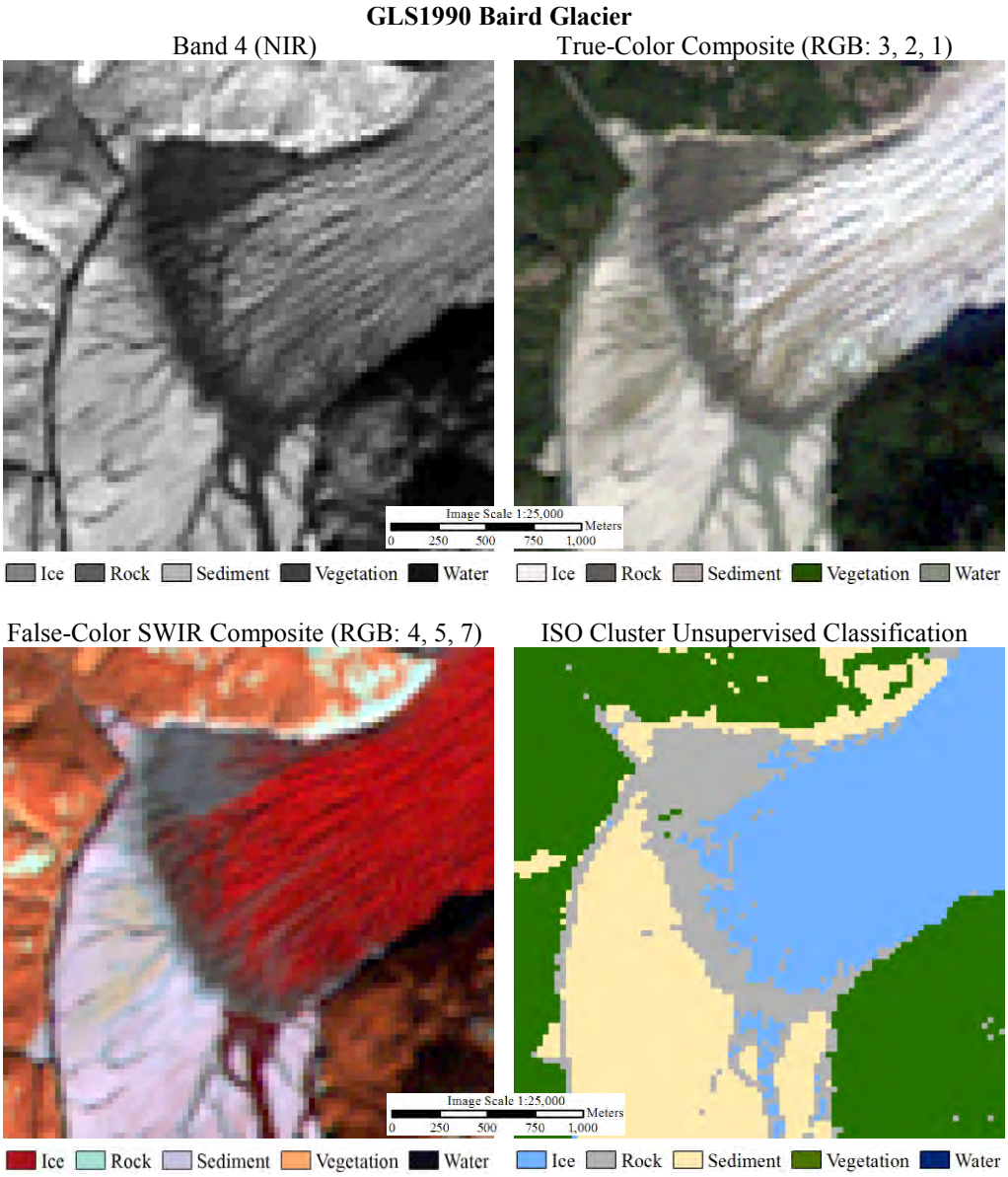

Figure 63. Baird Glacier in GLS1990 images used for glacier terminus delineation. The collecting sensor was Landsat 5 TM. The upper left image is Band 4 (NIR) image. The upper right image is a true-color composite image (RGB: 3, 2, 1). The lower left image is a false-color shortwave infrared composite (RGB: 4, 5, 7). The lower right image is an ISO Data Cluster Unsupervised Classification. Legends for each image are displayed below their respective images.

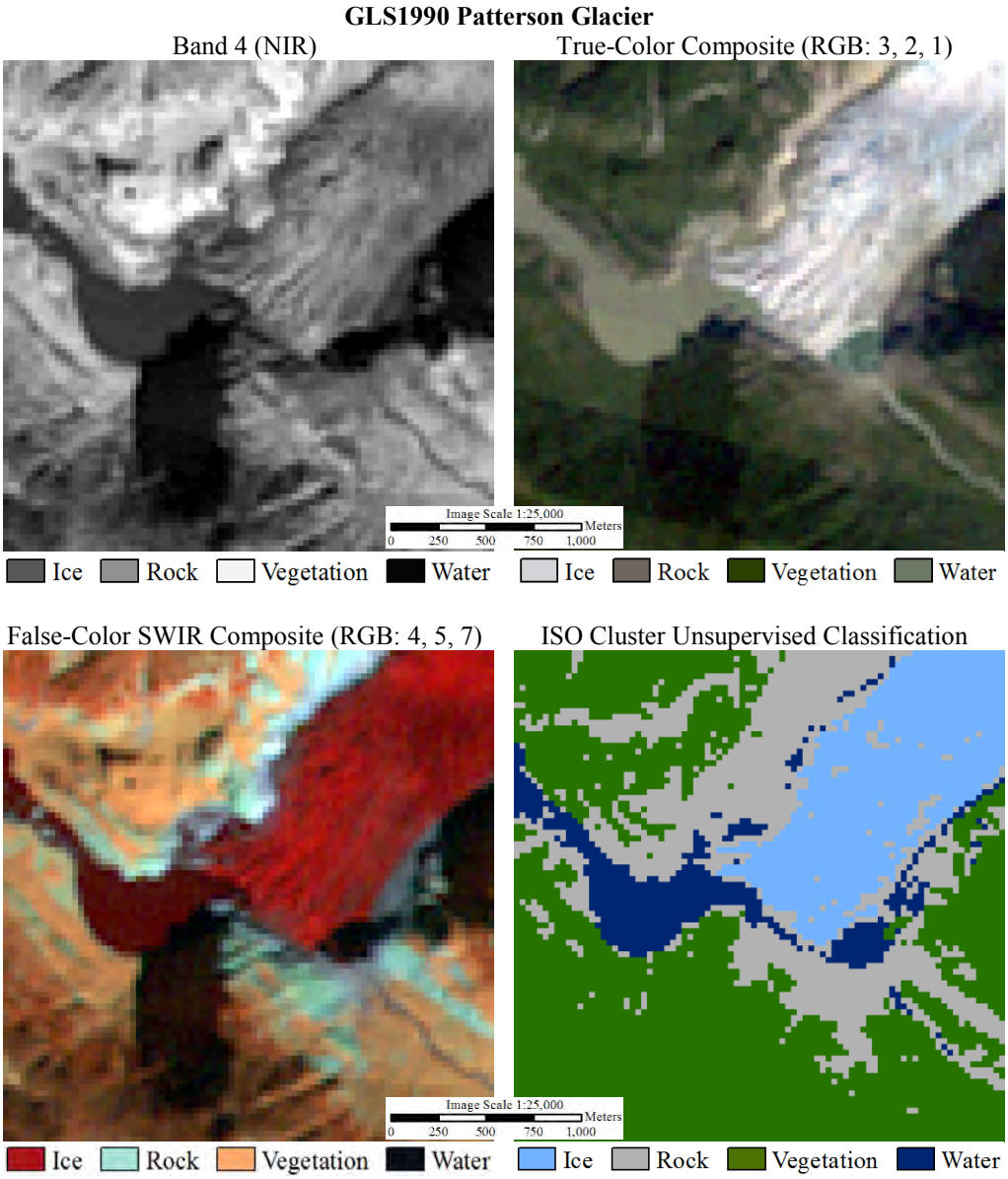

Figure 64. Patterson Glacier in GLS1990 images used for glacier terminus delineation. The collecting sensor was Landsat 5 TM. The upper left image is Band 4 (NIR) image. The upper right image is a true-color composite image (RGB: 3, 2, 1). The lower left image is a false-color shortwave infrared composite (RGB: 4, 5, 7). The lower right image is an ISO Data Cluster Unsupervised Classification. Legends for each image are displayed below their respective images.

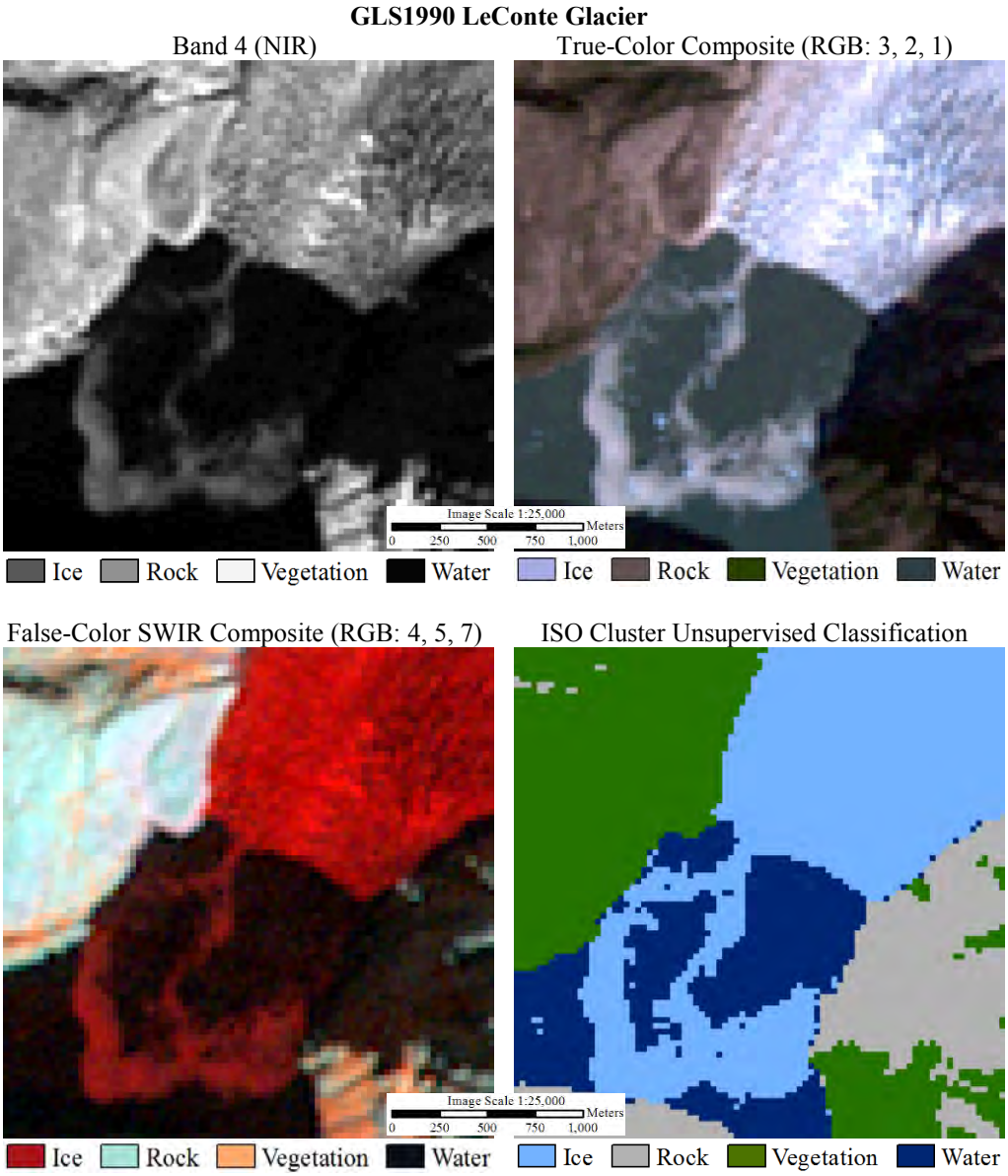

Figure 65. LeConte Glacier in GLS1990 images used for glacier terminus delineation. The collecting sensor was Landsat 5 TM. The upper left image is Band 4 (NIR) image. The upper right image is a true-color composite image (RGB: 3, 2, 1). The lower left image is a false-color shortwave infrared composite (RGB: 4, 5, 7). The lower right image is an ISO Data Cluster Unsupervised Classification. Legends for each image are displayed below their respective images.

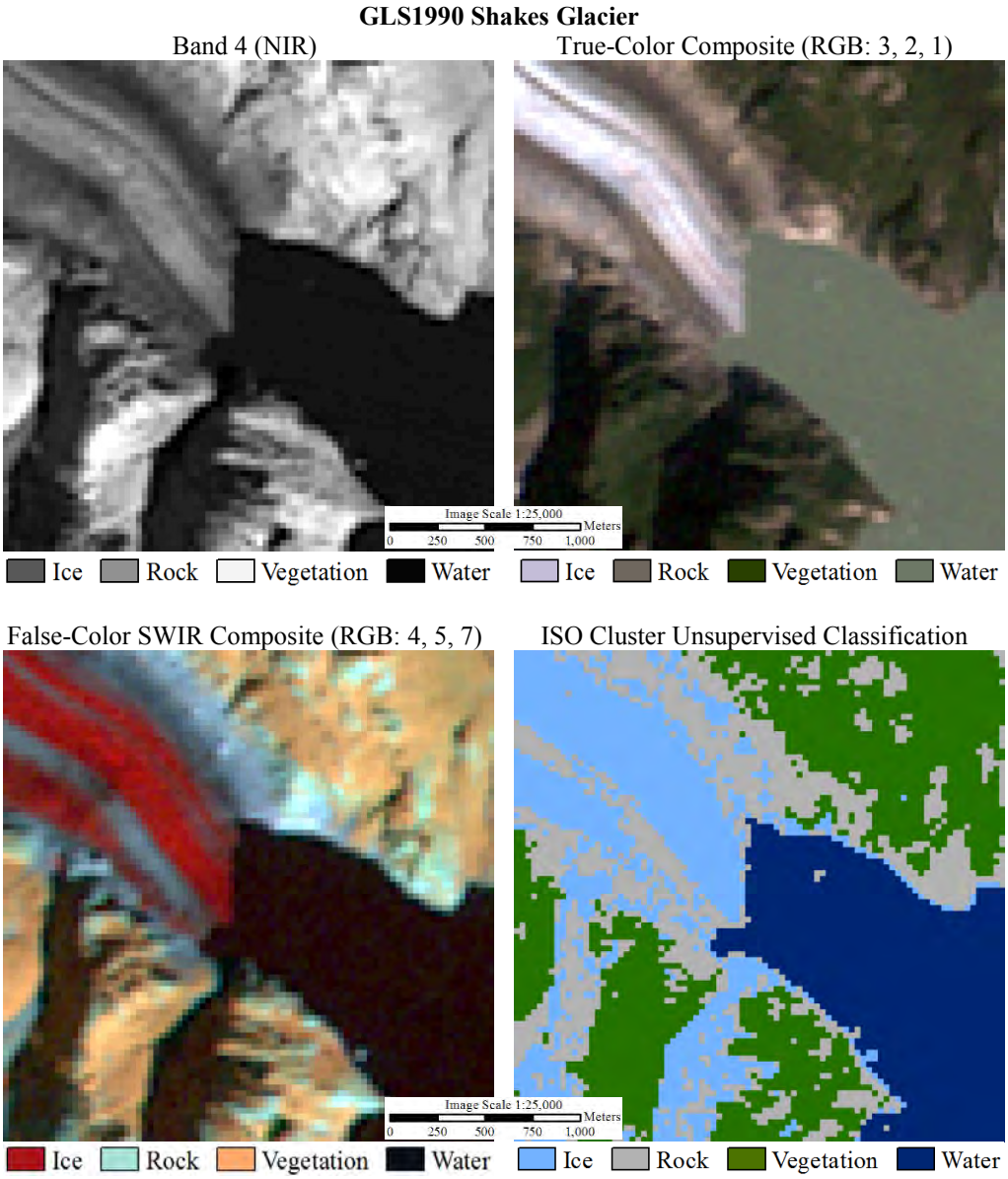

Figure 66. Shakes Glacier in GLS1990 images used for glacier terminus delineation. The collecting sensor was Landsat 5 TM. The upper left image is Band 4 (NIR) image. The upper right image is a true-color composite image (RGB: 3, 2, 1). The lower left image is a false-color shortwave infrared composite (RGB: 4, 5, 7). The lower right image is an ISO Data Cluster Unsupervised Classification. Legends for each image are displayed below their respective images.

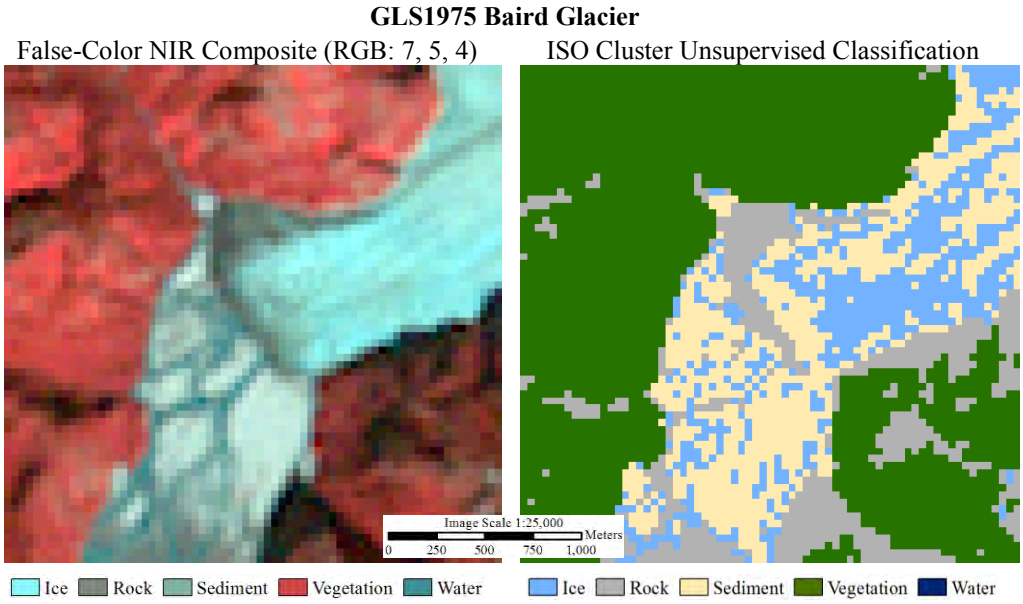

Figure 67. Baird Glacier in GLS1975 images used for glacier terminus delineation. The collecting sensor was Landsat 1 MSS. The lower left image is a false-color near-infrared composite (RGB: 7, 5, 4). The right image is an ISO Data Cluster Unsupervised Classification. Legends for each image are displayed below their respective images.

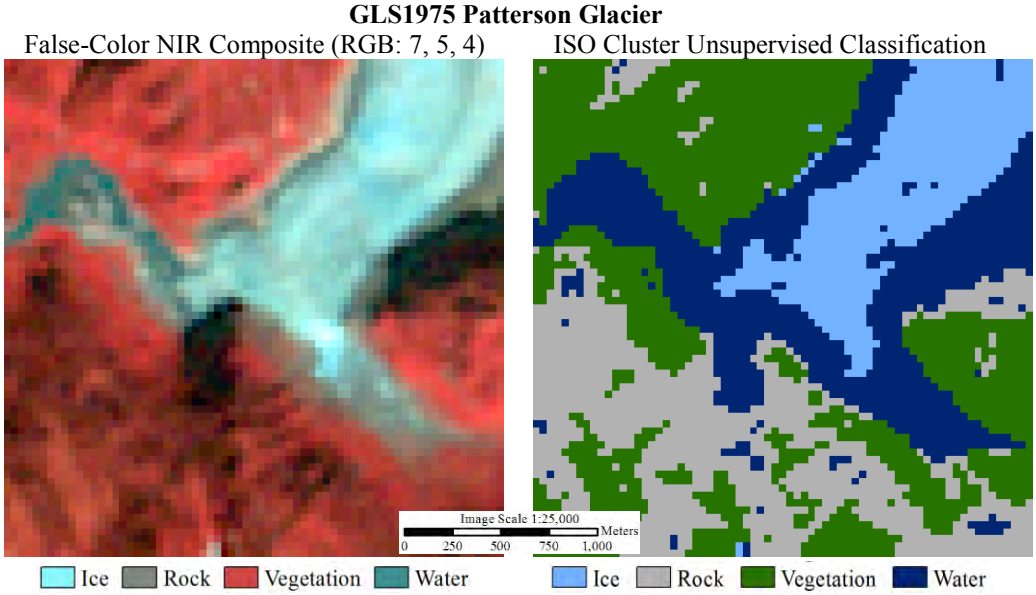

Figure 68. Patterson Glacier in GLS1975 images used for glacier terminus delineation. The collecting sensor was Landsat 1 MSS. The lower left image is a false-color near-infrared composite (RGB: 7, 5, 4). The right image is an ISO Data Cluster Unsupervised Classification. Legends for each image are displayed below their respective images.

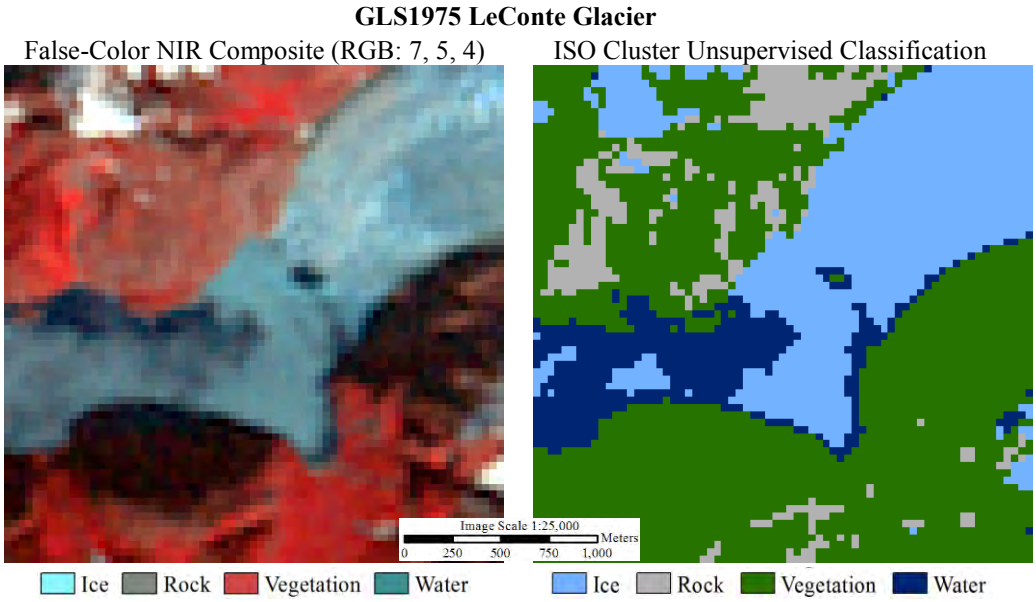

Figure 69. LeConte Glacier in GLS1975 images used for glacier terminus delineation. The collecting sensor was Landsat 1 MSS. The lower left image is a false-color near-infrared composite (RGB: 7, 5, 4). The right image is an ISO Data Cluster Unsupervised Classification. Legends for each image are displayed below their respective images.

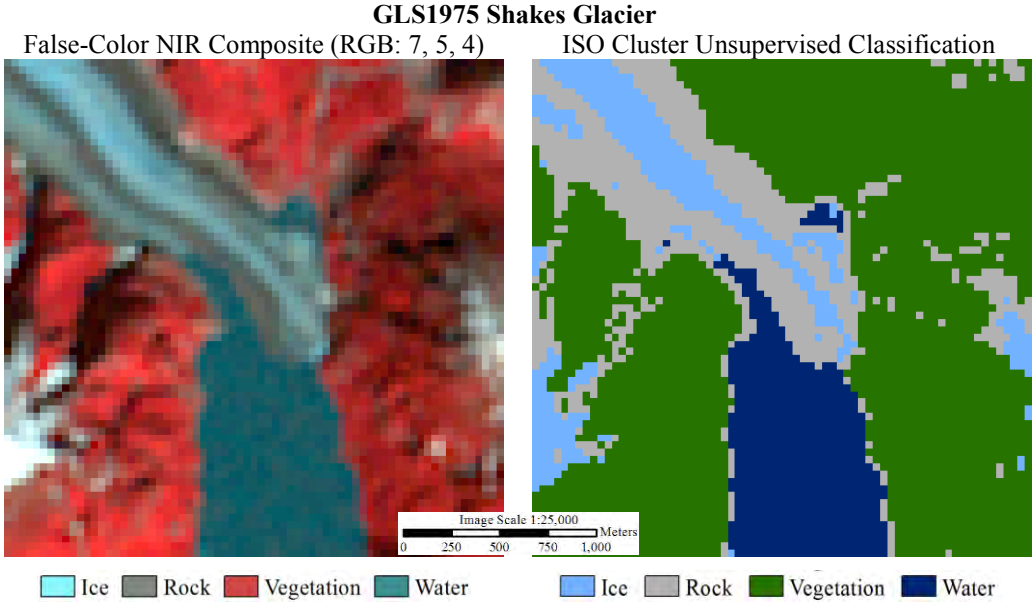

Figure 70. Shakes Glacier in GLS1975 images used for glacier terminus delineation. The collecting sensor was Landsat 1 MSS. The lower left image is a false-color near-infrared composite (RGB: 7, 5, 4). The right image is an ISO Data Cluster Unsupervised Classification. Legends for each image are displayed below their respective images.